2013

Role of Tyk2 in regulating energy expenditure and preventing obesity

Vidisha Raje
Virginia Commonwealth University

ROLE OF TYK2 IN REGULATING ENERGY EXPENDITURE AND PREVENTING OBESITY

A dissertation submitted in partial fulfillment of the requirements for the degree

of Doctor of Philosophy at Virginia Commonwealth University.

By

Vidisha Bipin Raje, M.Sc.

Advisor: Andrew C Larner, MD, PhD

Professor

Department of Biochemistry and Molecular Biology

Virginia Commonwealth University

Richmond, Virginia

July, 2013

Acknowledgements

I take this opportunity to thank all the people without whom this thesis would not have been possible.

First and foremost, I would like to express my gratitude towards my mentor Dr. Andrew Larner for giving me the freedom to explore, and providing all the guidance and support. Thanks boss for being so patient with me and making research exciting.

I would also like to thank my committee members: Dr. Joycle Lloyd, Dr. Daniel Conrad, Dr. Edward Lesnefsky and Dr. Keith Baker for providing invaluable guidance and support throughout this process. I would also like to acknowledge Dr. Tomek Kordula, for helping me with my cloning feats.

I am grateful to the administrative staff of Department of Life Sciences and Department of Biochemistry and Molecular biology - Jeanne, Larry, Gwen and Carmelda for dealing with all my queries and concerns. Thanks a lot guys.

My heartfelt gratitude towards my lab family- Jenny, Marta, Magda, Karol, Qifang and Jeremy and to my extended lab family- Divya, Tom and MJ. Thank you all for being there, keeping me motivated and entertained and making this PhD the greatest experience of my lifetime. You guys rock.

This thesis would not have been accomplished without the love and support of my friends and my family. I do not have enough words to express my gratitude towards my family. I would like to thank my parents- *aai* and *baba* for believing in me and letting me be. I also thank my sister for being there for me. My heartfelt gratitude towards all my

extended family-thank you all for all the love and support. My heartfelt love and gratitude to my husband Ninad, for always being there for me. I would like to dedicate this thesis to my grandmothers- my *aajis*, for being my strength and inspiration, always.

Table of Contents

List of Figures

List of Tables

Abbreviations

ADP : Adenosine di phosphate

ANT : Adenosine di phosphate

ATP : Adenosine tri phosphate

βAR : β adrenergic receptor

BAT : Brown adipose tissue

BMI : Body mass index

BMR : Basal metabolic rate

BN-PAGE : Blue native polyacrylamide gel electrophoresis

cAMP : Cyclic adenosine mono phosphate

C/EBP : CCAAT/enhancer binding proteins

ChIP : Chromatin immunoprecipitation

CHO : Chinese hamster ovary

Cidea : Cell death-inducing DFFA-like effector A

DNA : Deoxyribonucleic acid

DNP : 2,4 dinitrophenol

En1 : Engrailed like protein 1

Epr : Ephrin receptor

ETC : Electron transport chain

$FADH_2$: Flavin adenine dinucleotide dihydrogen

FDA : Food and drug administration

FDG : Fluoro deoxyglucose

FERM : Band 4.1 ezrin, radixin and moesin

FFA : Free fatty acids

GA : Gastrocnemius

GTT : Glucose tolerance test

IFN : Interferon

IFNAR : Interferon α/β receptor

IL : Interleukin

IP : Immunoprecipitation

IRS : Insulin receptor substrate

JAK : Janus kinase

KD : Kinase dead

LIF : Leukemia inhibitory factor

MCK : Muscle creatine kinase

mESC : Mouse embryonic stem cells

MHC : Myosin heavy chain

Mfn : Mitofusin

NADH : Nicotinamide adenine dinucleotide

NK : Natural killer

NLS : Nuclear localizing sequence

NMJ : Neuro-muscular junction

NMR : Nuclear magnetic resonance

NST : Non-shivering thermogenesis

PAGE : Polyacrylamide gel electrophoresis

PCR : Polymerase chain reaction

PET : Positron emission tomography

PGC1α : Peroxisome proliferator-activated receptor γ coactivator 1 α

PKA : Protein kinase A

PL : Plantaris

PPAR : Peroxisome proliferator-activated receptor

PRDM16 : PRD1-BF1-RIZ1-containing homologous domain containing protein 16

qPCR : Quantative realtime PCR

RNA : Ribonucleic acid

RyR : Ryanodyne receptor

RT : Room temperature

SE : Standard error

SEM : Standard error of mean

SERCA : Sarcoplasmic/endoplasmic reticulum calcium ATPase.

SKM : Skeletal muscle

STAT : Signal transducers and activators of transcription

TAG : Triacyl glycerol

TCA : Tricarboxylic acid cycle

Th2 : T helper

UCP : Uncoupling protein

WAT : White adipose tissue

WHO : World health organization

WT : Wild type

Abstract

Obesity develops when energy intake exceeds energy expenditure. Defect in the function of brown fat and skeletal muscle, two of the major tissues that contribute towards energy expenditure, lead to the development of obesity and metabolic syndrome. Our previous findings suggest that Tyk2 deficient mice become obese and develop the metabolic syndrome. Tyk2, which is a tyrosine kinase of the JAK-STAT signaling family, is important for optimal brown development and function. Since brown fat and skeletal muscle, both are derived from the Myf5+ lineage of mesenchymal stem cells, we also characterized the role of Tyk2 in the development and function of skeletal muscle. We found that Tyk2 deficient mice do not display a structural defect in skeletal muscle development; however, the function of skeletal muscle is severely impaired in these mice. Expression of troponins, which regulate the muscle contraction and muscle creatine kinase, which regulates the levels of phosphocreatine, a major fuel for skeletal muscle, is downregulated in Tyk2 deficient mice. Skeletal muscle mitochondria also display an abnormal morphology along with decreased respiration capacity, which is a function of decreased activity of complex IV of the electron transport chain. Interestingly, Tyk2 deficient mice also exhibit an increased proportion of fast, glycolytic, Type II fibers in the skeletal muscle. Using an in-vitro system for skeletal muscle differentiation, we found that Tyk2 levels increase during differentiation, suggesting a role for Tyk2 in proper development and function of the skeletal muscle.

Our previous studies suggested that a kinase-inactive (Tyk2KD) form of Tyk2 is also efficient in restoring the function of Tyk2 deficient brown fat preadipocytes. We generated transgenic mice that expressed a wild type (Tyk2WT) and kinase inactive

(Tyk2 KD) form of tyk2 in brown fat and skeletal muscle under Myf5 cre and in skeletal muscle using MCK cre mice. Expression of Tyk2 using the Myf5 cre (E8.0) reverts the obese and the metabolic phenotype observed in the Tyk2 deficient mice. Interestingly, expressing Tyk2 under MCK cre (E13.0) also reverts the obese phenotype, suggesting that the temporal and spatial expression of Tyk2 is critical in regulating energy expenditure.

Our studies also highlight the role of Tyk2, not as a kinase, but as a component of the transcriptional assembly regulating the expression of genes involved brown fat and skeletal muscle differentiation and function.

Chapter I: Introduction

Obesity is a global phenomenon affecting at least 200 billion adults to date. In the United States alone, over a third of the population is obese. Obesity in children and adolescents has also increased from 5% in the 1980s to 18% in 2012. Obesity is usually defined by the body mass index (BMI; weight in kilograms divided by length in squared meters, kg/m^2). A BMI >25 kg/m^2 represents overweight, >30 kg/m^2 obese and >40 kg/m^2 morbidly obese individuals (1). Incidence of Type II diabetes is also linked to obesity. As such, the world health organization (WHO) estimates that the number of diabetics will reach around 300 billion in 2025 (2).

Obesity is a result of increased energy intake and/or decreased energy expenditure. This excess weight is stored in adipose tissue, which consists of fat cells, or adipocytes, which have an incredible capacity for storing surplus energy in the form of lipid (3). Obesity is also associated with many abnormalities collectively known as the metabolic syndrome, including dyslipidemia, increased risk for cardiovascular disease, and abnormal glucose metabolism. All of these alterations can easily factor into the development of insulin resistance and type II diabetes (4).

Changing diet and lifestyle are the common treatments suggested for obesity, however, in morbidly obese patients, bariatric surgery has been the only effective treatment to date (1). Currently, there are drugs that aim at decreasing energy intake by acting on the satiety centers in the brain. Nonetheless, decreasing food intake is known to trigger the starvation response in mammals and hence these treatments become ineffective after a while (5). Developing alternative therapies that will enhance energy expenditure

in obese individuals is the need of the hour. Mammals have two major thermogenic tissues- Brown Adipose Tissue (BAT) and Skeletal Muscle (SKM), which are involved in regulation of energy expenditure. Increasing the thermogenic capacities of these tissues and hence increasing overall energy expenditure may provide an alternative means of combating obesity.

1.1: Brown Adipose Tissue in obesity

Mammals have two functionally different types of adipose tissues- white adipose tissue (WAT) and brown adipose tissue (BAT). WAT mainly functions as an energy store whereas the main function of BAT is to dissipate energy in the form of heat (6). Differences between BAT and WAT are listed in Table 1.1. In rodents BAT is present throughout life. Major depots are located primarily in the interscapular region and the axillae, whereas minor amounts exist near the thymus and in the dorsal midline region of the thorax and abdomen. The activity of BAT in non- hibernating animals is strictly related to the environmental temperature with cold exposure inducing its action. In neonates and hibernating animals, BAT serves as an important regulator of the body temperature via non- shivering thermogenesis.

Studies on rodent models suggest that BAT also plays an important role in prevention of obesity. Transgenic mice with ablated BAT exhibit metabolic syndrome (7). Uncoupling protein 1 (UCP1) is unique to brown fat and is responsible for dissipating the mitochondrial proton gradient, thus releasing this potential energy as heat. UCP1 null mice exhibit an obese phenotype (8). Additional examples of the relevance of BAT against the development of obesity come from genetically obese mouse models like the

ob/ob and db/db strains where BAT is dysfunctional (9). BAT activity is also lower in overweight and obese individuals compared to the lean individuals. Whereas BMI and body fat percentage showed an inverse correlation with BAT activity, resting metabolic rate exhibited a positive correlation with BAT activity. Interestingly, it has been observed that higher levels of BAT might protect against age-related obesity (6).

The presence of active brown fat depots in human newborns and its role in non-shivering thermogenesis has been well studied. However little was known about the presence of active brown fat depots in adult humans. It was a well-conceived notion that brown adipose tissue is rapidly lost postnatally, within the first (few) years of life, and that older adults do not possess more than vestigial amounts of brown adipose tissue (10).

The recent discovery with the use of fluorodeoxyglucose positron emission tomography (FDG PET) suggested that adult humans possess active brown fat depots (10) has sparked a renewed interest in using brown fat thermogenesis as a treatment for obesity.

Table 1.1: Differences between WAT and BAT (adapted from (11))

	WAT	**BAT**
Function	Energy storage in form of fatty acids, triglycerides, secretion of adipokines	Heat production, thermogenesis, low fat storage capacity
Location	Subcutaneous, abdominal, perirenal, gonadal	Intrascapular, paravertebral, axillary and perineal
Macroscopic Features	Sympathetic and parasympathetic innervation, small lobules of densely packed cells	Sympathetic innervation, Lobular organization with gland-like structure
Microscopic Features	One single large droplet, few, small elongated mitochondria	Multilocular, small lipid droplets, abundant, large, round mitochondria

1.1.1: Development of brown fat

Brown adipose tissue (BAT), a unique organ to mammals, is developed in the later stages of embryonic development (12). Its major function is dissipation of energy as heat, for defense against cold (12, 13). Brown fat, is developed from the Myf5+ lineage of mesenchymal stem cells (14), Myf5 is one of the earliest myogenic factors to be expressed and determines the myogenic lineage (15). Brown fat, hence, is a close relative of skeletal muscle than white adipose tissue (WAT). Functionally, WAT and BAT carry entirely different functions, the major function of WAT being storage of energy whereas of BAT being dissipation of energy as heat. Although, WAT and BAT share some common adipogenic factors in development, BAT development occurs early in embryogenesis, whereas it is not until after birth that WAT depots are developed (13). Let's take a quick look at some of the transcription factors important for BAT development.

a) C/EBP and PPARs

Peroxisome proliferator-activated receptors (PPAR) are ligand-activated transcription factors belonging to the nuclear receptor superfamily. The three known subtypes PPARα, PPARγ and PPARδ have different tissue distributions and play a key role as regulators of glucose and lipid homeostasis as well as in cell proliferation, differentiation and inflammatory responses (16). PPARγ plays a central role in differentiation of both brown and white adipocytes (17). The C/EBP (CCAAT/enhancer-binding proteins) family consists of 6 members- C/EBPα, C/EBPβ, C/EBPγ, C/EBPδ, C/EBPε and C/EBPζ (18). Of the C/EBP family, C/EBPα and C/EBPβ were identified as key transcription factors driving fat cell differentiation (18). C/EBPs function cooperatively

with PPARγ and promote a transcriptional cascade that promotes and maintains the stable differentiated state of adipocytes (19). Interestingly, ectopic expression of C/EBPβ in white fat cells has been shown to promote the expression of BAT selective genes (17).

b) PGC1α

PPARγ coactivator 1α (PGC1α) was identified from brown fat cells as a cold-inducible coactivator of PPARγ and other nuclear hormone receptors (20). PGC1α is an important regulator of mitochondrial biogenesis (21) and plays an important role in regulating the function of mitochondria-rich BAT. Ectopic expression of PGC1α in white adipocytes has been shown to induce the expression of UCP1 and promote differentiation toward the brown fat phenotype (22). Despite its importance in the thermogenic function of BAT, PGC1α still remains dispensable for differentiation of BAT.

c) PRDM16

PRD1-BF1-RIZ1-containing homologous domain containing protein 16 (PRDM16) was identified in a screen that involved determining the transcriptional factors selectively expressed in BAT (23). PRDM16 is highly enriched in BAT as compared to WAT and when ectopically expressed in white preadipocytes and fibroblasts, it can initiate complete brown fat differentiation. Expression of PRDM16 is not induced during cold exposure, suggesting that it is only acting as a brown fat determinant and not in its function. Interestingly, mutating the DNA binding residue in PRDM16 does not alter its ability to initiate brown fat differentiation nor its interaction with PGC1α, suggesting that PRDM16 acts in a transcriptional complex to regulate brown fat determination (23). Knockdown of PRDM16 in brown adipocytes induces the expression of skeletal muscle

specific genes like MCK, MyoD and Myogenin, suggesting that PRDM16 may also act as a Myf5+ lineage specific determinant (24).

1.1.2: Brown fat in Thermogenesis

Brown fat is mainly involved in maintaining the body temperature via nonshivering thermogenesis. Nonshivering thermogenesis is independent of shivering, which occurs in the skeletal muscle. Studies from the 1950s demonstrated that following norepinephrine injection, there was an increase in BAT thermogenesis. Recent studies have shown that cold induced adaptive thermogenesis is UCP1 dependent and requires activation of the sympathetic nervous system, of which norepinephrine is the primary signaling component (25). Cold induced responses can also be mimicked by injecting mice with norepinephrine. The hypothalamus motor neurons senses any changes in temperature and activates the sympathetic nervous system. Thermogenesis in BAT is activated by the nor-epinephrine released by the sympathetic nervous system, mainly by activation of the β_3 adrenergic receptors. This leads to an increase in intracellular cAMP concentration, downstream of the G-protein coupled β_3 adrenergic receptors and thus activation of PKA, which triggers lipolysis. Increased lipolysis lead to an increased cellular concentration of free fatty acids which are transported to mitochondria, leading to the activation of mitochondrial electron transport chain and the mitochondrial uncoupling protein UCP1 (26).

The mitochondrial electron transport chain (ETC) consists of a series of four complexes (Complex I-IV) and electron carriers (coenzyme Q,cytochrome c). The flow of electrons via these complexes pumps protons across the inner mitochondrial membrane, thus

generating a proton gradient across the inner mitochondrial membrane. The proton gradient then drives the synthesis of ATP as protons flow passively back into the mitochondrial matrix through a pore that is associated with ATP synthase (or complex V) to generate ATP from ADP and Pi.

The uncoupling proteins (UCPs) belong to a class of mitochondrial transporter proteins, spanning across the inner mitochondrial membrane. Similar to other mitochondrial proton channels like Adenine nucleotide transporter (ANT), UCP1 increases the permeability of the inner mitochondrial membrane, allowing the passage of protons against the gradient back into the mitochondrial matrix. This releases the stored potential energy and is lost as heat, rather than being converted into chemical energy in form of ATP by mitochondrial ATP synthase. UCP1 is primarily expressed in the brown fat, whereas UCP2 exhibits a global tissue distribution. UCP3 is restricted to the skeletal muscle. Besides UCP1, the role of other UCPs in uncoupling mitochondrial ETC from oxidative phosphorylation is not well characterized (27). BAT heavily relies on the mitochondrial uncouplers for generation of heat.

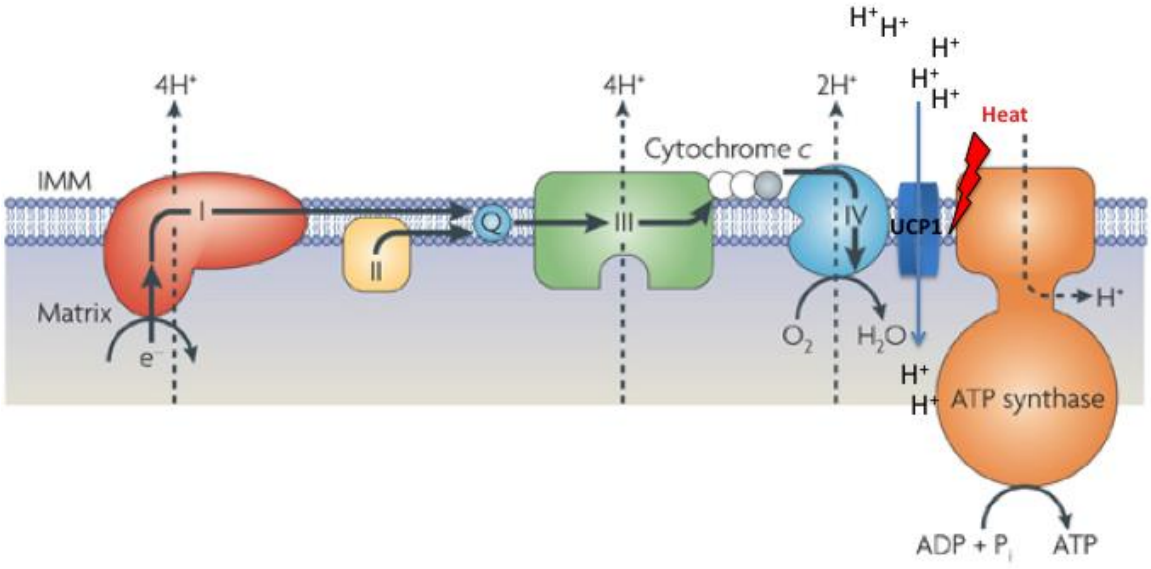

Figure 1.1: UCP1 along with mitochondrial electron transport chain: Mitochondrial oxidative phosphorylation begins with the entry of electrons into the ETC, which is impermeable to low-molecular-weight solutes. Electrons flow through the four membrane bound complexes (Complex I-IV) with the aid of the electron carriers. The transfer of the electrons generates a membrane potential ($\Delta\Psi_m$) across the inner mitochondrial membrane. UCP1 dissipates this proton gradient, thus releasing the potential energy as heat. (Modified from (28)).

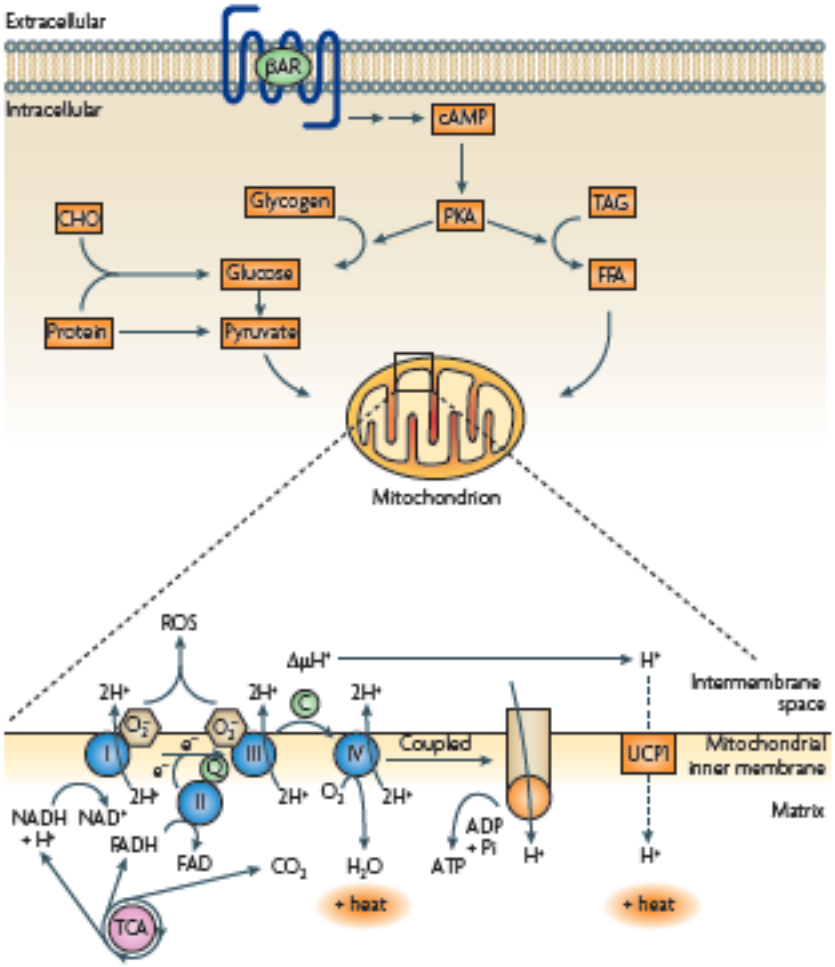

Figure 1.2: Norepinephrine mediated activation of non-shivering thermogenesis in brown fat. Thermogenesis occurs in brown adipocytes with the stimulation of β-adrenergic receptors (βARs), initiating a signal transduction cascade that produces cyclic AMP (cAMP) and activates protein kinase A (PKA), which then activates multiple enzymes responsible for converting the catabolic end products of macronutrients (carbohydrates, fats (triacylglycerols (TAG) and free fatty acids (FFA)) and proteins) into mitochondrial fuel. The electrons generated by the TCA cycle feed into the electron transport chain, generating a proton gradient, which is dissipated by UCP1 and heat is generated in this process (5).

1.2: Skeletal Muscle in obesity

Skeletal muscle is an important metabolic tissue in mammals. In humans, SKM comprises roughly 30-50% of the body mass and handles almost 80-95% of insulin mediated glucose uptake (29). Impaired glucose uptake and decreased oxidative capacity of skeletal muscle is one of the major contributors toward the pathophysiology of obesity and metabolic syndrome. Skeletal-muscle is also a non-adipose site for lipid accumulation (29) and plays an important role in fatty acid oxidation thereby controlling circulating lipid levels (30). Obesity and metabolic syndrome are correlated with the level of physical activity as well as the accumulation of intramyocellular lipids and fatty acid oxidation in SKM (30). Skeletal muscles are also specialized to dissipate energy directly as heat (figure 1.4) in response to external stimuli and hence important in energy expenditure (5). These studies suggest that a defect in SKM plays a significant role in the pathogenesis of obesity and metabolic syndrome.

1.2.1: Structure of Skeletal Muscle

Skeletal muscle, along with heart, is an important contractile tissue in mammals. The smallest contractile unit of skeletal muscle is termed as a sarcomere. A sarcomere consists of an assembly of thick filaments (myosin heavy and light chains) and thin filaments (actin) inserted between two z-discs and an M line running through the center (Figure 1.3). A complex of Troponins (Troponin T, Troponin I and Troponin C) and Tropomyosins sit on the thin filaments (31, 32).

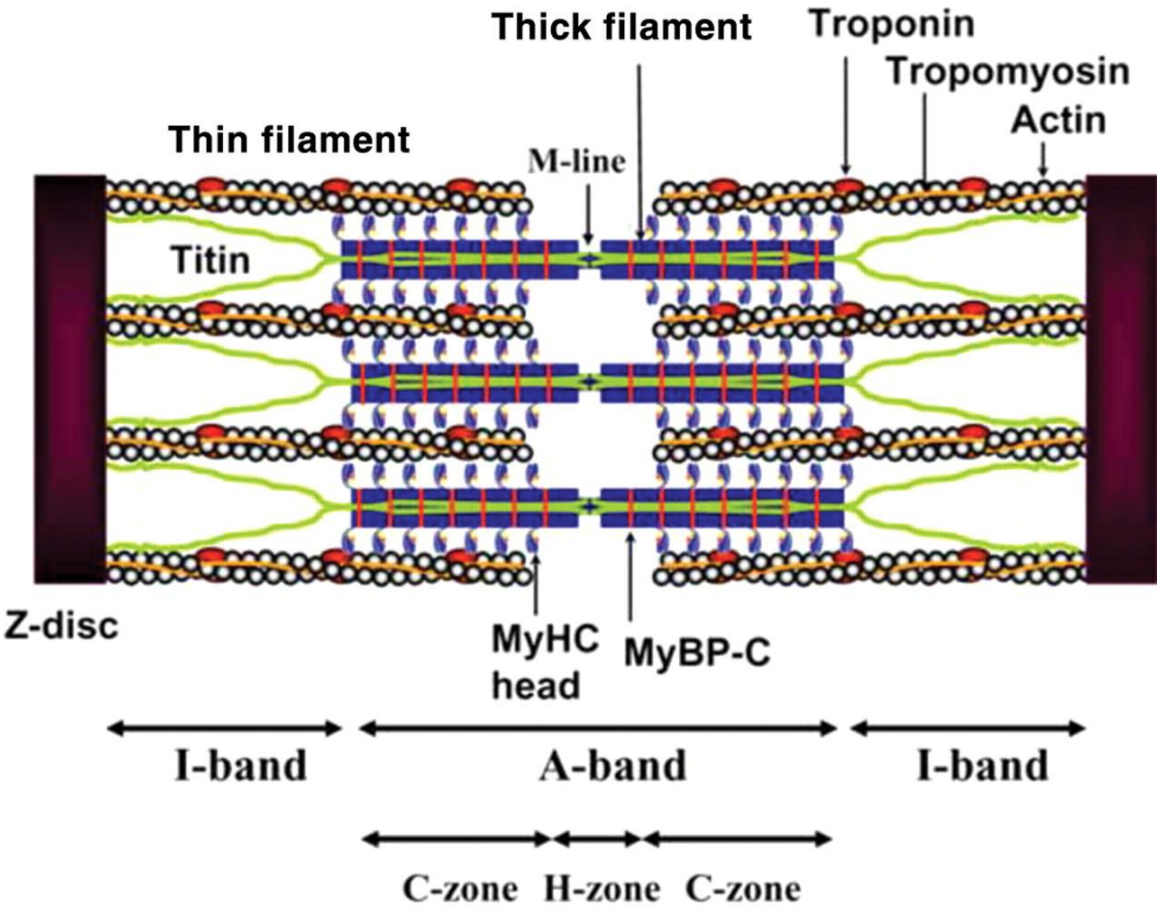

Figure 1.3: Structure of skeletal muscle: Sarcomeric assembly consists of a thick filament (composed of myosins) and a thin filament (composed of actin units) arranged between two Z-discs and an M line running through the center. Troponins and tropomyosines are arranged on the thin filament (31).

Muscle contraction is initiated by an incoming action potential from the nerve endings, transmitted via the acetylcholine receptors at the neuromuscular junction, which in turn triggers the calcium release from the sarcoplasmic reticulum via the Ryanodyne receptors (RyR) (5). The increase in cytosolic calcium concentration triggers calcium binding to the Troponins, which changes their confirmation, providing a binding site for the myosins. This leads to ATP hydrolysis by the myosins and a change in crossbridge linking between actin and myosin, thus initiating muscle contraction (33). Sarcoplasmic Reticulum Calcium ATPase (SERCA) pumps back the calcium in the sarcoplasmic reticulum to cease the contraction.

The ability of skeletal muscle to generate force depends on the type of Myosin heavy chain (MHC) present within the myofiber. Based on the MHC present, skeletal muscle fibers can be classified into four fiber types: TypeI, Type IIa, Type IIb and Type IIx. Differences between the fiber types are listed in Table 1.2. Type I fibers are the slow twitch fibers, which are oxidative in nature owing to their high mitochondrial content. They are important for endurance. Type II fibers are fast twitch fibers, IIa being moderately fast and IIb and IIx being extremely fast, rely on anaerobic glycolysis for energy, which makes them more prone to fatigue than Type I fibers (22). Interestingly, it has been observed that obese individuals and type II diabetics have an increased proportion of Type II fibers (29).

An important determinant of the skeletal muscle fiber types is PGC1α. PGC1α was shown to be preferentially expressed in Type I fibers (34)and also shown to induce mitochondrial biogenesis in skeletal muscle cells (35). Expression of PGC1α in Type II

fibers in transgenic mice lead to their conversion to the mitochondria rich, type I fibers (34) is the principal fiber type determinant.

Table1.2: Fiber types in skeletal muscle

	Type I fibers	**Type IIa fibers**	**Type IIx fibers**	**Type IIb fibers**
Contraction time	Slow	Moderateley fast	Fast	Fast
Resistance to fatigue	High	Fairly high	Moderate	Low
Activity used for	Aerobic	Long term anaerobic	Short term anaerobic	Short term anaerobic
Maximum duration of use	Hours	<30 mins	<5 mins	<1 min
Power produced	Low	Medium	High	Very high
Mitochondrial density	Very high	High	Medium	Low
Oxidative Capacity	High	High	Moderate	Low
Major Storage fuel	Triglycerides	Creatine phosphate, glycogen	ATP, creatine phosphate, glycogen	ATP creatine phosphate

1.2.2: Thermogenesis in Skeletal Muscle

Skeletal muscle, apart from brown fat, is an important organ for thermogenesis. Three types of thermogenesis occur in skeletal muscle- exercise induced thermogenesis, non-exercise induced thermogenesis and cold induced shivering thermogenesis (5). Exercise induced thermogenesis is a well studied mechanism of decreasing body fat. Non-exercise induced thermogenesis includes maintenance of general posture and other activities of daily life. The most well known mechanism of defending the body temperature in response to cold is shivering thermogenesis. Shivering is primarily a function of skeletal muscle and is the body's first response to cold. Shivering is known to increase oxygen consumption by up to 5 times the basal metabolic rate (BMR) and hence a very effective means of energy expenditure (36). A slight drop in core body temperature activates the primary motor nerve center in the hypothalamus and triggers the signal for skeletal muscle contraction. As the muscle contraction does not translate into work, the energy is released as heat. During cold exposure (4-8^{o}C), shivering initially sets in, (it can take place for days during longer periods of cold exposure), until it is replaced by non-shivering thermogenesis (NST), which is a primary function of brown fat. NST is also beneficial because it prevents from any tissue damage to the skeletal muscle because of excessive use. Recent studies have also shown that skeletal muscle can contribute to NST (37). Skeletal muscle possesses sarcolipin, which uncouples SERCA pump from the Ca^{2+} releasing Ryanodyne receptors and causes futile Ca^{2+} cycling, which leads to generation of heat. This effect was also observed in UCP1 deleted, brown fat ablated mice, suggesting that skeletal muscle is also capable of NST. A potential mechanism for skeletal muscle NST could be through mitochondrial

uncoupling, as occurs in BAT. Although skeletal muscle possesses UCP3, a homologue of UCP1, its role in mitochondrial uncoupling is highly debated (38). No specific uncoupling proteins like UCP1 have yet been identified in the skeletal muscle.

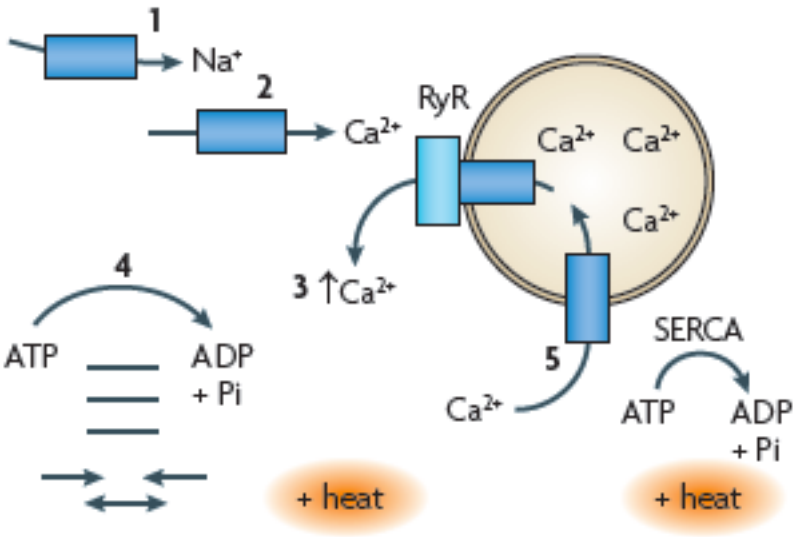

Figure 1.4: Shivering thermogenesis in Muscle. Neurotransmitter-mediated opening of cell-surface Na^+ channels (1) leads to release of Ca^{2+}into the cytoplasm from sources both outside the cell (2) and the sarcoplasmic reticulum (3) via the ryanodine receptor (RyR). Ca^{2+} release results in heat generation by ATP hydrolysis (4) during both muscle relaxation and actin–myosin crossbridge cycling during sustained contraction. Additional heat energy is released when Ca^{2+} ions are pumped back into the sarcoplasmic reticulum by the sarcoplasmic reticulum Ca^{2+} ATPases (SERCAs) (5) (5).

1.3: Brown fat and Skeletal Muscle- Two peas in a pod?

Given the common adipogenic features of both tissues, white fat and brown fat were though to share a common developmental lineage. However, recent studies have highlighted the fact that brown adipocytes carry a myogenic signature and are derived from Myf5+ progenitors that give rise to the muscle cells (24). Although little was known about the developmental origins of brown fat at this time, there were some studies that suggested the finding that brown fat shares a developmental origin with skeletal muscle. Hasty *et al* showed that myogenin mutant mice have defects in forming skeletal muscle, but showed increased brown fat bundles in cervical and interscapular regions (39). This finding was confirmed by Kablar *et al* almost 10 years after Hasty *et a*l reported their findings, that mice deficient in the myogenic transcription factors Myf5/Myod, have defects in muscle formation, but they show an increased expression of adipose tissue in place of muscle bundles (40). They however did not distinguish whether the excess adipose tissue was white or brown. Lineage tracing experiments by Atit *et al* suggested that some populations of brown fat, skeletal muscle and dermis all arise from Engrailed1 (En1) expressing population of the dermamyotome cells, which depends on the Wnt signaling pathway (41). Microarray experiments from the Swedish group Cannon and Nedergaard (42) again confirmed the myogenic signature of the brown fat. Another set of independent studies identified PRDM16 as the 'master regulator' that controlled the brown fat to skeletal muscle cell fate of the Myf5+ cells (24). Interestingly, when PRDM16 was knocked out, the Myf5+ cells assumed a myogenic fate, suggesting that PRDM16 plays an inhibitory role on differentiation of Myf5+ cells into skeletal muscle. Given the common features of brown fat and skeletal muscle (abundance of

mitochondria, regulation of energy expenditure and thermogenesis), these two tissues make an attractive target for the treatment of obesity.

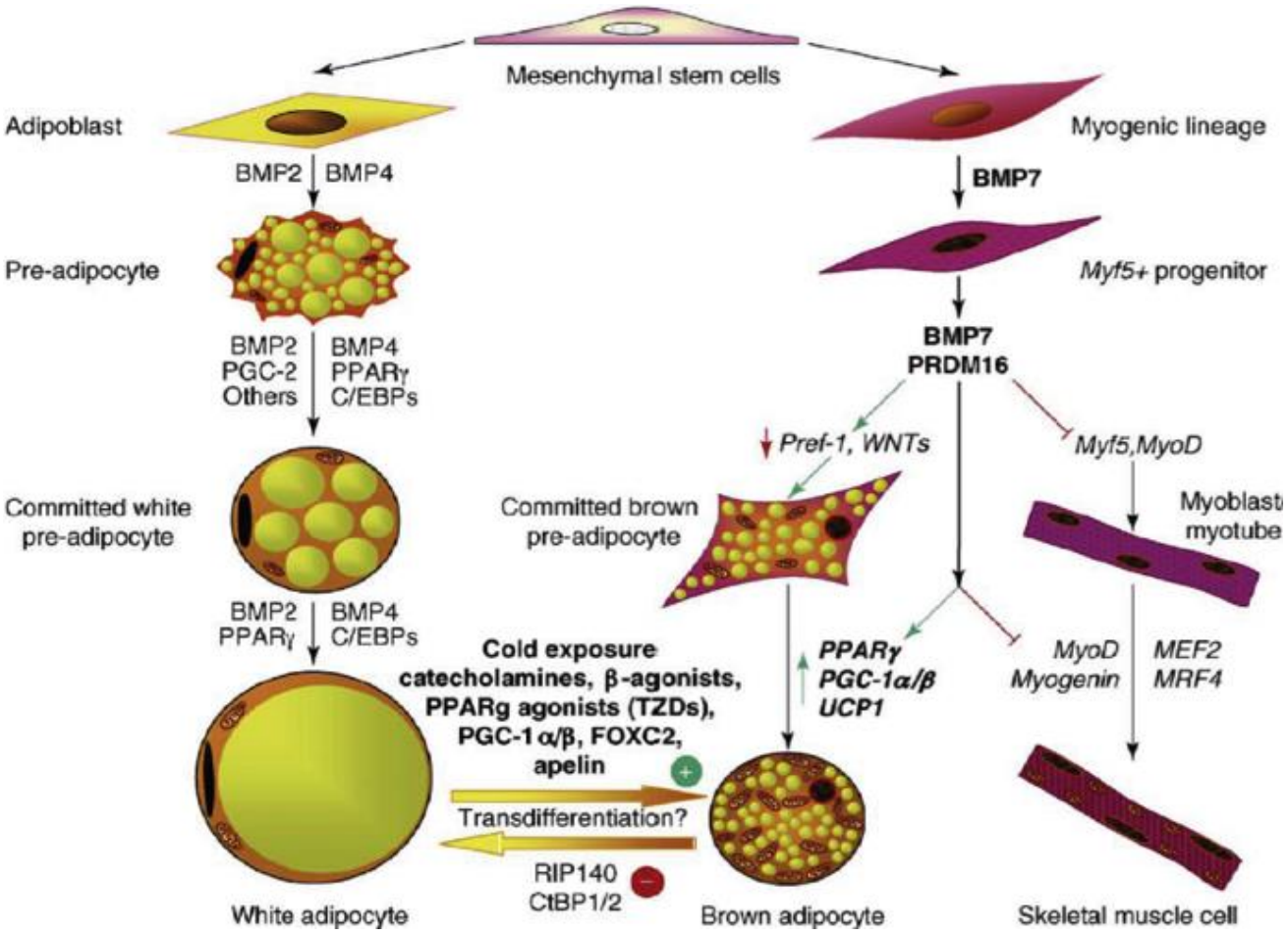

Figure 1.5: Brown fat and skeletal muscle share a common developmental origin.

(11)**.**

1.4: Mitochondria in obesity and metabolic syndrome

Mitochondria are important organelles in eukaryotes involved in the production of chemical energy in form of ATP from oxidation of nutrients consumed. Mitochondria have an inner and outer membrane, intermembrane space and a matrix. The inner membrane is highly invaginated, forming numerous cristae. Breakdown of glucose by glycolysis and tri-carboxylic acid cycle and oxidation of fatty acids generates substrates (NADH and $FADH_2$) that feed in to the electron transport chain (ETC) located in the inner mitochondrial membrane (43). As mentioned in section 1.1.2, flow of electrons across the ETC generates a proton gradient, which is harnessed by the ATP synthase to generate ATP by phosphorylation of ADP.

Mitochondria play an important role in metabolic regulation and hence affect the whole body energy homeostasis. Dysfunction of mitochondria can affect energy expenditure and hence lead to the development of obesity (43). Studies on insulin resistant individuals have highlighted the role of mitochondrial dysfunction- including decreased number of mitochondria, decreased expression of the subunits of the electron transport chain and also smaller mitochondria in skeletal muscle (30, 44). The mitochondria not only show decreased respiration capacity, but also defective cristae formation and overall structure. Interestingly expression of PGC1α, which is known to regulate mitochondrial biogenesis, is downregulated in patients with Type II diabetes, suggesting a co-relation between mitochondria number and development of insulin resistance (22).

Mitochondria are important for skeletal muscle function, which handles almost 80% of insulin mediated glucose uptake and also for production of adequate amounts of ATP required for skeletal muscle contraction. Dysregulation of mitochondrial function in

skeletal muscle affects their ability to generate enough ATP, thereby decreasing the necessary force production required for muscle contraction. This affects the overall muscle function (43), leading to impaired substrate utilization (glucose and fatty acids), which can lead to the development of obesity and metabolic syndrome (45).

Mitochondria also possess uncoupling proteins (UCP1, UCP2, UCP3) (46)in their inner mitochondrial membranes. UCP1 is primarily present in brown fat whereas UCP2 shows a more global distribution. UCP3 is present mainly in the skeletal muscle. So far, only UCP1 is considered to be a true ‘uncoupling’ protein. UCP1 dissipates the ETC proton gradient as heat, thereby increasing energy expenditure. Brown adipose tissue is also extremely rich in mitochondria and any functional defects in mitochondria translate into decreased energy expenditure and thermogenesis, which can ultimately result in development of obesity (43).

1.5: The JAK-STAT pathway

Discovered in the early 1990s while studying the actions of Interferon on cells, the JAK-STAT pathway is still being unraveled after twenty years. The JAKs (Janus kinases/ Just Another Kinases) and STATs (Signal Transducers and Activators of Transcription) are a part of the signal transduction scheme acting downstream of the Interferon (IFN) and cytokine receptors and are important for initial innate immune responses. The JAK-STAT pathway is also involved in regulating a multitude of cellular processes including cell growth, differentiation and immune responses (47).

The cytokine receptors are comprised of a single transmembrane domain and an extracellular domain that promotes ligand binding (48). Binding of a ligand causes receptor homo or hetero dimerization or multimerization, depending on the ligand. The receptors themselves lack any kinase activity, but receptor associated JAKs are brought in close proximity and they auto and trans phosphorylate each other, leading to their activation. Activated JAKs phosphorylate specific phosphotyrosine residues on the receptor, which provides a binding site for the SH2 domain possessing STATs. The STATs are also phosphorylated by JAKs, which releases them from the receptors, allows them to dimerize, translocate to the nucleus and activate transcription of respective genes (47, 49-51).

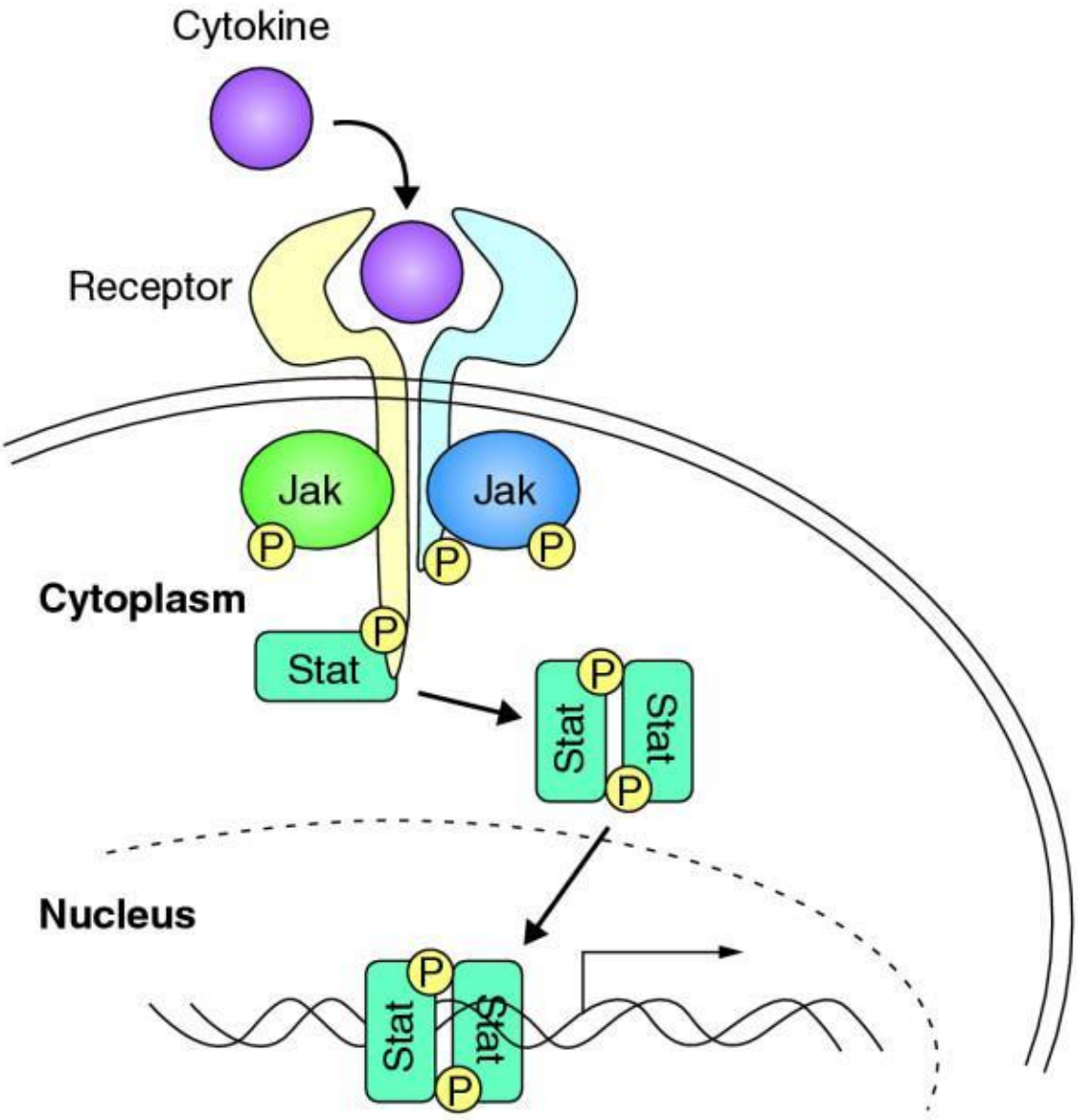

Figure 1.6: The classical JAK-STAT pathway (Adapted from (50)**)**

1.5.1: JAK family of tyrosine kinases

Mammals have four JAKs- JAK1, JAK2, JAK3 and Tyk2 and seven STATs (STAT1-4, STAT5A, 5B and 6). JAK1, JAK2 and Tyk2 are ubiquitously expressed, whereas JAK3 expression is restricted to the hematopoietic lineage (48, 50). JAKs are 120-140kd proteins and share a common structure. The N-terminus of JAKs contains a Band 4.1 ezrin, radixin and moesin (FERM) domain (JH6-JH7) and an SH2-like domain (JH3-JH4). The FERM domain of JAKs is implicated in mediating interaction with the cytokine receptors. At the C-terminus, JAKs possess a kinase like (pseudokinase) domain (JH2) and a kinase domain (JH1). The kinase like domain does not possess an ATP binding catalytic site, however it is important for complete kinase activity of JAKs (48)The phenotypes of JAK knockout mice are listed in Table 1.3. Apart from STATS, JAKs are known to have other targets including SOCS proteins, IRS1/2, Grb2 and c-abl, (48).

JAKs are found on the plasma membrane, associated with their receptors; however recent studies have provided a completely new perspective on JAK localization and function. JAK2 has been shown to be present in the nucleus of numerous cell types including hematopoietic cells, where it was shown to directly phosphorylate Y41 on histone H3 (52). JAK1, along with JAK2 was also found to be constitutively present in the nucleus of CHO cells (53). Interestingly, JAKs also affect transcription of genes which are not STAT dependent. Tyk2 also shows constitutive localization in the nucleus of human fibrosarcoma cells (54). Tyk2, along with the receptor complex, was also shown to bind the promoters of IFN inducible genes following interferon treatment of cells (55). The FERM domain contains an arginine rich region, which is thought to be the putative nuclear localization sequence (NLS) for JAKs (54).

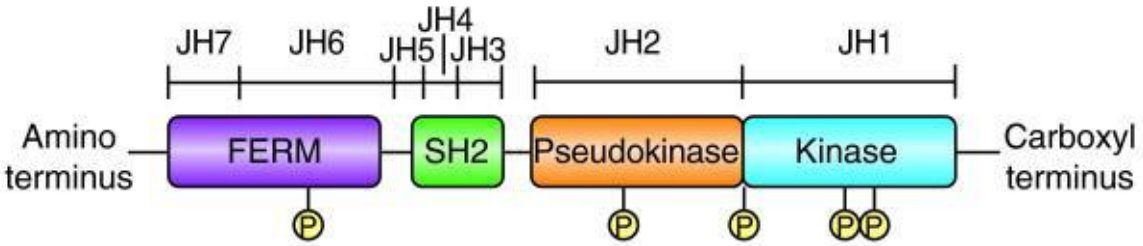

Figure 1.7: Schematic structure of JAKs (Adapted from (50)**)**

Table 1.3: Phenotypes of JAK knockout mice (Adapted from (50)**)**.

Gene	Phenotype of mouse knockout	Cytokines whose signaling requires this Jak
Jak1	Viable but early postnatal lethal owing to neurological deficits; SCID	Families of receptor with the shared subunits γc or gp130; IFNs
Jak2	Embryonic lethal owing to a defect of erythropoiesis	IL-3; family of receptors with the shared subunit gp130; IFN-γ hormone-like cytokines (EPO, GH, PRL, TPO)
Jak3	SCID, viable and fertile	Family of receptor with the shared subunit γc
Tyk2	Viable and fertile; susceptible to parasite infection; resistant to LPS; resistant to collagen-induced arthritis	IL-12; LPS

1.5.2: Tyk2 - structure, function and what we already know.

Tyk2 was the first of the JAKs to be discovered (56), and was found to play an important role in IFNα/β signaling (57). Most of the early studies on Tyk2 were carried out in Tyk2 null human fibrosarcoma cells (58). Tyk2 requires the presence of both kinase like domain and kinase domain for full catalytic activity (59). Point mutations in the kinase like domain also lead to impaired kinase activity of Tyk2 (60). Tyk2 has two Tyrosines in the kinase domain (Y1051/1052 in mice), phosphorylation of both is important for complete ligand dependent activation of Tyk2, however mutation of the YYs does not impair the kinase activity of Tyk2 (61). Interestingly, mutation of catalytic lysine K930 in the ATP binding pocket of Tyk2 renders it kinase inactive, and is not phosphorylated basally, however it is still capable of being phosphorylated upon IFN treatment (61). While deletion of the N-terminus of Tyk2 has no direct effect on its catalytic activity, it is indispensible for stabilizing interaction of Tyk2 with its receptors (62).

Tyk2 knockout mice were generated by three independent groups- Shimoda *et al* replaced the first coding exon with a neo resistant gene cassette (63), Karshigoff *et al* disrupted exons 3-9 (64) and Sheehan *et al* deleted the 5”UTR and the first coding ATG (65). A naturally occurring mutant mouse of Tyk2 was also reported (66), containing a single point mutation in the pseudokinase domain. Tyk2 knockout mice are viable and fertile. Interestingly, as opposed to what was observed in the in-vitro model, Tyk2 knockout mice were found to be dispensable for their role in IFNα/β signaling (63, 64). Tyk2 however plays an important role in protection from bacterial, protozoan and viral infections by activating IL12 mediated IFNγ production in NK and T cells (67). Tyk2 also plays an important role in allergic inflammations by regulating the downregulation of Th2

mediated antibody production and recruitment of eosinophils in the airways (68). Interestingly, Tyk2 knockout mice are Th2 skewed and also show increased IgE production (68). Tyk2 deficient pro-B cells were shown to have a decreased mitochondrial respiration capacity (69). Recent studies from our lab have highlighted a novel role of Tyk2 in obesity. It was found that Tyk2 deficient mice become obese with age (70) and develop the classical hallmarks of metabolic syndrome (Insulin resistance, glucose intolerance). These mice do not have an increased energy intake, however they clearly have a deficiency in energy expenditure. Brown fat, a key thermogenic tissue, was developmentally and functionally defective in Tyk2 knockout mice. These mice also cannot survive in the cold past 12 hours, whereas a wild type a mouse can survive in cold i.e $4^{o}C$ for up to weeks/months. This suggests that in the absence of Tyk2, there is both, an impaired shivering response mediated by skeletal muscle and non-shivering thermogenesis mainly mediated by the brown fat. Interestingly, Tyk2 knockout mice also show exercise intolerance (69) when exercised on a treadmill, suggesting that they may have defects in their skeletal muscle function.

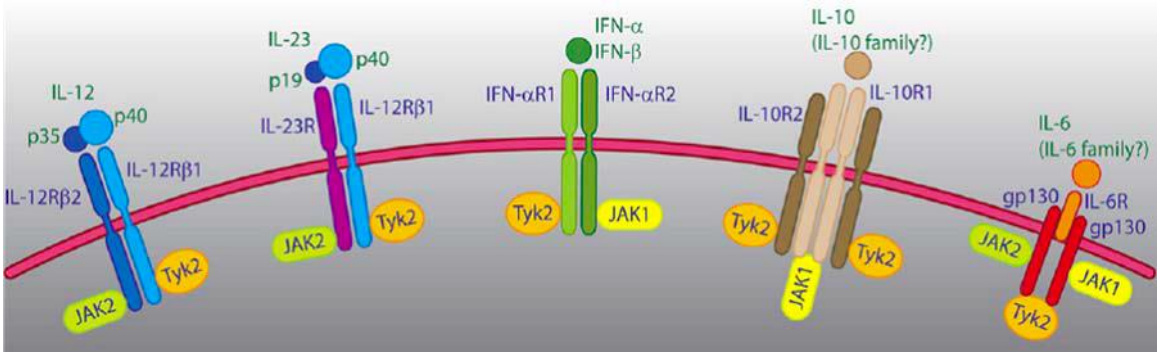

Figure 1.8: Tyk2 and its various activator cytokines (71)**.** Tyk2 is usually found in combination with other JAKs (JAk1 and JAK2) at the cytokine (IL and IFN) receptors.

Two cases of Tyk2 deficiency in humans have been reported to date (72, 73). Minegashi *et al* reported a 22 year old Japanese patient that displayed a Hyper-IgE like syndrome. Similarly, Kilic *et al* reported an 8 year old Turkish patient that exhibited a trend for elevated serum IgE levels, but not as significantly elevated as the Japanese patient. Interestingly, both patients were susceptible to bacterial and viral infections. Diagnosis of Tyk2 deficiency reported in the Turkish patient is fairly recent and hence limited observations are reported till date, including deafness and a mental condition. Studies on Japanese patient are consistent with the observations reported in Tyk2 mice, including restricted response to IFNα/β, increased proportion of Th2 cells and decreased IFNAR1 expression.

Given the skewed physiology observed in Tyk2 deficient mice and also human subjects, more detailed studies on Tyk2 will help consolidate the role it plays and its targets in the various physiological functions, which will help develop novel strategies to overcome those deficiencies.

The following studies presented in this thesis highlight the role of Tyk2 in the lineage specific determination of brown fat and skeletal muscle and also in their function.

Chapter II: Materials and Methods

2.1: Reagents and antibodies

All chemicals and reagents were purchased from Sigma-Aldrich or indicated otherwise. Antibodies were purchased from Cell Signaling (mouse monoclonal Stat3), Sigma-Aldrich (mouse monoclonal alpha-tubulin), Abcam (rabbit polyclonal UCP1, rabbit polyclonal PRDM16, mouse monoclonal CEBPβ, rabbit polyclonal PGC1α). Rabbit Tyk2 antisera was a kind gift of Dr. Birgit Strobl (University of Veterinary Medicine, Vienna, Austria). Mouse monoclonal antibodies, MHC2b (antibody developed by Stefano Schiaffino), myogenin (antibody developed Woodring Wright) and MyHC (antibody developed by Helen Blau) were obtained from the Developmental Studies Hybridoma Bank, developed under the auspices of the NICHD and maintained by University of Iowa, Department of Biology, Iowa City, IA-52242. MHC2a (goat polyclonal antibody) was a kind gift from Dr. Zhen Yan (University of Virginia, Charlottesville, VA).

2.2: Animals

All the mice were bred and maintained in the MCV/VCU animal facility according to Institutional Animal Care and Use Committee (IACUC) regulations. Male mice were used for these studies. Tyk2 deficient mice (C57BL/6) were kindly provided by Dr. Ana Gamero (Temple University School of Medicine, Philadelphia, USA). Mice carrying a transgene encoding the Wild Type (WT) or Kinase Dead (KD) form of Tyk2, including an upstream loxP- flanked stop sequence in the ubiquitously expressed Rosa26 locus were generated. These mice were crossed 5 generations to Tyk2-/- mice (on C57Bl6/J background) to eliminate interference from endogenous Tyk2 in the studies. Control

animals were obtained by crossing WT and KD transgenics with a wild type (Tyk2+/+) mouse (on C57Bl6/J background) for 5 generations. Mice (transgenic WT and KD on Tyk2-/- and Tyk2+/+ background) expressing the WT or KD form of Tyk2 in BAT (brown adipose tissue) and SKM (skeletal muscle) were obtained by crossing WT or KD transgenic animals with mice expressing the Cre recombinase under control of the Myf5 promoter, allowing Myf5 lineage-specific expression of Cre (24). SKM and Heart specific expression of WT or KD form of Tyk2 was obtained by crossing the transgenic mice with mice expressing Cre recombinase under control of MCK promotor (Muscle Creatine Kinase) (74). Animals from the same mixed background strain generation were compared. Mice were genotyped to confirm the expression of the transgene and the specific cre recombinase.

2.3: Genotypings

Mice were genotyped using a modified HotSHOT genomic DNA isolation protocol. Briefly, a tail snip was taken and incubated in 75µL of alkaline buffer (25mM NaOH, 0.2mM EDTA,pH 12.0) for 30minutes at 95°C. Samples were then cooled on ice and then 75µL of neutralization buffer (40mM Tris-HCl, pH2.0) was added. Samples were vortexed and then centrifuged at 16,000xg for 5 minutes at room temperature. Then 100µL of the reaction (approximately 100ng/µL) was removed and stored at -20°C until used for genotyping. To determine the genotype of the mice, the following PCR reactions were set up. For Rosa, 2µL DNA, 0.3µl of 10µM Rosa1, 0.3µl of 10µM Rosa2, 0.3µl of 10µM EGFP1 and 0.3µl of 10µM EGFP2 Primers,12.5µL 2x GoTaq Hot Start Green Master Mix (Promega, Madison, WI) and 5.3 µL dH_2O were added to a PCR tube. The following PCR cycles were used 1) 95°C for 4minutes, 2) 95°C for 30

seconds, 60°C for 30 seconds, 72°C for 45 seconds repeated 35 cycles 3) 72°C for 7 minutes. Myf5 cre PCR was set as follows- 2μL DNA, 1.5μl of 10μM Myf5F, 1.5μl of 10μM Myf5R, 1.5μl of 10μM Myf5 mutant Primers,12.5μL 2x GoTaq Hot Start Green Master Mix (Promega, Madison, WI) and 6 μL dH_2O. For Tyk2 genotyping, PCR was set as follows- 2μL DNA, 1.0μl of 10μM Tyk2F, 1.0μl of 10μM Tyk2R, 1.0μl of 10μM Primers,12.5μL 2x GoTaq Hot Start Green Master Mix (Promega, Madison, WI) and 8.5μL dH_2O. For Neo genotyping, PCR was set as follows- 2μL DNA, 1.0μl of 10μM Tyk2F, 1.0μl of 10μM Neo8, 1.0μl of Neo9 10μM Primers,12.5μL 2x GoTaq Hot Start Green Master Mix (Promega, Madison, WI) and 8.5μL dH_2O. The following PCR cycles were used for Myf5, Tyk2 and Neo: 1) 95°C for 3minutes, 2) 95°C for 30 seconds, 55°C for 30 seconds, 72°C for 30 seconds repeated 35 cycles 3) 73°C for 5 minutes. For MCK cre genotyping, PCR was set as follows- 2μL DNA, 1.0μl of 10μM MCK F, 1.0μl of 10μM MCK R, 1.0μl of 10μM Primers,12.5μL 2x GoTaq Hot Start Green Master Mix (Promega, Madison, WI) and 8.5μL dH_2O. The following PCR cycles were used 1) 95°C for 3 minutes, 2) 95°C for 30 seconds, 50°C for 30 seconds, 72°C for 45 seconds repeated 35 cycles 3) 72°C for 10 minutes. The PCR products were resolved on a 1% agarose/TBE gel with EtBr (ethidium bromide) to visualize the bands. Sequences of primers used for genotypings are listed in Table 2.1.

2.4: Cell Culture

Brown fat preadipocytes were isolated as previously described (75, 76). Interscapular brown adipose tissue was isolated from newborn Tyk2+/+, Tyk2-/-, Tyk2-/-+WT, Tyk2-/-+KD mice, minced and subjected to collagenase A digestion (1.5 mg/ml in isolation

buffer containing 123 mM NaCl, 5 mM KCl, 1.3 mM $CaCl_2$, 5 mM glucose, 100 mM HEPES and 4% BSA) for 40 min at 37^{o}C. The digested tissue was filtered through a 70μM filter. Collected cells were centrifuged at 1500 rpm at room temperature for 5 min and then resuspended in 1 ml of primary culture medium (Dulbecco's modified Eagle medium, 4500 mg/L glucose Gibco, Carlsbad, CA) containing 20% FBS, 20 mM HEPES and 1% penicillin-streptomycin), transferred into 12 well plates and grown in a humidified atmosphere of 5% CO_2 and 95% O_2 at 37°C. After 3 days of culture, cells were immortalized by infection with puromycin resistance retroviral vector pBabe encoding SV40 Large T antigen. 24 hrs after infection cells were split into 10 cm dishes and maintained in primary culture media for the next 24 hrs and then subjected to selection with puromycin at a concentration of 2 μg/ml in DMEM with 20% FBS for one week.

For differentiation, brown preadipocytes were grown to 100% confluence in the differentiation medium: DMEM containing 4500 mg/L glucose, 10% FBS, 20 nM insulin and 1 nM triiodothyronine. Fully confluent cells were incubated for 48 h in differentiation medium supplemented with Induction medium- 0.5 mM isobutylmethylxanthine (IBMX), 0.5μM dexamethasone and 0.125 mM indomethacin. After 48 hrs of induction, cells were maintained in differentiation medium for 5 days.

2.5: Constructs and viral transductions

293T cells, used as packaging cells, were grown in complete DMEM medium containing 10% FBS and 1% penicillin-streptomycin. Cells were transfected in 10 cm dishes using Fugene reagent, 5μg plasmid and 5μg of helper vector. (Roche Diagnostics, Indianapolis, IN) according to the manufacturer's instructions. Media was changed 24

hrs after transfection. The virus-containing medium was collected 48 hrs after transfection, centrifuged for 10 min at 500 x g and filtered through 0.45 µm filter. Viral supernatants were added to the cells for 24 hrs in the presence of Polybrene (8 µg/ml polybrene, Chemicon Int., Temecula,CA), then diluted twice with the fresh medium. The next day the viral supernatant was removed and replaced by fresh medium.

2.6: Mitochondrial preparation

Skeletal muscle mitochondria were prepared as described previously (77) with a few modifications. Briefly, muscles were minced finely with a blade, trimmed clean of visible fat and connective tissue, and placed in 4 ml of modified Chappell-Perry (CP) buffer (buffer CP1: 100 mM KCl, 50 mM 3-(N-morpholino) propanesulfonic acid (MOPS), 1 mM ethylene glycol-bis(2-aminoethylether)-N,N,N′,N′-tetraacetic acid (EGTA), 5 mM MgSO47H2O) supplemented with trypsin (8 mg per 2g of wet tissue). After 20 min incubation at 4°C on a rotator, the digestion was stopped by adding an equal volume of CP2 (CP1 supplemented with 5% defatted BSA). The tissue was homogenized using a motor-driven Teflon-glass Potter homogenizer (3x). The supernatant was transferred to a 50ml falcon tube and centrifuged at 1000 ×g for 5 min at 4°C. Mitochondria containing supernatant was transferred to fresh eppendorfs and spun at 7800xg for 10 mins at 4°C. Mito pellet was washed 3x with CP1 buffer. The final mitochondrial pellet after 3 washes was resuspended in CP1 buffer and protein concentration was measured using the Lowry method.

2.7: Blue Native-PAGE

Electrophoresis of mitochondrial proteins in native conditions was performed using NativePAGE Novex Bis-Tris Gel System (Invitrogen, Carlsbad,CA), according to the manufacturer's instructions with modifications. All chemicals purchased from Invitrogen or stated otherwise. Briefly, mitochondria were solubilized in cold 1x NativePAGE Sample Buffer containing DDM (*n*-dodecyl-β-D-maltoside) in the ratio of 1.6 g of detergent per 1 g mitochondrial protein or containing digitonin in the ratio of 6 g of detergent per 1 g protein. After 15 min of incubation on ice, the samples were centrifuged at 16,000 x g for 30 min at 4^{o}C and supernatants transferred to the new tubes. The protein concentration of the lysates was determined using Bio-Rad protein assay. Prior to the electrophoresis, 30 µg of the extract was combined with Coomassie blue G-250 dye (detergent/dye ratio of 8 g per 1 g). Blue Native-PAGE was run using 4 – 16% gradient Novex NativePAGE Bis-Tris gels and NativePAGE Running Buffer. The conditions of a run were as follows: low temperature (4^{o}C) run, 150 V constant for 60 min, then the voltage was increased to 250 V constant for the remainder of the run (about 60 min), upper (inner) chamber contained dark blue cathode buffer (NativePAGE running buffer mixed with 0.02% Coomassie blue G-250 dye) which was exchanged after the dye front reached 1/3rd of the gel into the light blue cathode buffer (0.002% G-250). After the run gels were subjected to Coomassie staining. For Coomassie protein staining, the native gels were first placed in 100 ml of Fix solution (40 % methanol, 10 % acetic acid) and microwaved on high 60 (950 – 1100 watts) for 45 seconds followed by 30 min of incubation on an orbital shaker at RT. This procedure was repeated once and gels were immersed in EZBlue Coomassie Brilliant Blue G-250 colloidal protein stain

(Sigma-Aldrich, Saint Louis, MO) and left on orbital shaker for overnight at RT. Next day, staining solution was decanted and gels were de-stained using ultrapure water until the desired background was obtained, and they were then scanned.

2.8: In Gel complex assays

Following BN-PAGE on mitochondria samples solubilized in 10% DDM, the gel was stained as follows for determining the activity of individual ETC complexes.

Complex I: Gel was incubated with 2mM Tris-HCl, pH 7.4, 0.1mg/mlNADH and 2.5mg/ml nitroblue tetrazolium at RT for 20 mins.

Complex II: Gel was incubated with 4.5mM EDTA, 10mM KCN, 0.2mM phenazine methosulfate, 84mM succinic acid and 50mM nitroblue tetrazolium in 1.5mM phosphate buffer, pH 7.4 at RT for 3 hrs.

Complex IV: Gel was incubated in 5mg diaminobenzidine dissolved in 9ml of 50mM sodium phosphate, pH 7.2, 1ml catalase (20mg/ml), 10mg cytochrome c and 750mg sucrose at RT for 3 hrs.

The color development for bands was preserved by fixing the gels in 50% methanol with 10% acetic acid for 15 mins. The fixed gels were stored in 10% acetic acid. The resulting bands were quantified by densitometry with the help of Image-J software.

2.9: Oxygen Consumption assay

Polarographic measurement of oxygen consumption by intact mitochondria was performed in a glass chamber equipped with Clark-type oxygen electrode (Strathkelvin Instruments, Glasgow, Scotland) as previously described (75). The measurements were done at 30^{o}C in 500 µl of a respiration buffer (80 mM KCl, 50 mM MOPS, 1 mM EGTA,

5 mM KH2PO4 and 1 mg/ml defatted BSA, at pH 7.4). For glutamate/malate-dependent respiration (complex I) 300 µg of mitochondrial protein was used. For succinate-dependent respiration (complex II), 200 µg of mitochondrial protein was used, and for TMPD (N,N,N′,N′-tetramethyl-p-phenylenediamine)/ascorbate (complex IV), 100 µg of protein was used. Next, the selected substrates for complex I (20 mM glutamate+5 mM malate), complex II (20 mM succinate with 7.5 µM rotenone), or complex IV (1 mM TMPD/20 mM L- ascorbate with 7.5 µM rotenone) of the respiratory chain were added to the chamber. State 3 respiration was initiated by the addition of 0.2 mM ADP (final concentration) followed by state 4 respiration. After state 4 was attained, 2 mM ADP was added to the chambers to measure maximum rate of state 3 respiration. Finally, 0.04 mM uncoupler DNP (2,4-dinitrophenol) was used to measure the uncoupled respiration rate. In case of TMPD/ascorbate, only maximum rate of state 3 (2 mM ADP) was measurable. At the end of that measurement, 2 mM azide was added to determine the specificity of complex IV-dependent oxygen consumption.

ADP-stimulated (state 3) and ADP-limited (state 4) respirations were defined and calculated according to the method of Chance and Williams (75).

2.10: Histology

Skeletal muscle was fixed in 10% formalin and were paraffin-embedded. Multiple sections were prepared and stained with hematoxylin and eosin (H&E) at the Pathology Research Service Facility (VCU Medical Center, Richmond, VA).

2.11: Electron microscopy

Skeletal muscle was fixed in 2% paraformaldehyde- 2% glutaraldehyde in 0.1 M cacodylate buffer. The tissue samples were processed and analyzed at the Microscopy Core Facility at the Department of Anatomy and Neurobiology (VCU Medical Center, Richmond, VA).

2.12: Oil red O staining

The Oil red O staining was used to test for lipid accumulation in fully differentiated cells. Plates with cells were rinsed once with PBS and then fixed with buffered formalin for 1 hr at room temperature. Fresh Oil red O working solution was prepared by adding 6 ml of the stock solution (0.5 g Oil red O in 100 ml of 2-propanol) to 4 ml of dH_2O, mixed and filtered through Whatman filter paper. Following fixation the cells were incubated for 1hr at room temperature with Oil red O stain. Then plates were carefully rinsed several times with dH_2O and air-dried before collecting images under the inverted microscope.

2.13: RNA extraction and real-time qPCR

Total RNA was isolated with TRI Reagent (Molecular Research, Cincinnati, OH), according to the manufacturer's instructions. Briefly tissues were harvested and minced finely and resuspended in 1ml TRI-reagent. Samples were incubated for 30 mins on a rotator-shaker at 4°C.Then 250μL cholorform was added to the Tri Reagent and the samples were vortexed for 30 seconds and spun down at 13,200 rpm for 10 minutes at 4°C. The aqueous phase was taken and 500μL of isopropanol was added. Samples were vortexed and then incubated at -20^{o}C for 30 minutes. RNA was pelleted at 13,200 rpm for 15 minutes at 4°C. The supernatant was removed and the RNA pellet was

washed with 75% ethanol. The samples were then centrifuged at 13,200 rpm for 10 minutes at 4°C. Supernatant was removed and RNA pellet was dried at 37°C. RNA was then re-suspended in the appropriate amount of DEPC H_2O depending pellet size and then incubated at 55°C for 10 minutes. Isolated RNAs were treated with DNase (Promega, Madison, WI) in a 1:10 ratio with DNase and Buffer and incubated at 37°C for 30 minutes. The treatment was stopped by using Stop Buffer (Promega, Madison, WI) in a 1:10 ratio and incubated at 65°C for 10 minutes. RNA concentration was measured using a nanodrop. cDNA was synthesized from 2 µg of RNA with the Tetro cDNA Synthesis Kit (Bioline, Taunton, MA). 2µg RNA, 1µL Random Hexamer Primer Mix, 1µL 10mM dNTPs mix were preheated at 95°C for 1 minute then cooled to 4°C. Then the 5x RT Buffer, 200U Reverse Transcriptase, 10U RNase Inhibitors, and DEPC H_2O was added to a final volume of 20µL. The PCR was set as follows: 42°C for 50 minutes, 70°C for 15 minutes and then cooled to 4°C.

Real-time qPCR was performed using SensiMix SYBR and Fluorescein Kit (Bioline, Taunton, MA) according to manufacturer's instruction. . Briefly, the cDNA was diluted to 1:20 ratio and then 5µL of the cDNA was used as the template for the reaction. The reaction mixtures for internal controls were prepared as followed: 12.5µL of SYBER Green mix, 1µL 5µM forward primer, 1µL 5µM reverse primer, and 5.5µL of dH_2O. For any other gene the mixture reaction is as followed: 12.5µL of SYBER Green, 2.5µL 5µM forward primer, 2.5µL 5µM reverse primer, and 2.5µL dH_2O. All the samples were assayed in duplicates and analyzed using a CFX96 Real-Time PCR Detection System (Bio-Rad, Hercules, CA). Table 2.2 contains a full list of the primer sequences. Primers

for Jak1 and Jak2 were purchased from SuperArray (Qiagen SABioscience, Frederick, MD).

2.14: Protein Extraction

Cells were lysed in ice-cold extraction buffer (20 mM HEPES, 300 mM NaCl, 10 mM KCl, 1 mM $MgCl_2$**,** 20% glycerol, 1% Triton X-100) with added protease (COMPLETE-Roche) and phosphatase inhibitor cocktails (Roche, Indianapolis, IN) for 30 min at 4°C. For isolation of protein from tissues, tissues were harvested and minced finely with a blade and incubated with ice-cold extraction buffer for 30 mins on a rotator-shaker. After lysis, cell debris was removed from the lysates by centrifugation at 13,000 x g for 10 min at 4°C. The protein concentration in the supernatants was determined using a Bio-Rad protein assay (Bio-Rad, Hercules, CA).

2.15: Western blot analysis

Equal amounts of protein were mixed 1:1 with 2X Laemmli sample buffer containing 1 mM β-mercaptoethanol. Samples were incubated at 95°C for 5 mins and separated using SDS-PAGE electrophoresis (Running buffer: 25 mM Tris, 192 mM glycine, 0.1%SDS). The proteins were transferred to Immobilon-P polyvinyldifluoridine membrane (activated by methanol) and soaked in transfer buffer (70% methanol, Tris-Hcl) (Millipore, Billerica, MA) using a semi-dry transfer apparatus (Bio-Rad, Hercules, CA). Membranes were blocked for 1 h at room temperature with 5% non fat dry milk in TBS-T buffer (20nM Tris-HCl, pH 7.5, 500mM NaCl, and 0.05% Tween-20) and then incubated overnight at 4^oC with the indicated primary antibodies in 5%BSA in TBS-T. The blots were washed 3x in TBS-T. Secondary antibody was added (5% non fat dry

milk in TBS-T buffer) for 1h at room temp. Samples were washed 3x in TBS-T and then developed using ECL-Plus (Pierce Thermo Scientific, Rockford, IL).

2.16: Immunoprecipitation

250µg whole cell extracts were diluted with in an IP buffer pH 7.4 (150 mM NaCl, 50mM Tris-HCl, 1% Triton, 1 mM EDTA with added protease and phosphatase inhibitor cocktails (Roche, Indianapolis, IN) at 0.5µg/µl concentration. Samples were incubated overnight at 4°C with Tyk2 antibodies (1:100 dilution) and 20µl agarose beads or control IgG and agarose beads. Immunoprecipitates were washed five times with 1xPBS with protease and phosphatase inhibitor cocktails. Beads were resuspended in laemlli buffer with 1 mM β-mercaptoethanol. Samples were incubated at 95°C for 5 mins and beads were pelleted. The supernatant was separated by SDS-PAGE and blotted with indicated antibodies.

2.17: Chromatin Immunoprecipation (ChIP) assay

Tissues were isolated from mice, minced finely and resuspended in 20ml media supplemented with 750µl formaldehyde for crosslinking. The samples were incubated on a shaker 37°C for 20 minutes. To stop crosslinking, 125mM glycine was added and samples were incubated on a shaker at RT for another 10 mins. The samples were then spun down at 4°C, 450xg for 10 minutes. The supernatant was removed and pellet was resuspended in 5ml PBS (supplemented with protease inhibitors). The samples were then homogenised using a glass homogenizer till the homogenate was clear. This homogenate was filtered using a 70µM cel strainer to get a single cell suspension. Homogenate was aliquoted into eppendorf tubes and frozen at -80°C. Samples were

then thawed and spun at 4°C , 7000rpm for 5 minutes. The pellet was resuspended in 1ml of lysis buffer (1%SDS, 10mM EDTA pH8.0, 50mM Tris-HCl, pH 8.0) and sonicated 10x 10 sec on-20 sec off cycle. The samples were then spun 4°C, 7000rpm for 10 minutes. Supernatant (chromatin) was pre-cleared as follows: 100µl supertanant+1ml IP buffer (0.01%SDS, 1.1% Triton X, 1.2mM EDTA, 16.7mM Tris-HCl, pH 8.0, 16.7mM NaCl) with inhibitors + 10µl ChIP beads (3x washed protein G sepharose beads resuspended in equal volume of ChIP buffer with 10µl 1mg/ml BSA/ 100µl beads and 5µl 10mg.ml red herring DNA/100µl beads) on rotator at 4°C for 30 minutes. Beads were pelleted to give a pre-cleared chromatin. 200µl was saved as input. IP was set as follows: 1ml pre-cleared chromatin + 5µl antibodies on rotator at 4°C overnight. The next day, 50µl ChIP beads were added and samples were incubated on a rotator at 4°C for 2hrs. Beads were spun down at 6000 rpm at 4°C for 1 min and were washed 2x (10mins rocking at 4°C followed by a spin at 6000 rpm for 1 min) with each of the following buffers: ChIP buffer I (0.1%SDS, 1% Triton X, 2mM EDTA, 20mM Tris-HCl, pH 8.0, 150mM Nacl), ChIP buffer II (0.1%SDS, 1% Triton X, 2mM EDTA, 20mM Tris-HCl, pH 8.0, 500mM Nacl), ChIP buffer III (0.25M LiCl, 1% NP.-40, 1% Sodium Deoxycholate, 1mM EDTA, 20mM Tris-HCl, pH 8.0) and ChIP buffer IV (10mM Tris-HCl, pH 8.0, 1mM EDTA). DNA was then eluted from the beads by adding 200µL ChIP elution buffer (1%SDS, 0.1M $NaHCO_3$) and rocking for 15 mins at RT. The beads were pelleted at 6000 rpm. The supernatant (and also input sample that was saved previously) was reverse cross-linked by adding 8µl 5M NaCl followed by o/n incubation at 65°C. 1ml PB was addded and samples were purified on miniprep colums. Final DNA

was eluted with 50µl buffer EB. This DNA was then used to set up qPCR for respective promoters.

For setting up ChIP from cells, 1% formaldehyde was added to the media for 10mins to fix cells. The cells were then washed with ice-cold PBS supplemented with 125mM Glycine and protease inhibitors. The cells were scraped off in 1ml of PBS, transferred to an eppendorf and pelleted at 6000 rpm, 4°C for 4 mins. The pellet was resuspended in 1ml ChIP lysis buffer and protocol was followed as described above.

2.18: Site-Directed Mutagenesis

Site-Directed mutagenesis was carried out according to manufactures instructions (Strategene). Briefly, a PCR reaction was set as follows-5 µl of 10× reaction buffer, X µl (50 ng) of dsDNA template, 1µl (125 ng) of oligonucleotide forward primer, 1 µl (125 ng) of oligonucleotide reverse primer, 1 µl of dNTP mix , 1 µl pfu turbo, ddH2O to a final volume of 50 µl. The PCR was set as follows: 1) 95°C for 30 sec 2) 95°C for 30 seconds, 55°C for 30 seconds, 68°C for 1min/kb of plasmid length, repeated 35 cycles 3) 72°C for 10 minutes. The PCR product was digested with Dpn1 at 37°C for 1 hr. 2 µl of the digested product was then transformed into XL-gold ultracompetent cells (On ice for 15 minutes, heat shock at 42°C for 50 sec, ice for 2 mins. Add 950 µl SOC medium and shake at 37°C for 1hr. 50 µl of transformed bacteria was plated onto an ampicillin selection plate and incubate o/n at 37°C). The resulting colonies were screened for the mutation.

2.19: Statistical analysis

Results are presented as the mean ± SE. Statistical comparison was performed using two-tailed Student's t-test. While interpreting the data results a p-value less than 0.05 was considered statistically significant and annotated by *.

Table 2.1: List of Primers for Genotyping

Primer	Sequence
Myf5 F	CGT AGA CGC CTG AAG AAG GTC AAC CA
Myf5 R	CAC ATT AGA AAA CCT GCC AAC ACC
Myf5 mutant	ACG AAG TTA GGT CCC TCG AC
Rosa1 F	CAA CGC CCA CAC ACC AGG TTA G
Rosa1 R	GCA CGT TTC CGA CTT GAG TTG CC
EGFP1 F	GCA AGC TGA CCC TGA AGT TCA TC
EGFP1 R	TCG TCC ATG CCG AGA GTG ATC C
MCK F	ATG TCC AAT TTA CTG ACC G
MCK R	CGC CGC ATA ACC AGT GAA AC
Tyk2 F	TGG ACA AAA TGG AGT GAG TGT AAG
Tyk2 R	CTG GGT CAT GGC TGG AAA AGC CCA
Neo8	GAT CGG CCA TTG AAC AAG ATG
Neo9	CGC CAA GTC CTT CAG CAA TAT

Table 2.2: List of Primers for qPCR

Primer	Sequence
UCP1	F: CTG GGC TTA ACG GGT CCT C R: CTGGGCTAGGTAGTGCCAGTG
PRDM16	F: CAGCACGGTGAAGCCATTC R: GCGTGCATCCGCTTGTG
Cidea	F: TGC TCT TCT GTA TCG CCC AGT R: GCC GTG TTA AGG AAT CTG CTG
MHCI	F: GCCAACTATGCTGGAGCTGATGCCC- R: GGTGCGTGGAGCGCAAGTTTGTCATAAG
MHC2a	F: GGCACAAACTGCTGAAGCAGAGGC R: GGTGCTCCTGAGGTTGGTCATCAGC
MHC2b	F: GAGCTACTGGATGCCAGTGAGCGC- R: CTGGACGATGTCTTCCATCTCTCC
MHC2x	F:GGCAGCAGCAGCTGCGGAAGCAGAGTCTGG R: GAGTGCTCCTCAGATTGGTCATTAGC

titin	F: GGA TGG AAA GGC TAT TGC AC R: CCT CGG TGT CTT CAG CT
Ryr1	F: GCCATCCTCAGACCCTAGC R: CACTGCAGGACCACTTCATC
Serca1	F: ACTGGGGTCAGAACTTCGTG R: CCAGGGGGTGATGTGTTTCT
TnnT1	F: CTTTGATTCCCCCGAAGATT R: CCTTTTTCCGCTGTTCAAAG
TnnT3	F: CGCTGAGAAGGAGCGGGAA R: GCCAGGTAGCTGCTGTAGT
TnnI1	F: AGCCCTCTTCACCTGTCTCA R: TTACGGGAGGCAGTGATCTT
TnnI2	F: GATCTCAGGATGGGAGATGAG R:TCTTTCTCCAGCTCTGTGGC
TnnC2	F: CACCTTTGGGTGGTGGAGT R: GCCTTGAACTCAGCGATCAT

Chapter III: Results

3.1: Tyk2-/- mice have normal skeletal muscle morphology

Our previous studies have shown that Tyk2-/- mice have defects in brown adipose tissue (BAT) formation (70). Since brown adipose tissue and skeletal muscle are derived from the same lineage of Myf5+ve mesenchymal stem cells (24), we wanted to investigate if SKM of Tyk2-/- mice have any structural defects. Gastrocnemius, plantarius and soleus muscle from 12 week old mice were isolated, fixed, sectioned and stained with Hematoxylin and Eosin. As seen in Figure 3.1, Tyk2-/- mice exhibit a normal skeletal muscle fiber formation and structure. This suggests that Tyk2 is not required for differentiation of skeletal muscle.

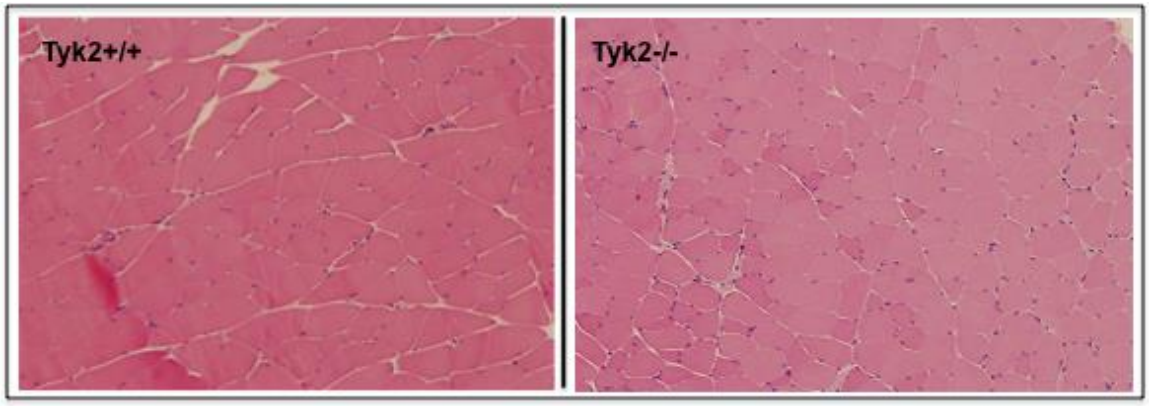

Figure 3.1: Tyk2-/- mice have a normal skeletal muscle morphology: Hematoxylin and Eosin staining of Gastrocnemius muscle of 12 week old Tyk2+/+ and Tyk2-/- mice.

3.2: Skeletal muscle of Tyk2-/- mice is not hypertrophied

NMR studies on Tyk2-/- mice indicated that 3 month old Tyk2-/- mice have increased lean mass as compared to Tyk2+/+ mice (Gornicka et al, unpublished). To determine whether the increased muscle mass is due to increased muscle hypertrophy or increased number of muscle fibers, we measured individual muscle fiber area using image-J software. As seen in Figure 3.2A, Tyk2-/- mice do not show an increase in fiber size nor do they have increased number of fibers in a muscle cross section. We also weighed individual Gastrocnemius, plantaris and soleus muscle from Tyk2+/+ and Tyk2-/- mice. As seen in Figure 3.2B, the gross weights of individual muscle types are not significantly changed. This suggests that the increase in muscle mass is not due to hypertrophied muscle, but an overall increase in the body muscle mass.

A

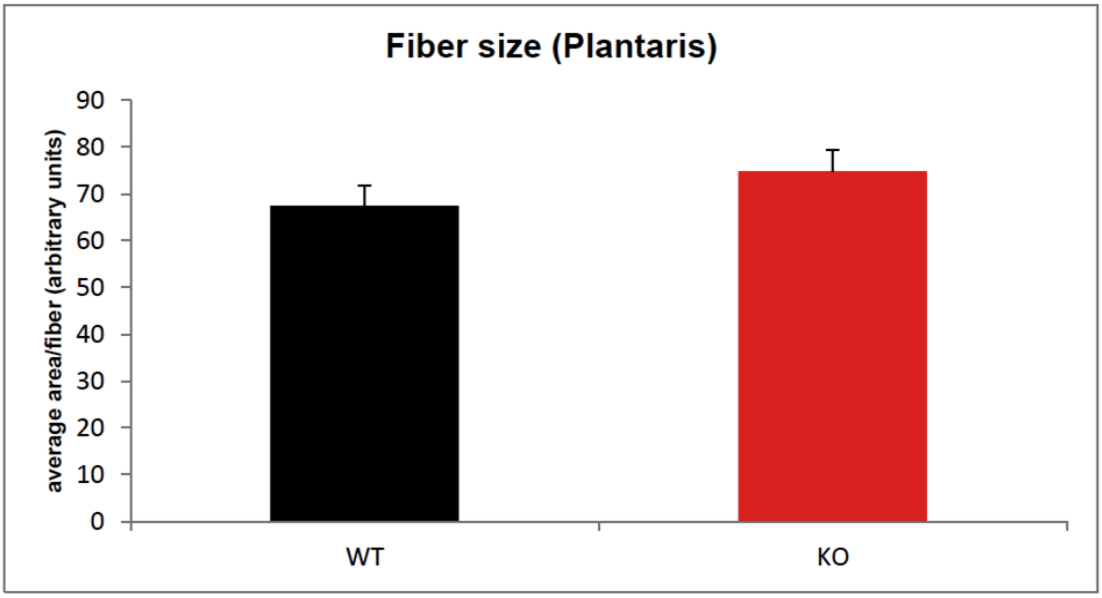

B

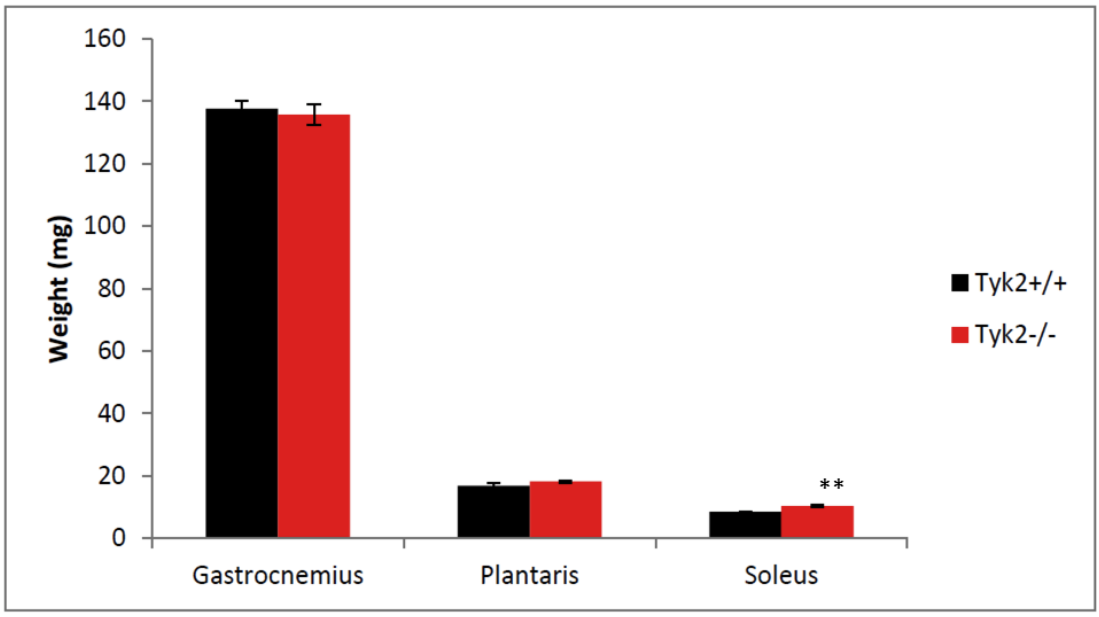

Figure 3.2: Skeletal muscle of Tyk2-/- mice is hot hypertrophied. A) Quantification of muscle fiber area of a muscle cross section from figure 3.1, using Image-J software (n= 6). B) Weights of individual muscle types isolated from 12-14 week old Tyk2+/+ and Tyk2-/- mice (n=6), **p<0.01. Data are expressed as mean ± SEM.

3.3: **Expression of muscle transcription factors is unaltered in SKM of Tyk2-/- mice**

Our previous studies indicate that BAT of Tyk2-/- mice show increased expression of skeletal muscle specific genes (70), most likely due to an imbalance in commitment of the Myf5+ progenitors towards skeletal muscle, mediated by PRDM 16 (24). Since Tyk2-/- mice also have increased muscle mass, we investigated whether there is also an imbalance in the expression level of muscle specific genes in the skeletal muscle of Tyk2-/- mice. As seen in figure 3.3, expression levels of the muscle transcription factors MyoD and myogenin, and the uncoupling protein, UCP3, are not changed in Tyk2-/- mice. Interestingly, the levels of muscle creatine kinase (MCK) are downregulated in Tyk2-/- mice. MCK is responsible for phosphorylation of creatine, which is one of the major fuels utilized by SKM. This would suggest an imbalance in energy utilization (78)in Tyk2-/- mice.

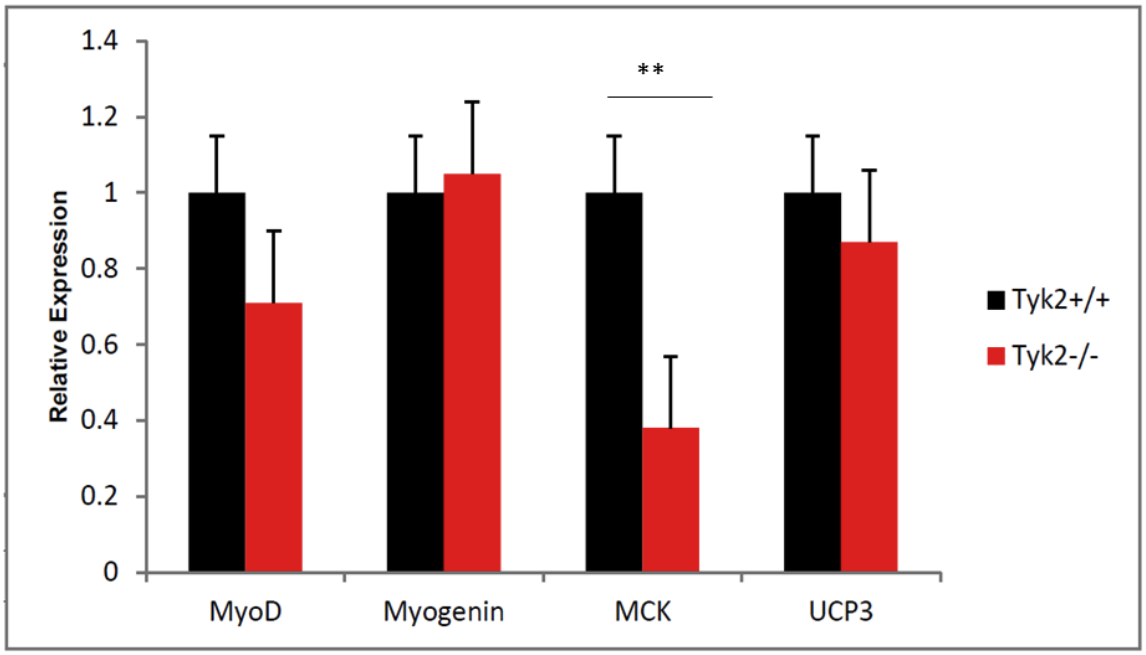

Figure 3.3: Expression of muscle specific mRNAs in Tyk2-/- mice: q-RT PCR on gastrocnemius muscle of 12-14 week old Tyk2-/- and Tyk2+/+ mice. (n=6-8 mice per group), **p<0.01. Data are expressed as mean ± SEM.

3.4: Tyk2-/- mice may exhibit contractile defects

Since muscle contraction is an important function of the skeletal muscle, we wanted to determine if Tyk2-/- mice exhibit any contractile defects. We measured the expression of different troponins, which are a part of the sarcomeric assembly and involved in muscle contraction. qRT-PCR analysis on SKM of 12-14 week old mice showed that the expression of troponins is downregulated in Tyk2-/- mice (Figure 3.4). This suggests that Tyk2-/- may play a role in regulating contractility of the skeletal muscle.

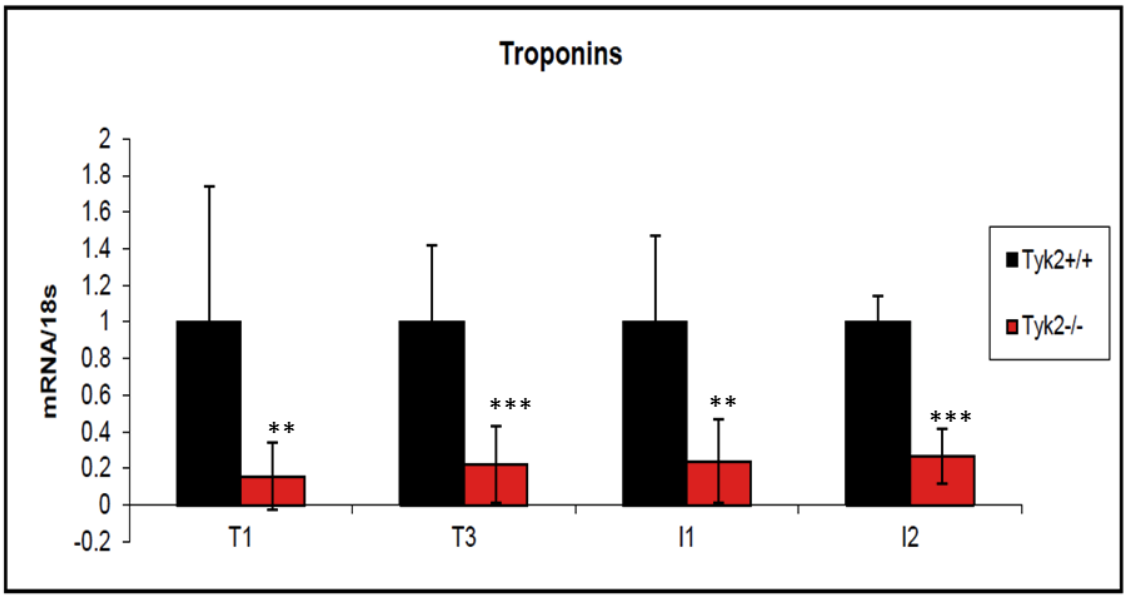

Figure 3.4: Tyk2-/- mice may exhibit contractile defects: Expression of troponins T1, T3, I1 and I2 in GA muscle of 12-14 week old mice measured by qRT-PCR. (n=6-8 mice per group). **p<0.01, ***p<0.0001. Data are expressed as mean ± SEM.

3.5: Tyk2-/- mice may exhibit defects in calcium signaling

Since calcium release triggers muscle contraction, we wanted to determine if Tyk2-/- mice show a defect in calcium release which could affect the muscle contraction. We measured the expression of Ryanodyne and SERCA receptors which are responsible for calcium release and calcium take-up after a stimulus. Figure 3.5 suggests that Tyk2-/- mice may exhibit a defect in calcium mediated contraction and could affect the muscle function and its thermogenic capacity.

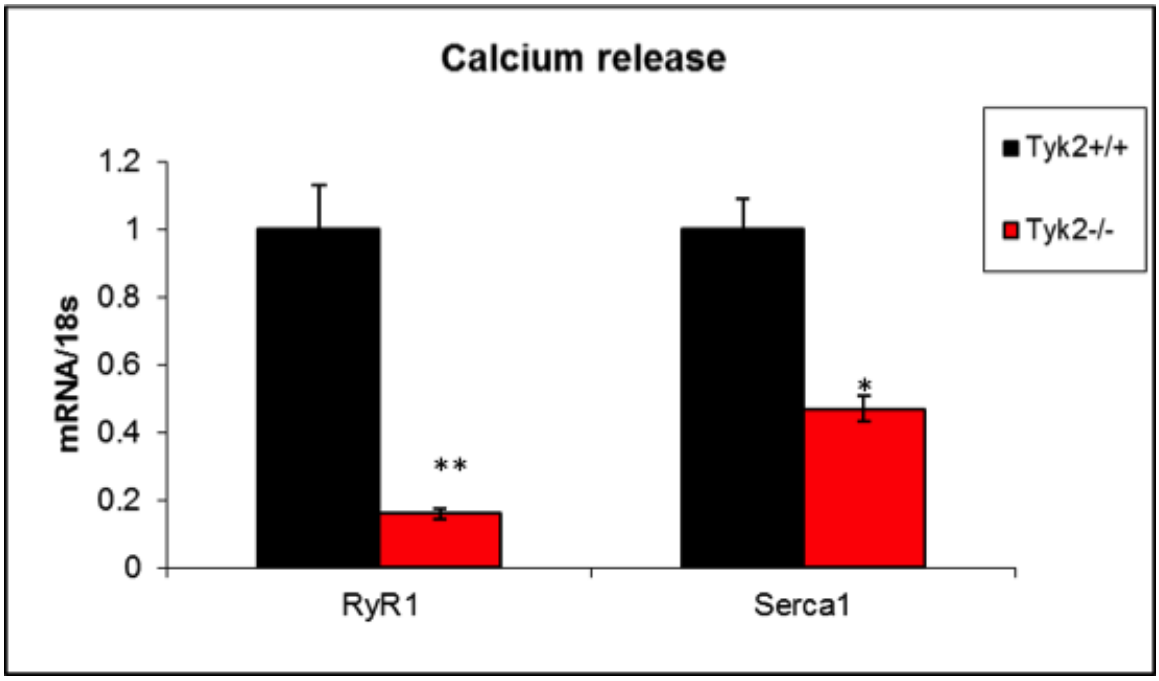

Figure 3.5: Tyk2-/- mice have decreased expression of mRNAs regulating calcium release: Expression of SERCA and Ryanodyne receptors in GA muscle of 12-14 week old mice measured by qRT-PCR. (n=6-8 mice per group). *p<0.05, **p<0.01. Data are expressed as mean ± SEM.

3.6: Tyk2-/- do not show defects in sarcomere assembly

Our previous studies have shown that Tyk2-/- mice may have a defect in shivering thermogenesis which is a function of skeletal muscle contraction (70). We wanted to determine if these contractile defects in SKM function were due to a disorganised sarcomere assembly. We isolated gastrocnemius, plantarius and soleus muscle from Tyk2+/+ and Tyk2-/- mice and subjected them to electron microscopy. The electron micrographs (Figure 3.6) reveal an organised structure of the sarcomere assembly in Tyk2-/- mice, suggesting that the defects in SKM function in Tyk2-/- mice is not due to a defect in structural assembly of the skeletal muscle.

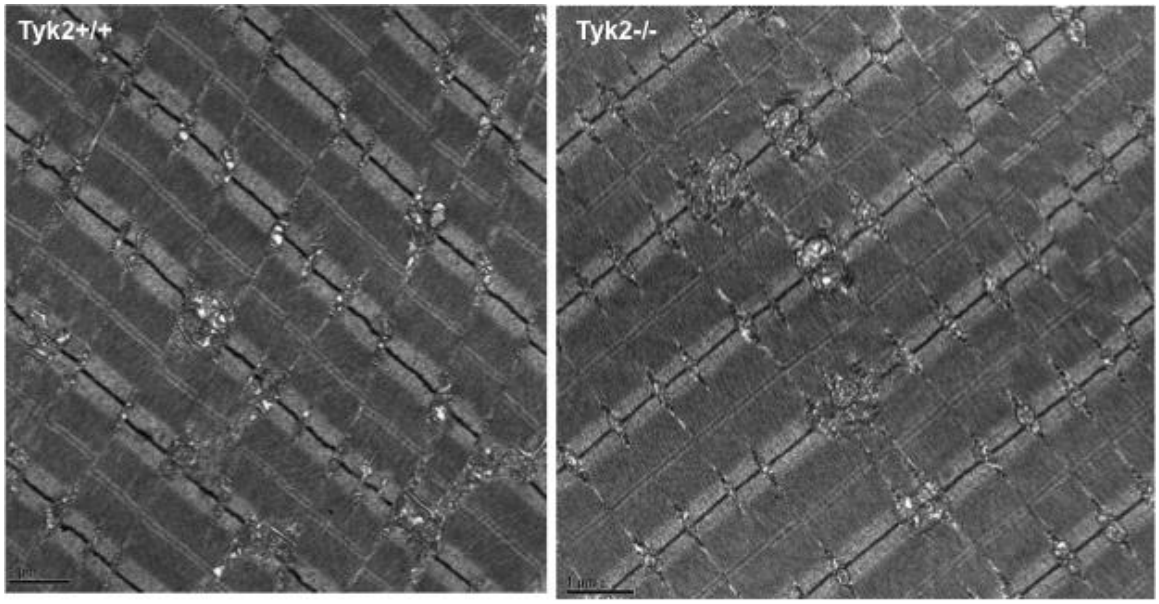

Figure 3.6: Tyk2-/- mice exhibit a normal skeletal muscle structure: Electron micrographs of GA muscle, in 12 week old mice, showing the sarcomere assembly. N = 4-6 mice per group.

3.7: Tyk2-/- mice do not have defects in neuro-muscular junction assembly

The neuro-muscular junction (NMJ) is responsible for transmitting signals from the incoming nerve to the skeletal muscle in response to various stimuli including cold exposure, which is responsible for inducing muscle contraction. Since Tyk2-/- mice exhibit defects in stimuli induced muscle contraction, we wanted to determine whether the defect was due to improper transmission of the incoming signal or due to the downstream effectors involved in muscle contraction. To determine this, we isolated individual muscle types (gastrocnemius, soleus, plantaris, tibelis anterior, diaphragm) and stained them with labelled α-bungarotoxin from snake venom, which binds specifically to the Acetylcholine receptors at the NMJ. As seen in figure 3.7, both Tyk2+/+ and Tyk2-/- exhibit a normal NMJ assembly (characterized by pretzel shaped staining), suggesting that the defects in Tyk2-/- mice lie downstream of the NMJ.

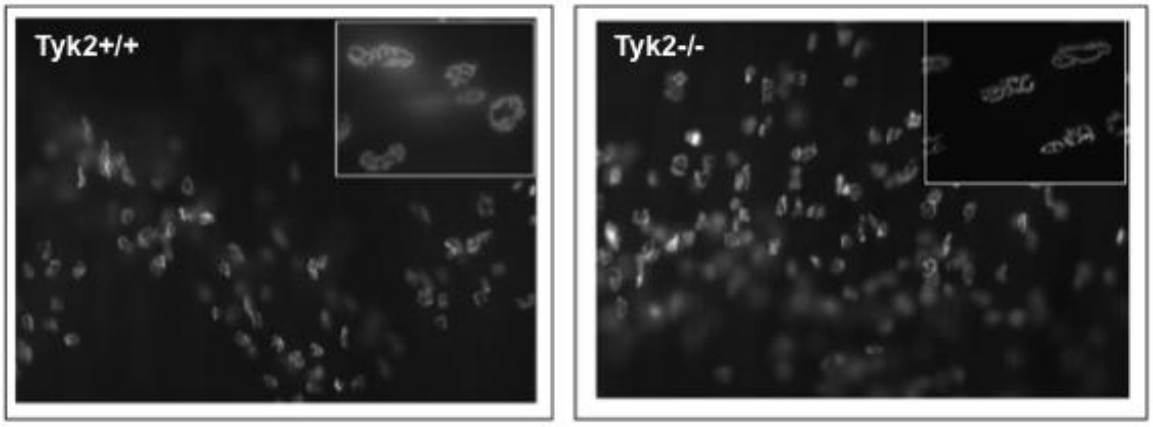

Figure 3.7: Tyk2-/- mice have a normal NMJ assembly: a-bungarotoxin staining of acetyl choline receptors at the NMJ assembly in GA muscle of 12 week old Tyk2+/+ and Tyk2-/- mice. N= 3 mice per group.

3.8: Contractile defects in Tyk2-/- are SKM specific

Apart from skeletal muscle, heart is another contractile tissue with similar contractile apparatus. As seen in Figure 3.8, expression of titin, one of the sarcomeric assembly proteins is downregulated in SKM, but is unchanged in the heart. This suggests that the defect lies specific to the contractile apparatus of skeletal muscle.

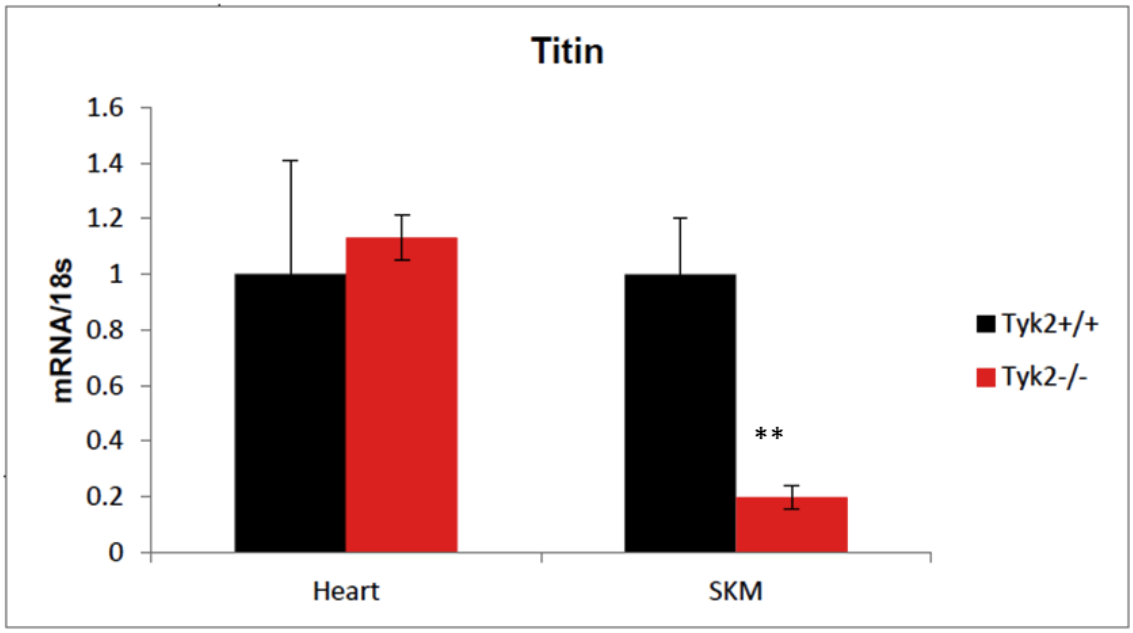

Figure 3.8: Contractile defects in Tyk2-/- mice are skeletal muscle specific: Expression of Titin in GA muscle and heart of 12-14 week old mice measured by qRT-PCR. (n=6-8 mice per group). **p<0.01. Data are expressed as mean ± SEM.

3.9: Tyk2-/- mice have increased glycolytic fibers

Fast-twitch fibers (glycolytic) contain low numbers of mitochondria and are responsible for short term muscle activities. Slow-twitch fibers (oxidative) are rich in mitochondria and are responsible for endurance functions. Our previous studies demonstrate that Tyk2-/- mice are exercise intolerent (69) and show a relatively lower endurance capacity. Since oxidative fibers and mitochondria play an important role in endurance function, we wanted to determine whether Tyk2-/- mice show an increased proportion of glycolytic fibers which could contribute to this phenotype. As seen in Figure 3.9, Tyk2-/- mice show an increased expression of MHC2b (the glycolytic fiber specific myosin heavy chain) and a decresed expression of MHC2a (the oxidative fiber specific myosin heavy chain) in gastrocnemius (mixed muscle). However, the expression of total myosin heavy chains or myogenin (marker of terminal muscle differentiation) are unchanged. This suggests that the decreased endurance phenotype is contributed by the increased proportion of fast-twitch fibers.

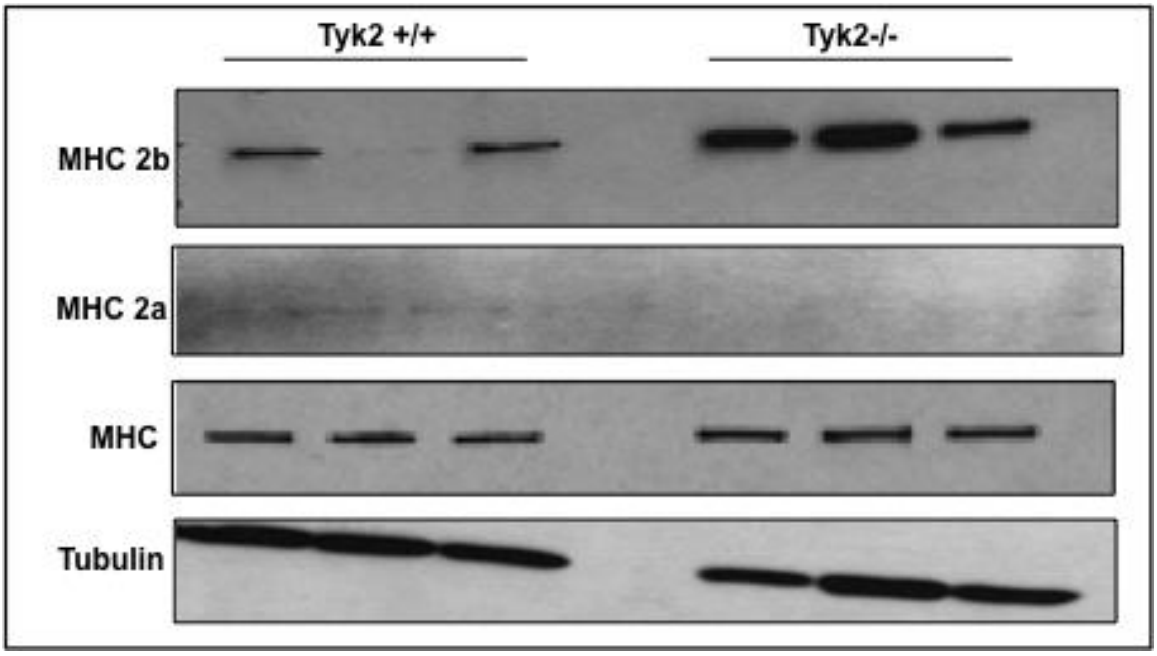

Figure 3.9: Tyk2-/- mice have an increased proportion of glycolytic fibers: Protein expression of MHCs for Type I (MHC2a), Type II (MHC2b) and total MHCs in whole cell extract on GA muscle of 12-14 week old mice was analysed by western blot.

3.10: PGC1α is downregulated in SKM of Tyk2-/- mice

PGC1α plays an important role in skeletal muscle function as it is the key factor that determines the different fiber types (fast-twitch versus slow-twitch) and also is involved in mitochondrial biogenesis. Since Tyk2-/- mice showed a decrease in the slow, oxidative fibers, we wanted to determine if PGC1α was one of the contributing factors. RNA was isolated from gastrocnemius muscle of 12 week old mice and PGC1α expression was determined by qRT-PCR. As seen in Figure 3.10, Tyk2-/- mice exhibit decreased PGC1α expression, and this downregulation is skeletal muscle specific, suggesting that PGC1α is one of the contributing factors towards the Tyk2-/- phenotype.

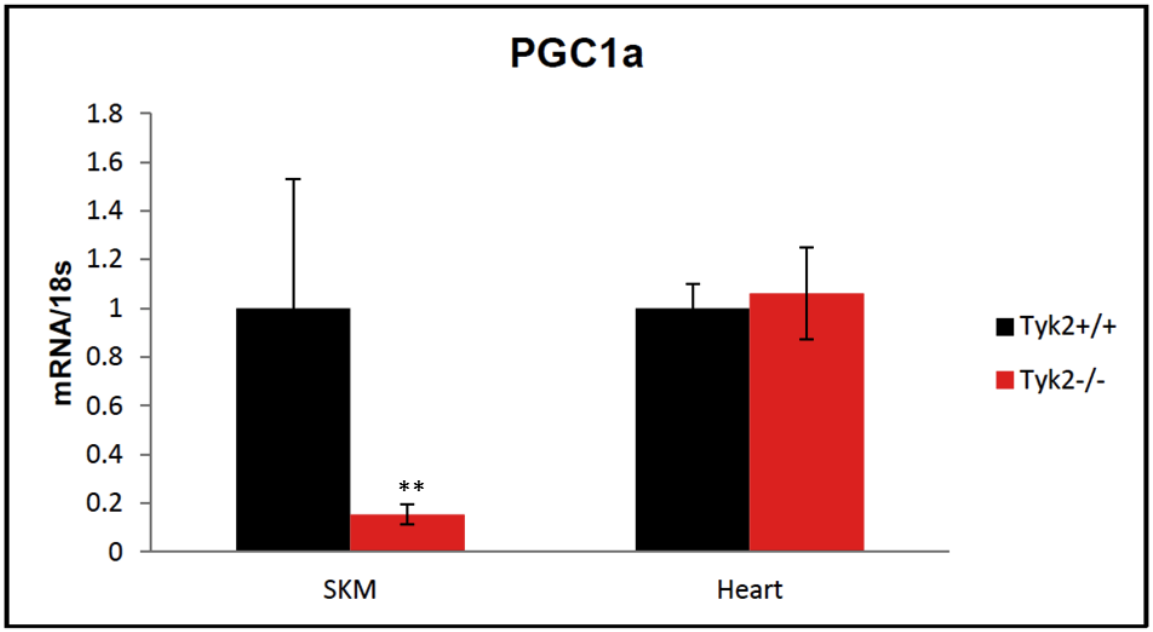

Figure 3.10:PGC1α is downregulated in Tyk2-/- mice: Expression of PGC1α in GA muscle and heart of 12-14 week old mice measured by qRT-PCR. (n=6-8 mice per group). *p<0.05. Data are expressed as mean ± SEM.

3.11: Tyk2-/- mice exhibit altered mitochondria morphology in SKM

From the previous figure, we know that PGC1α expression is downregulated in SKM of Tyk2-/- mice. Since PGC1α is also the master regulator of mitochondrial biogenesis, we wanted to determine whether the mitochondria morphology and number was affected in SKM of Tyk2-/- mice. Electron micrographs on gastrocnemius (glycolytic) (Figures 3.11C, 3.11D) and soleus (oxidative) (Figures 3.11A, 3.11B) muscles of 12 week old mice reveal that the number of mitochondria is not changed, however the morphology is grossly altered (Figures 3.11A, 3.11C). Mitochondria in Tyk2-/- mice appear smaller as compared to Tyk2+/+ mice in both Type I (mitochondria-rich) and Type II (mitochondria-poor) fibers and also show deformed cristae formation. This suggests that Tyk2 may play a role in regulating the mitochondrial structure.

A

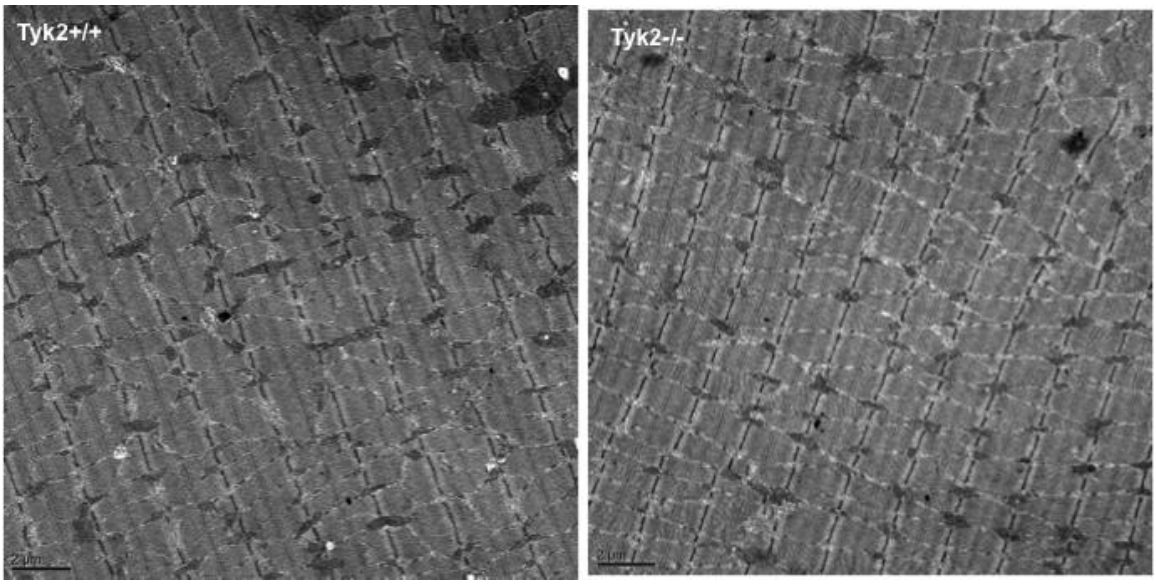

B

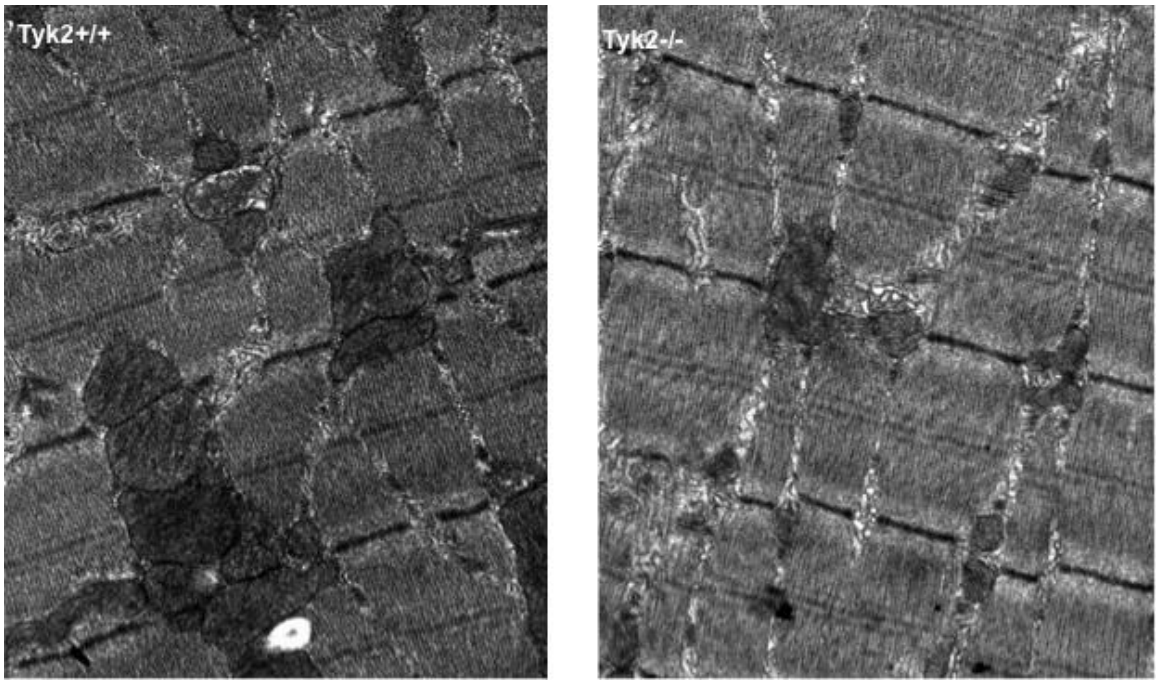

C

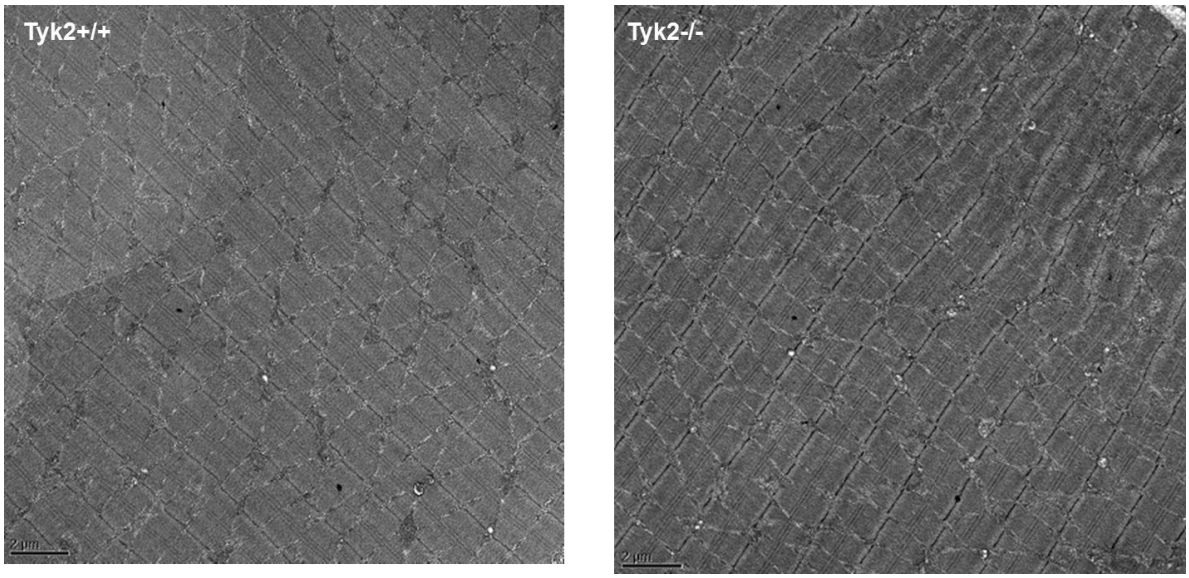

D

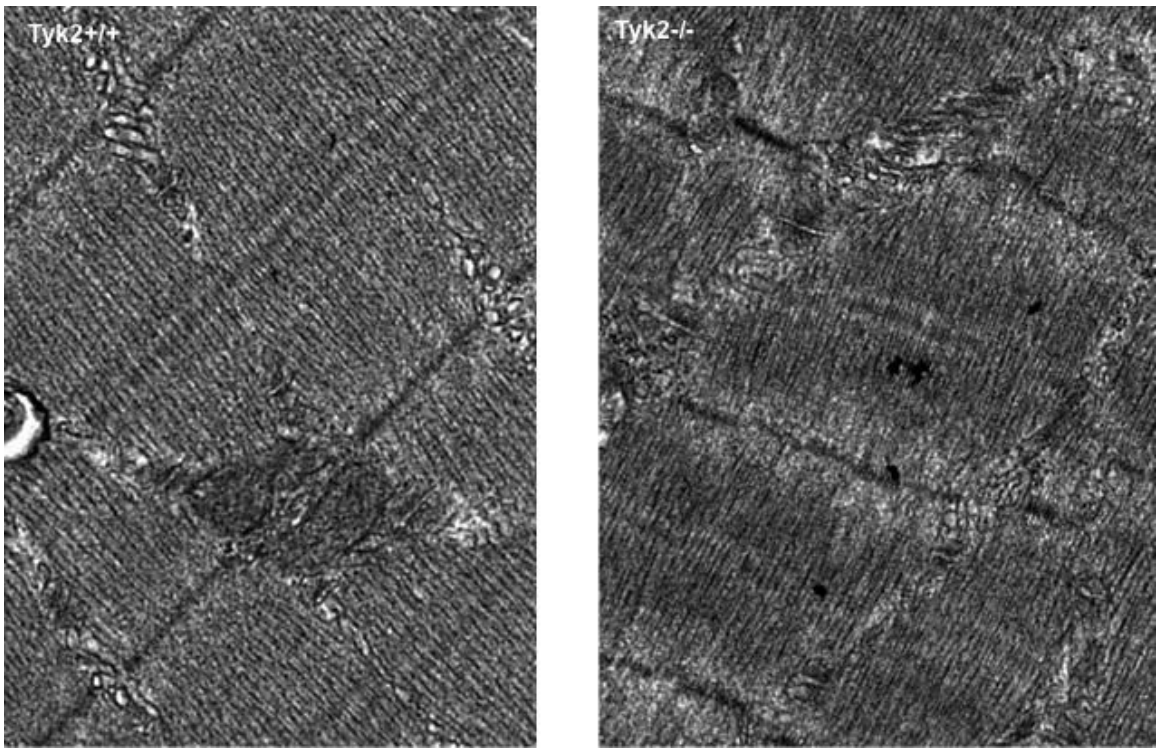

Figure 3.11:Mitochondria in Tyk2-/- mice are deformed: Representative Electron micrographs of Soleus (A),(B) and plantaris (C),(D) muscle in 12 week old Tyk2+/+ and Tyk2-/- mice.

3.12: Tyk2-/- mice exhibit defects in mitochondrial respiration

Next, we wanted to determine whether the mitochondria exhibit a defect in function along with the structural defects. We isolated mitochondria from skeletal muscle of 12-14 week old Tyk2+/+ and Tyk2-/- mice and measured respiration on isolated mitochondria using a Clark-type oxygen electrode. We measured electron flow through Complex I, Complex II and Complex IV by adddition of specific substrates. As seen in Figure 3.12, Tyk2-/- mice exhibit decreased Glutamate-Malate (complex I), succinate (complex II) and TMPD-ascorbate (Complex IV) dependent respiration. This could be due to a defect in activities of all ETC complexes or Complex IV which is the last one in the chain. Figure 3.12, also shows that State 3 (ADP-dependent) and State 4 (ADP-independent) respiration are both lower in Tyk2-/- mice. DNP and azide uncoupled respiration is also decreased, suggesting that the defects lie in electron flow through ETC and not in ATP synthase (Complex V).

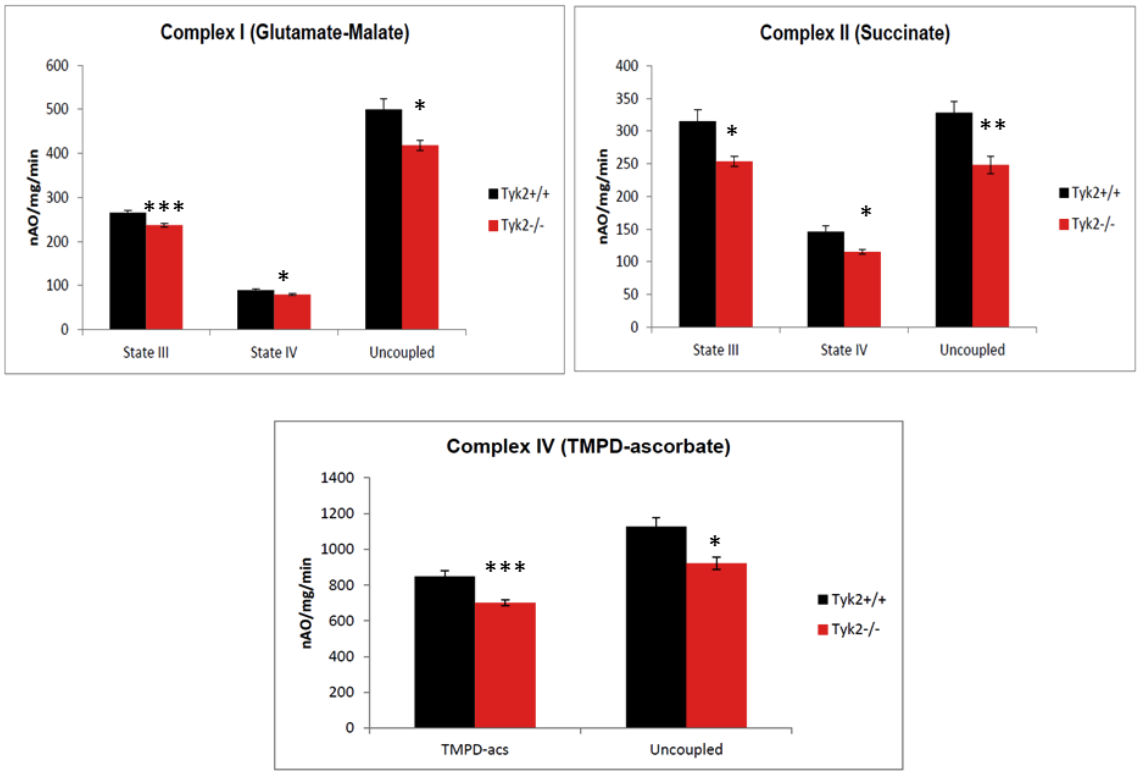

Figure 3.12: Tyk2-/- mice exhibit a defect in mitochondrial respiration: Oxygen consumption was measured from isolated mitochondria of 12-14 week old Tyk2+/+ and Tyk2-/- mice using specific substrates (Glutamate-malate for Complex I, succinate for complex II and TMPD-Ascorbate for complex IV) in a Clark-type oxygen electrode. State 3 (ADP dependent), State 4 (ADP-independent), and uncoupled (DNP for complex I and II and azide for complex IV) values are represented in the figure. (n= 10-12 mice per group) *p<0.05.

3.13: Tyk2-/- mice exhibit defect in CIV activity

To identify which ETC complex contributed to decreased in oxygen consumption in skeletal muscle mitochondria, we measured activities of the different ETC complexes using an In-gel assay. Isolated mitochondria from skeletal muscle of 12-14 week old mice were resolved on a Blue-Native gel to separate the individual complexes and enzymatic activities were measured based on colorimetric analysis (79). Figure 3.13 suggests that the defect lies in activity of Complex IV, which could contribute to the overall decreased mitochondrial respiration.

A

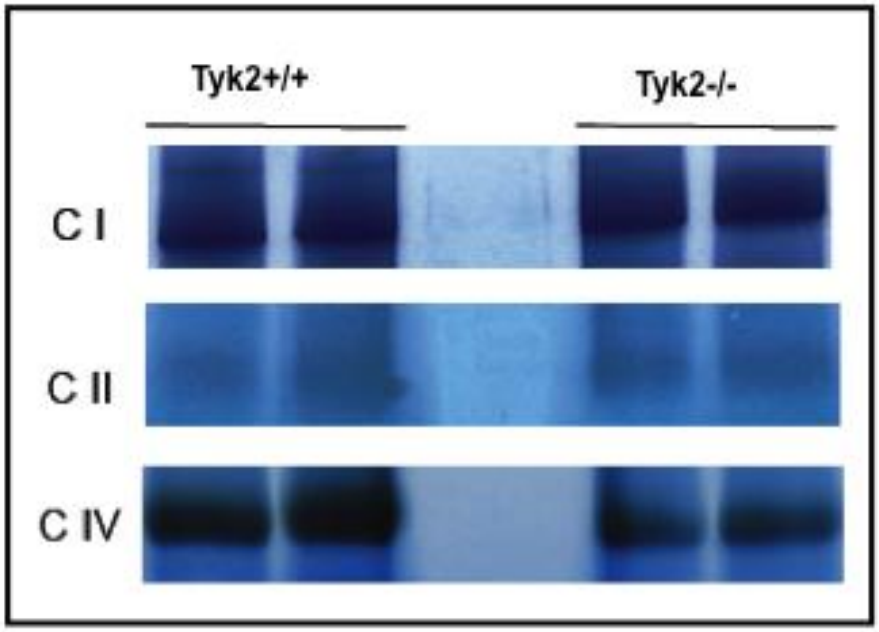

B

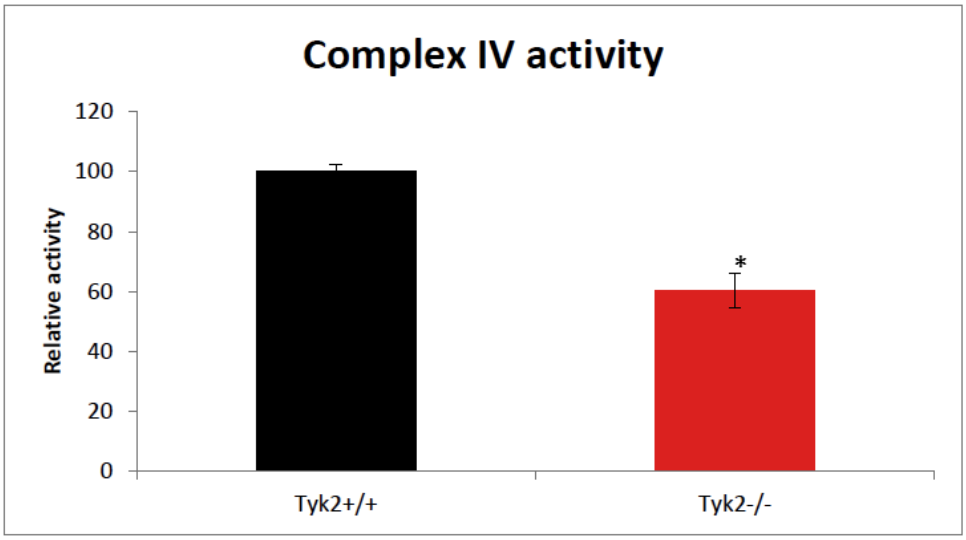

Figure 3.13: Complex IV activity is decreased in Tyk2-/- mice: (A) Activities of complex I, complex II and complex IV were measured on isolated mitochondria from 12-14 week old Tyk2+/+ and Tyk2-/- mice using an In-gel assay afterBN-PAGE. (B) Quantification of Complex IV activity from (A) using Image-J software. N=4-6 mice per group, *p<0.05.

3.14: Decreased ComplexIV activity in Tyk2-/- mice is not due to a defect in assembly of the ETC

Decreased complex IV activity in the SKM mitochondria of Tyk2-/- mice could be due to decreased expression of complex IV proteins or a defect in overall assembly of the ETC complexes. Figure 3.14A shows that Tyk2-/- mice do not show any changes in the expression or assembly of the different ETC complexes, nor the expression of mitochondrial proteins (Figure 3.14B) is different between Tyk2+/+ and Tyk2-/- mice, suggesting that the defect is activity of complex IV is not due to a structural defect in the assembly of ETC components.

A

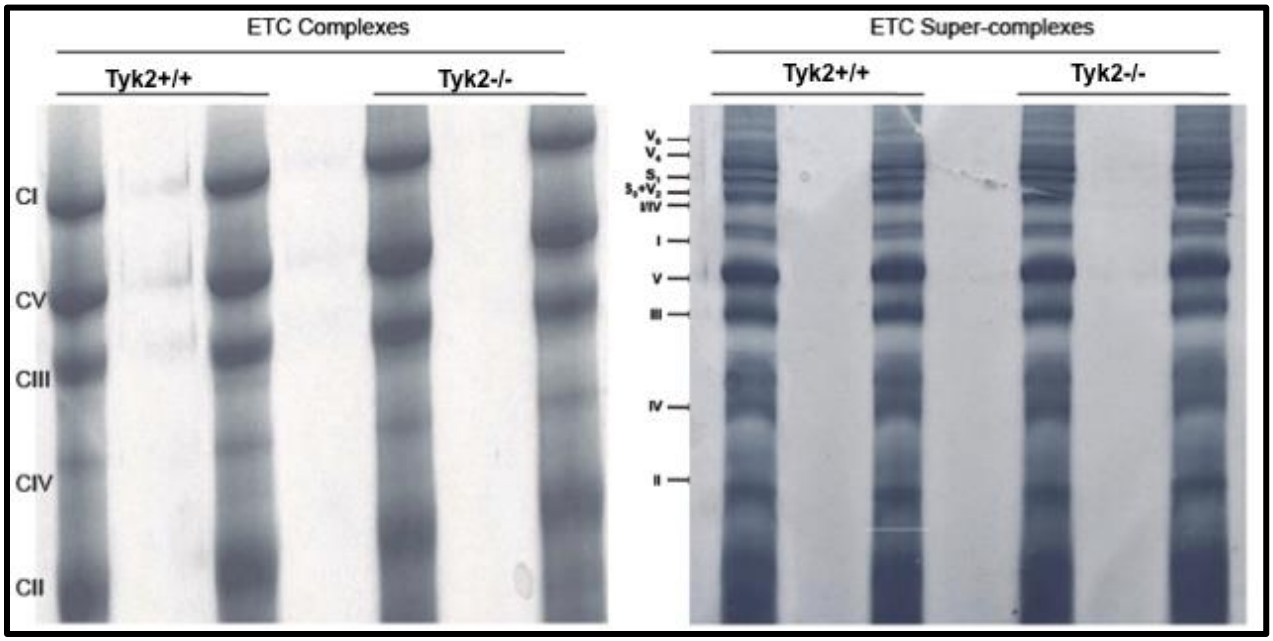

B

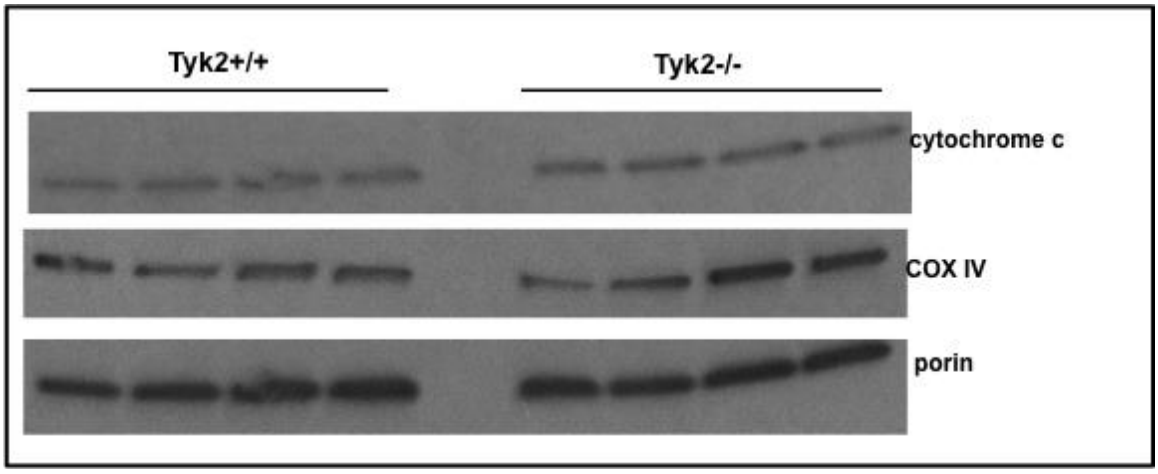

Figure 3.14: Decreased ComplexIV activity in Tyk2-/- mice is not due to a defect in assembly of the ETC: Mitochondria were isolated from 12-14 week old Tyk2+/+ and Tyk2-/- mice and resolved on BN-PAGE. Mitochondria solobilised with DDM show ETC complexes while mitochondria solubilised using digitonin show ETC supercomplex formation. B) Western blot on isolated mitochondria from 12-14 week old Tyk2+/+ and Tyk2-/- mice.

3.15: Tyk2-/- mice exhibit SKM defects from birth

We wanted to determine whether the defects seen in SKM of Tyk2-/- mice are present from birth or they develop with age. We isolated RNA from skeletal muscles from 1-3 day old newborn pups and measured the expression of troponins and MHCs by qRT-PCR. As seen in Figure 3.15 A, expression of troponins is downregulated in Tyk2-/- mice suggesting that the pups also exhibit contractile defects. Figure 3.16B shows that expression of MHCI, the slow-oxidative type muscle fiber MHC is downregulated, suggesting that Tyk2-/- mice exhibit a developmental defect in SKM function.

A

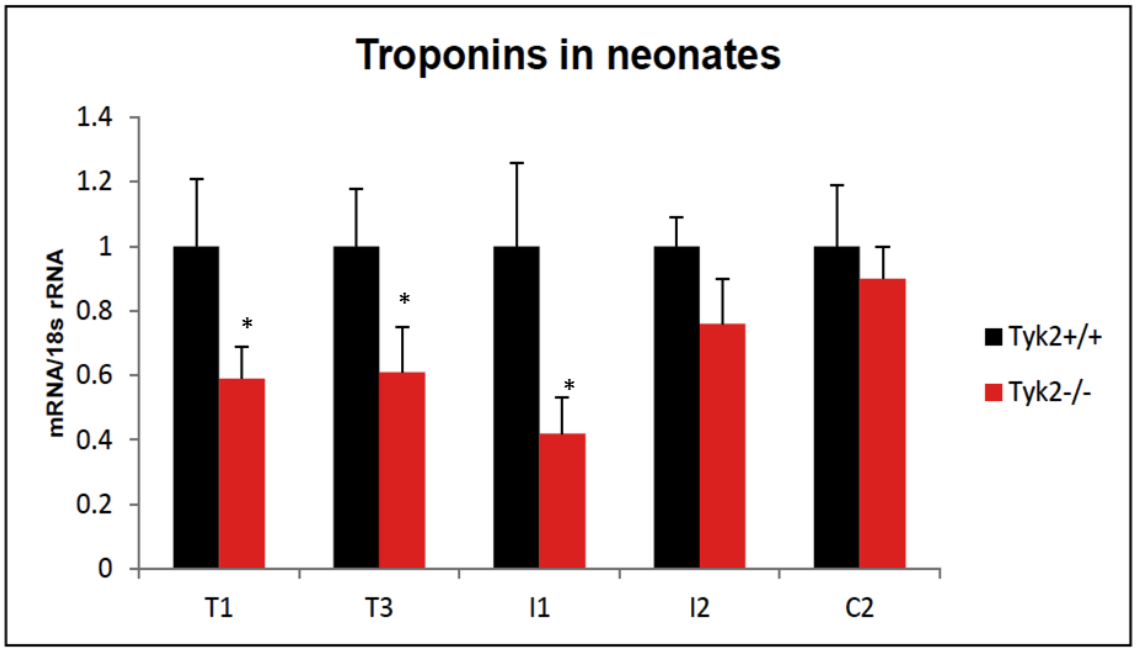

B

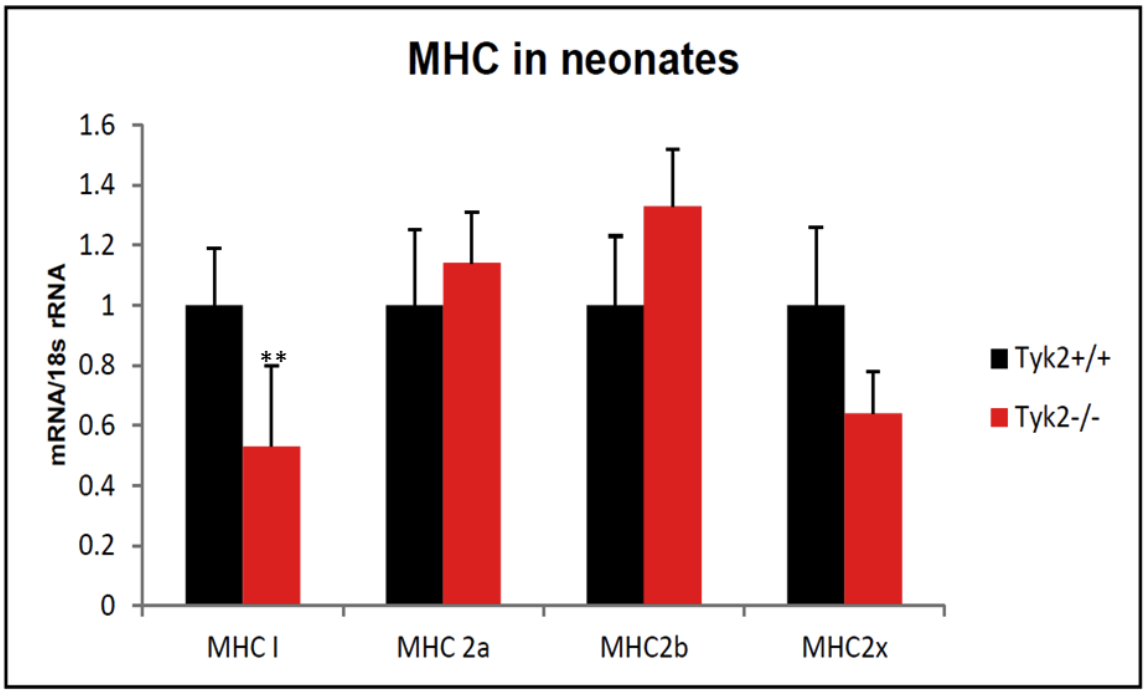

Figure 3.15: Tyk2-/- mice exhibit SKM defects from birth: Expression of Troponins (A) and Myosin Heavy Chains (B) in skeletal muscle 1-3 day old newborn pups measured by qRT-PCR. (n=8-10 mice per group). *p<0.05. **p<0.01. Data are expressed as mean ± SEM.

3.16: Tyk2 is induced during differentiation of C2C12 myocytes

To determine if Tyk2 is involved during the differentiation of SKM, we used an in-vitro approach. We measured the levels of Tyk2 RNA and protein during the differenetiation of C2C12 myocytes. As seen in Figure 3.16A, Tyk2 is barely detectable in undifferentiated, proliferating myocytes. However, Tyk2 levels increase (~20 fold) soon after C2C12 myocytes are induced for differentiation and the upregulation is maintained in differentiated myocytes. We also measured the expression of Jak1 and Jak2 (Figure 3.16B), which are known to be involved in myogenic differentiation. Jak1 is known to be upregulated during the proliferation stage (80)and Jak2 is known to be involved in the differentiation of C2C12 myocytes (81). This suggests that Tyk2 may be involved in differentiation of myocytes and is indispensable for SKM function.

A

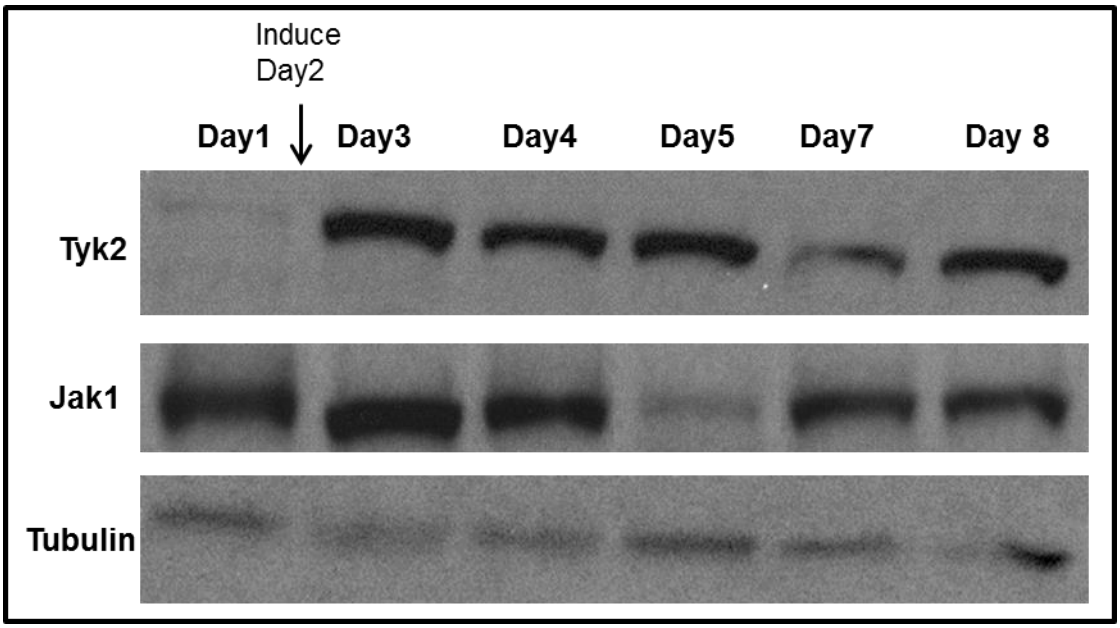

B

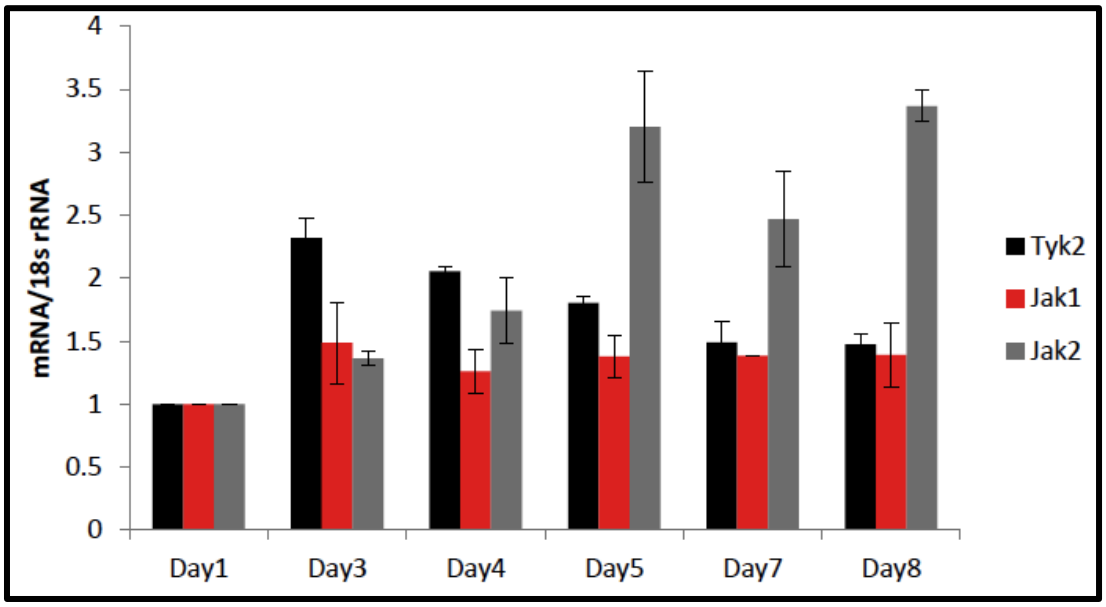

Figure 3.16: Tyk2 is induced during differentiation of C2C12 myocytes: Western blot analysis (A) and qPCR (B) on whole cell extracts of C2C12 myocytes during the course of differentiation.

3.17: Restoring expression of Tyk2 in BAT and SKM (Myf5 cre)

We next wanted to determine whether restroring the expression of Tyk2 in the Myf5 positive progenitors- BAT and SKM, will reverse the obese phenotype in Tyk2-/- mice. Our preliminary results showed that restoring the expression of Tyk2 (Tyk2 WT) in Tyk2-/- brown preadipocytes can differentiate into brown fat in-vitro (70). We also expressed kinase inactive Tyk2 (Tyk2 KD) in Tyk2-/- preadipocytes as a control for kinase activity. To our surprise, expression of Tyk2 KD also induced differentiation of brown fat preadipocytes in vitro. To further investigate the role of kinase inactive Tyk2, we generated mice carrying Tyk2 (Tyk2 WT) and kinase inactive Tyk2 (Tyk2 KD) transgene. These mice were bred with Tyk2-/- mice on C57/Bl6 background. These mice were then crossed to Myf5 cre mice (on Tyk2-/- background) to generate transgenic mice that expressed either Tyk2 WT ($Tyk2WT^{Myf5}$) or Tyk2 KD ($Tyk2KD^{Myf5}$) proteins. Tyk2-/- littermate control animals carried the inactive transgene. Tyk2+/+ control animals were generated in a similar fashion, the only difference being that they expressed endogenous Tyk2 and carried an inactive transgene. As seen in figure 3.17, the transgene was expressed only in BAT and SKM, but not other tissues.

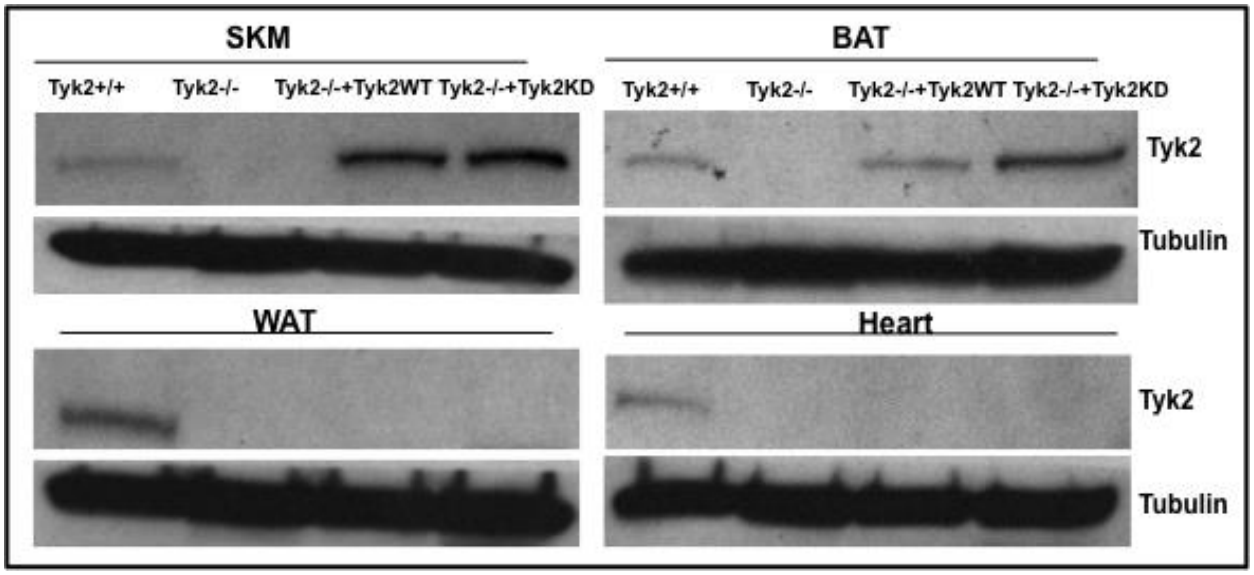

Figure 3.17: Expressing Tyk2 in the Myf5 lineage: Whole cell extracts from BAT, SKM, WAT and Heart from Tyk2+/+, Tyk2-/-, Tyk2-/-+Tyk2WT, Tyk2-/-+Tyk2KD mice were analysed by western blot forTyk2 levels in 4 week old male mice. N= 3-4 mice per group.

3.18: Tyk2 expression in BAT and SKM restores the obese phenotype

The first question that we wanted to address using the transgenic model was whether mice expressing Tyk2WT^{Myf5} and Tyk2KD^{Myf5} revert their obese phenotype. Mice were weighed every week for 6 months. The weights are plotted in Figure 3.18. Figure 3.18A shows that the lean phenotype is restored in both Tyk2WT^{Myf5} and Tyk2KD^{Myf5} mice as early as 12 weeks of age and is maintained till the mice are 6 months old (Figure 3.18B). This suggests that kinase activity of Tyk2 is not required for its role in regulating the obese phenotype and that restoring expression of Tyk2 in BAT and SKM is sufficient to revert the obese phenotype of Tyk2-/- mice.

A

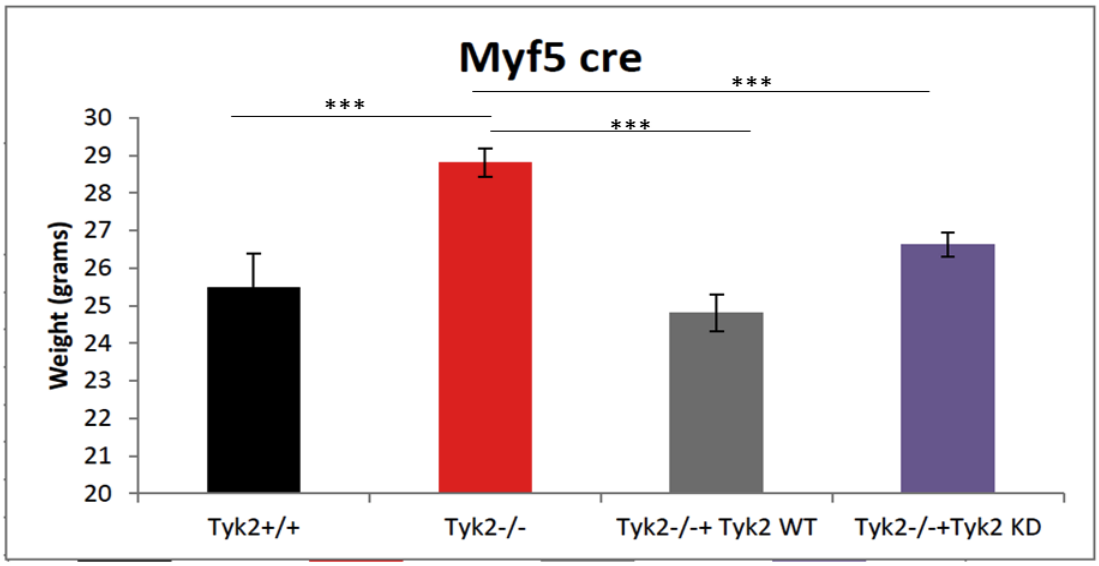

B

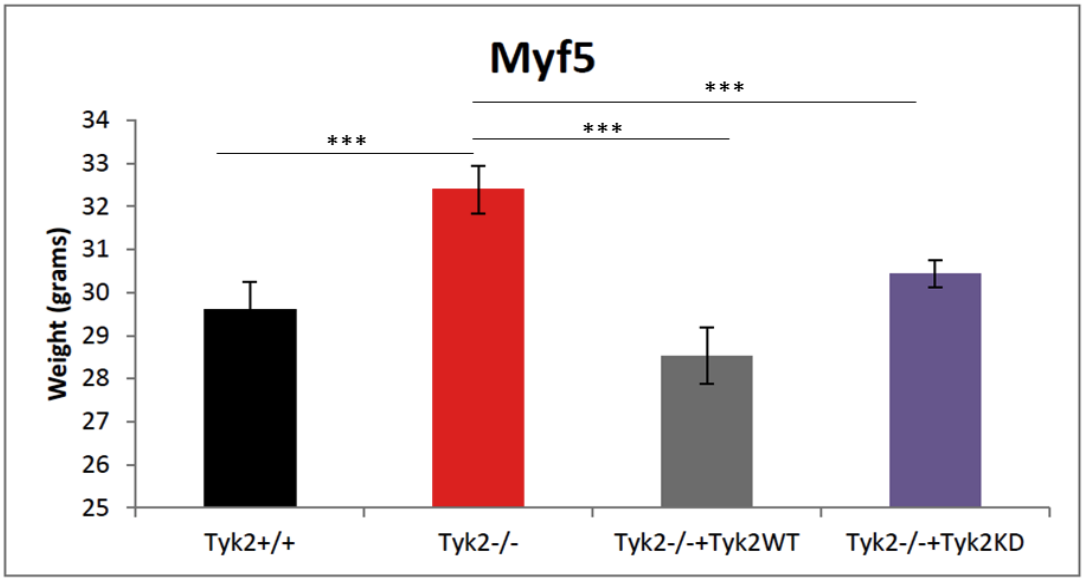

Figure 3.18: Tyk2 expression in BAT and SKM restores the obese phenotype: Body weight of mice at 12 weeks (A) and 24 weeks (B) fed a breeder chow diet. (n= 15-24 mice per group). ***p<0.0001. Data are expressed as mean ± SEM.

3.19: Tyk2 expression in BAT (Myf5 cre) restores the brown fat phenotype in primary preadipocytes

To determine whether brown fat development was restored in mice expressing $Tyk2WT^{Myf5}$ and $Tyk2KD^{Myf5}$, we isolated preadipocytes from 1-3 day old newborn pups and subjected them to in-vitro differentiation. As seen in Figure 3.19A, expression of Tyk2WT and Tyk2KD restored the expression of brown fat specific genes (UCP1, cidea, PRDM16) and fat specific genes (PPARα, PGC1α). Also, muscle specific genes (MCK, MyoD) that were upregulated in Tyk2-/- mice were downregulated back to their normal levels in both Tyk2WT and Tyk2KD preadipocytes (figure 3.19B). This suggests that expression of Tyk2 in myf5 cre restores the brown fat phenotype in these mice.

A

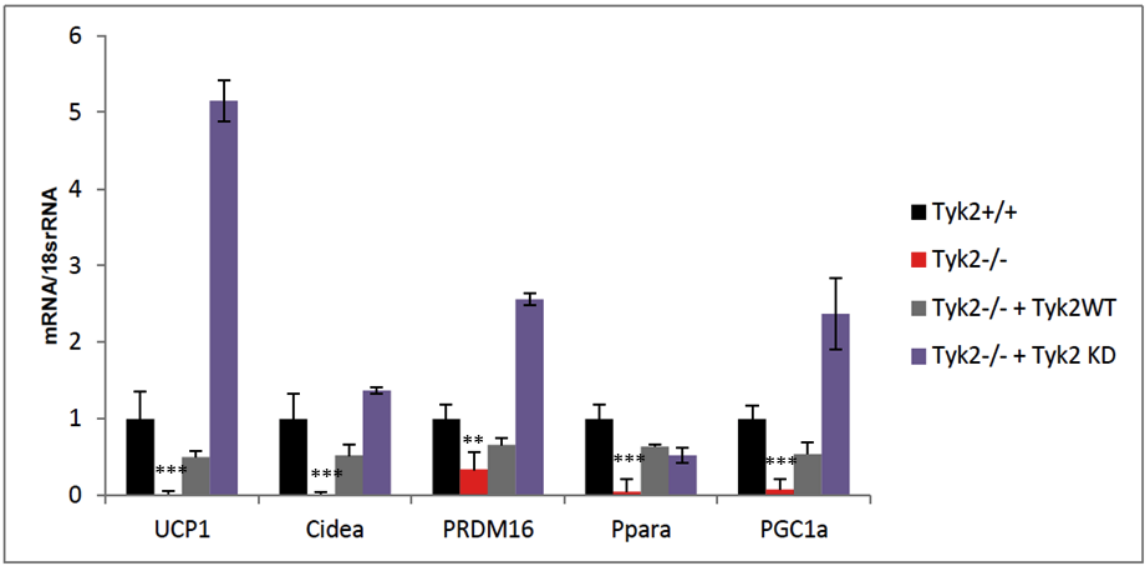

B

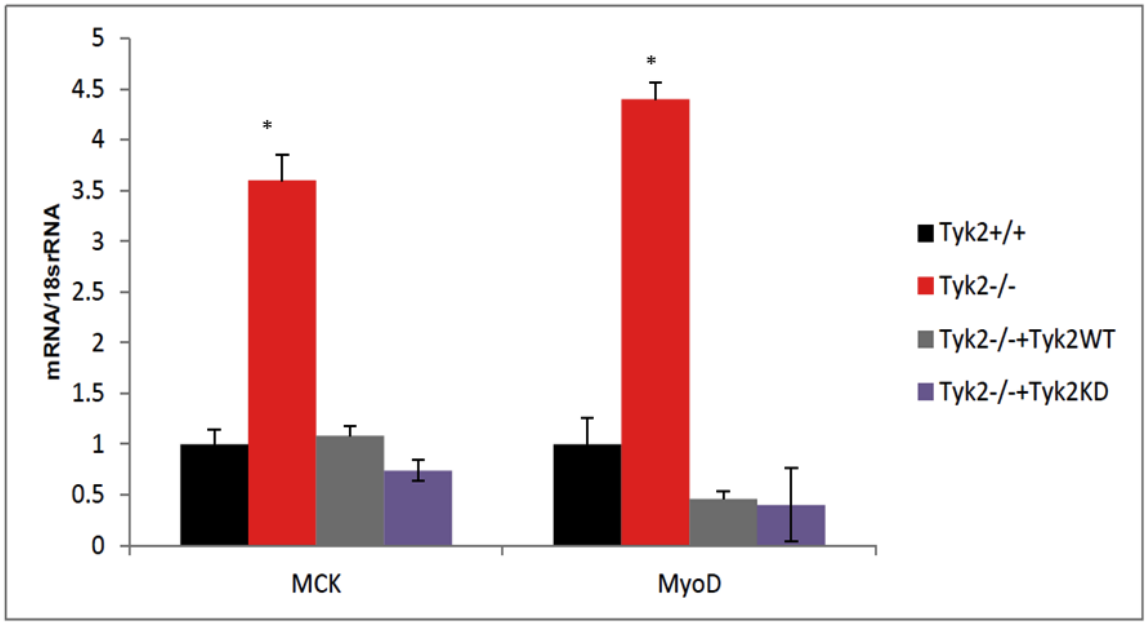

Figure 3.19: Expression of Tyk2 in BAT rescues the brown fat phenotype: Expression of brown fat specific genes (UCP1, cidea, PRDM16) and fat specific genes (PPARa, PGC1a) (A) and muscle specific genes (MCK, MyoD) (B) in differentiated primary brow fat adipocytes measured by qRT-PCR. (n=3-5 mice per group). *p<0.05. **p<0.01. Data are expressed as mean ± SEM.

3.20: Restoring Tyk2 expression in BAT and SKM restores the thermogenic function of these tissues

Since Tyk2-/- mice showed a defective response to cold exposure, we next determined whether Tyk2WT^{Myf5} and Tyk2KD^{Myf5} transgenics restored their ability for cold tolerance. 12-14 week old mice were subjected to cold stress at 4^{o}C for a period of 12 hours. Core body temperature was monitored at regular intervals. Figure 3.21 shows that both Tyk2WT^{Myf5} and Tyk2KD^{Myf5} can maintain the core body temperature as effectively as the Tyk2+/+ mice. This shows that function of SKM and BAT is not dependent on kinase activity of Tyk2.

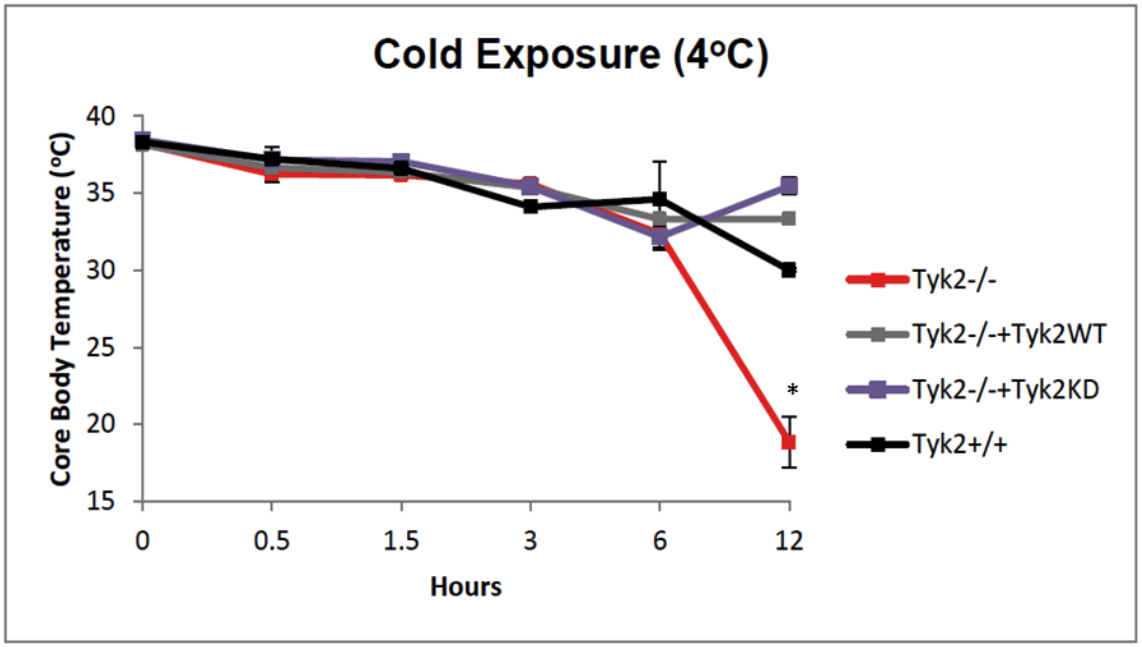

Figure 3.20: Tyk2 expression in BAT and SKM restores the thermogenic function of these tissues: Core body temperature measured at 0.5, 1.5, 3, 6 and 12 hours using a rectal thermometer in 12-14 week old mice placed at 4^{o}C for 12 hours. (n=3-7 mice per group) $p<0.05$. Data are expressed as mean ± SEM.

3.21: Restoring Tyk2 expression in the SKM alone reverts the obese phenotype in Tyk2-/- mice

Since SKM is an important tissue controlling energy expenditure, we wanted to determine whether expressing Tyk2WT and Tyk2KD only in the SKM, but not BAT, of Tyk2-/- mice is sufficient to revert the obese phenotype. We crossed the Tyk2WT and Tyk2KD transgenic mice on Tyk2-/- background to mice carrying the cre recombinase under the MCK (muscle creatine kinase) promoter. This allows expression of the transgene in SKM and heart, but not BAT. The mice generated (along with Tyk2-/- and Tyk2+/+ controls) were weighed every week for a period of 6 months. As seen in Figure 3.21A, at 12 weeks, $Tyk2WT^{MCK}$ and $Tyk2KD^{MCK}$ mice are significantly lighter than Tyk2-/- mice, but are still heavy compared to Tyk2+/+ mice. Interestingly, at 24 weeks (figure 3.21B), the $Tyk2KD^{MCK}$ mice show a complete reversal of obese phenotype, whereas $Tyk2WT^{MCK}$ mice show a moderate reversal. The effects seen are SKM specific, as the expression of genes involved in BAT function are downregulated, as in Tyk2-/- mice (Figure 3.21C). This suggests that expressing Tyk2 in the SKM alone can overcome the weight gain in Tyk2-/- mice and that kinase inactive form of Tyk2 is more effective in reversal of obese phenotype in Tyk2-/- mice.

A

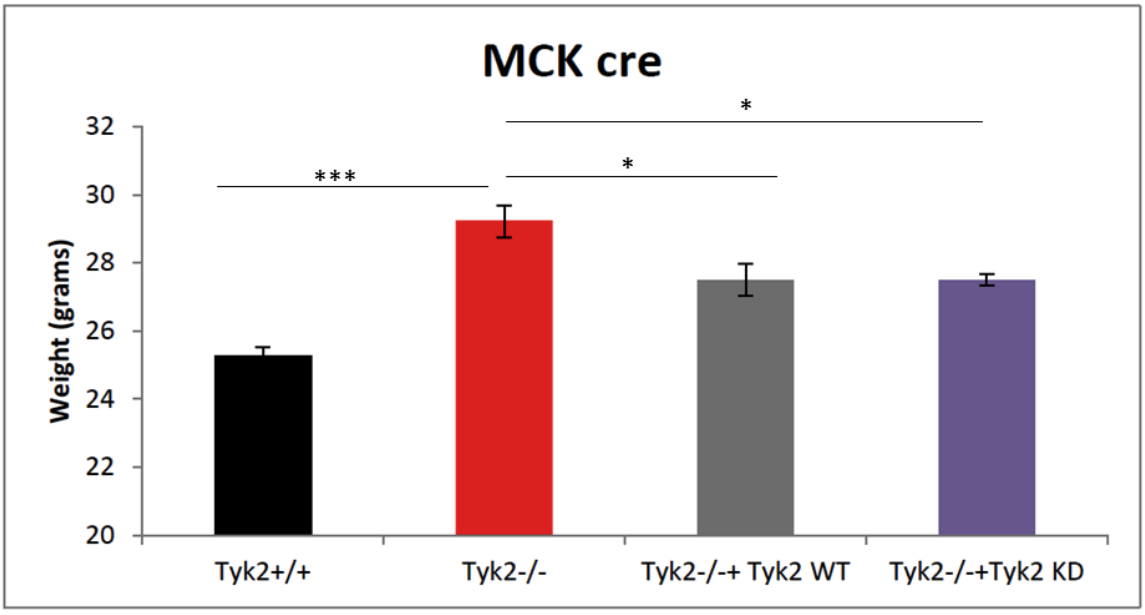
MCK cre
Weight (grams)
32
30
28
26
24
22
20
***
*
*
Tyk2+/+
Tyk2-/-
Tyk2-/-+ Tyk2 WT
Tyk2-/-+Tyk2 KD

B

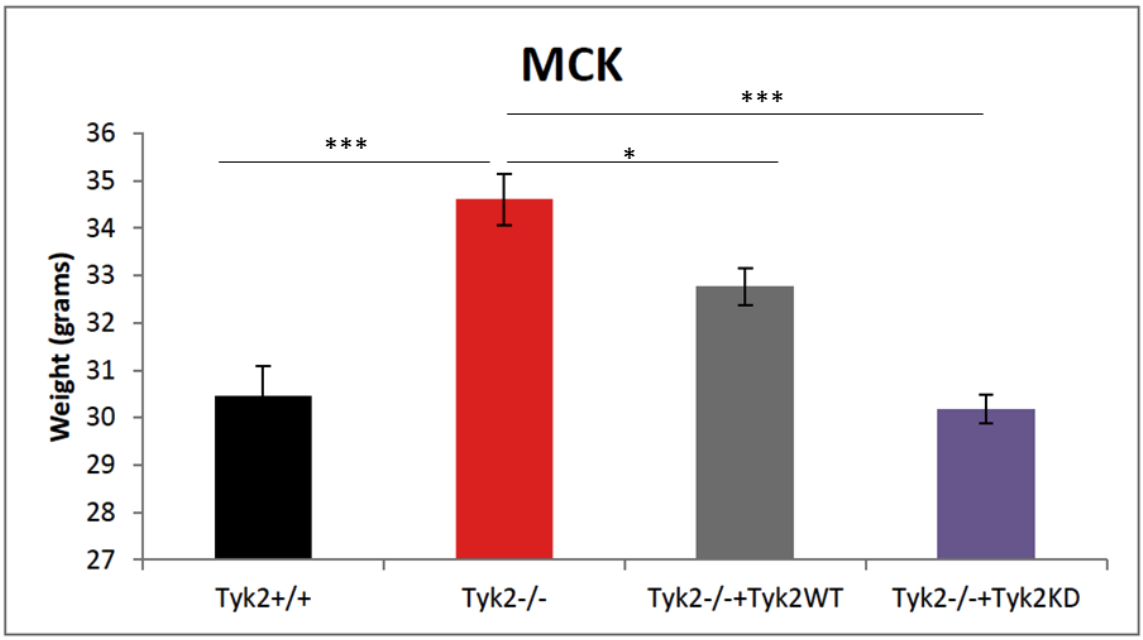
MCK
Weight (grams)
36
35
34
33
32
31
30
29
28
27
***
***
*
Tyk2+/+
Tyk2-/-
Tyk2-/-+Tyk2WT
Tyk2-/-+Tyk2KD

C

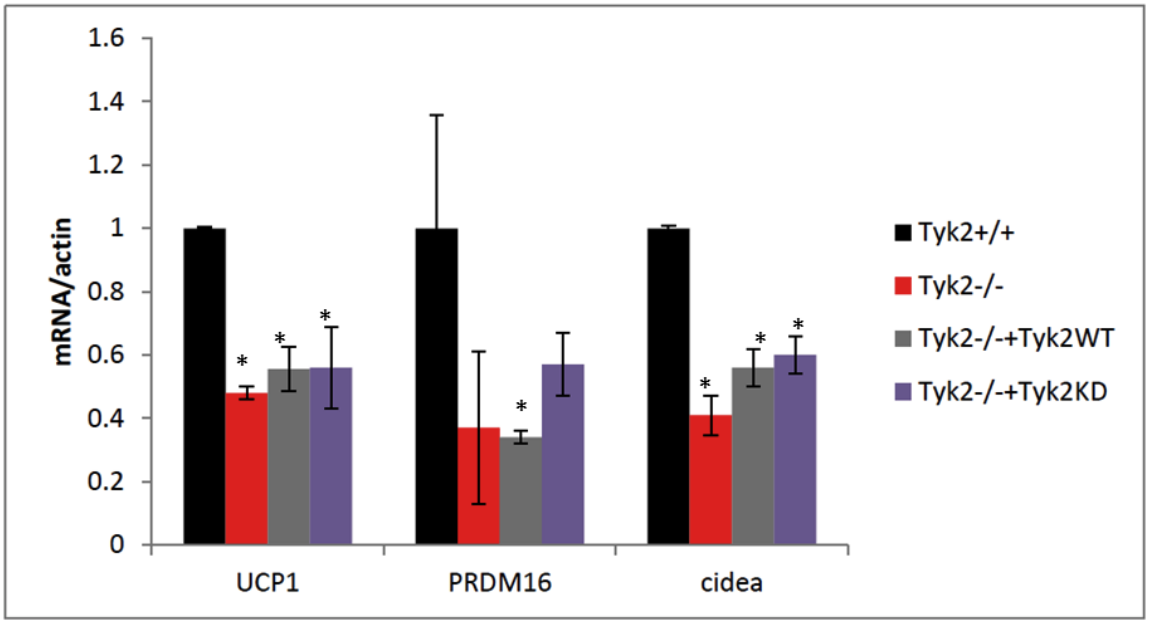

Figure 3.21: Tyk2 expression in SKM alone partially reverts the obese phenotype in Tyk2-/- mice: Body weight of mice at A) 12 weeks B) 24 weeks fed a breeder chow diet. (n= 5-24 mice per group) C) Expression of BAT specific genes-UCP1, PRDM16 and cidea in BAT of 24 week old mice analysed by qPCR. ***p<0.0001, **p<0.01, *p<0.05. Data are expressed as mean ± SEM.

3.22: FERM domain of Tyk2 is required for the control of obesity

From the previous figures, we can conclude that kinase activity of Tyk2, as a function of K927 in the JH1 domain, is dispensable for its role in regulating obesity, suggesting that Tyk2 may act as an adaptor protein and not as a kinase. Reports suggest that the N-term FERM domain is important for protein-protein interaction of Tyk2. To determine whether the FERM domain is involved in mediating function of Tyk2 in obesity, we generated FERM domain deletion of Tyk2. Brown fat preadipocytes from Tyk2-/- mice were infected with these constructs and differentiated in- vitro. Oil-red O staining was used as a marker for differentiation. As seen in figure 3.22, deletion of FERM domain in both WT and KD forms of Tyk2, did not restore the differentiation of Tyk2-/- preadipocytes. This suggests that the FERM domain of Tyk2 may be involved in regulation of its function in obesity.

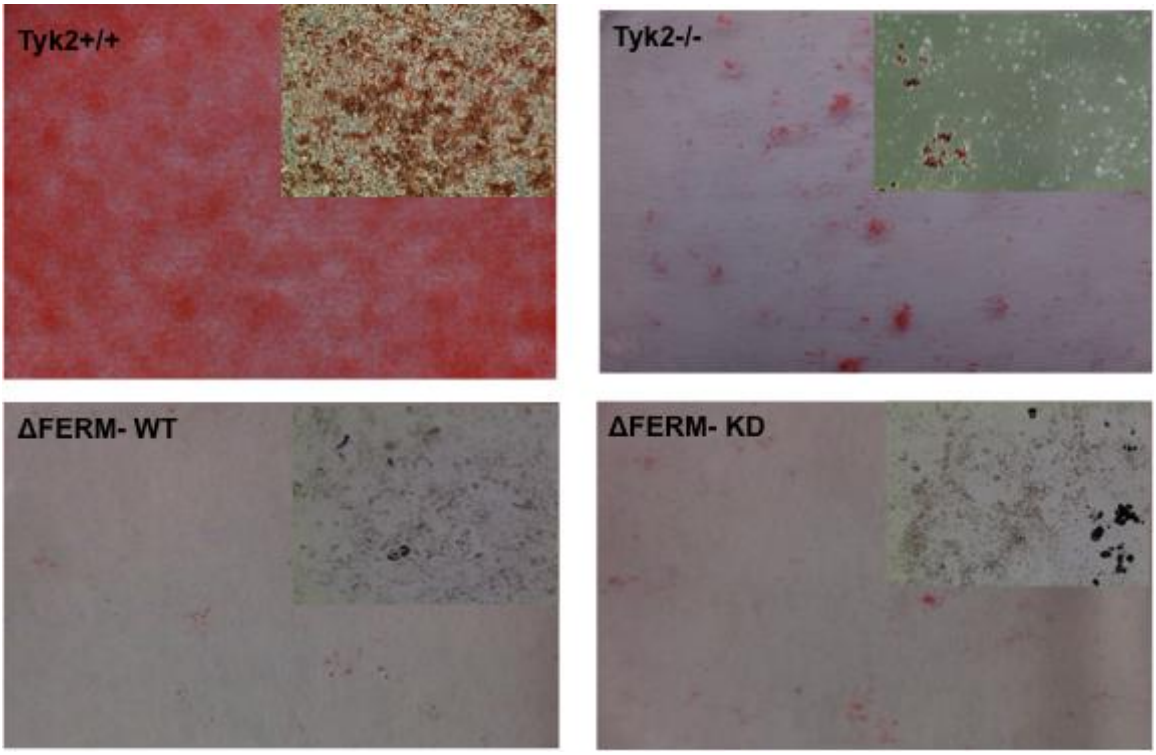

Figure 3.22: FERM domain of Tyk2 is important for its role in regulating obesity: Brown fat preadipocytes infected with the FERM domain deleted forms of Tyk2, sorted by FACS to selects cells expressing the tyk2 constructs (GFP) .Oil red-O staining was carried out after differentiation N = 3.

3.23: Tyk2 interacts with transcription factors involved in BAT differentiation and function

It has been well defined that the FERM domain of Tyk2 contains a nuclear-localization sequence (NLS) (54) and that Tyk2 also binds to the promoter region of IFN inducible genes along with its receptors IFNAR1 and IFNAR2 (55). We wanted to investigate whether the function of Tyk2 in obesity is because of its nuclear interactions. We immunoprecipitated Tyk2 from BAT of $Tyk2WT^{Myf5}$ and $Tyk2KD^{Myf5}$ mice and determined its interaction with transcription factors involved in BAT differentiation (PRDM16, C/EBPβ) and function (PGC1α,). As seen in Figure 3.25A, both Tyk2WT and Tyk2KD interact with PRDM16, C/EBPβ and PGC1α, suggesting that Tyk2 may be a part of the transcriptional complex regulating brown fat differentiation and function. We also performed a chromatin immunoprecipitation assay (ChIP) in brown fat of Tyk2+/+ mice with Tyk2 antibody and determined Tyk2 binding at the promoter regions of brown fat genes, UCP1 and PRDM16. As seen in Figure 3.23B, we did observe Tyk2 binding at these promoters and this binding is highly specific (figure 3.23C), suggesting a role for Tyk2 in regulating expression of genes involved in brown fat differentiation and function.

A

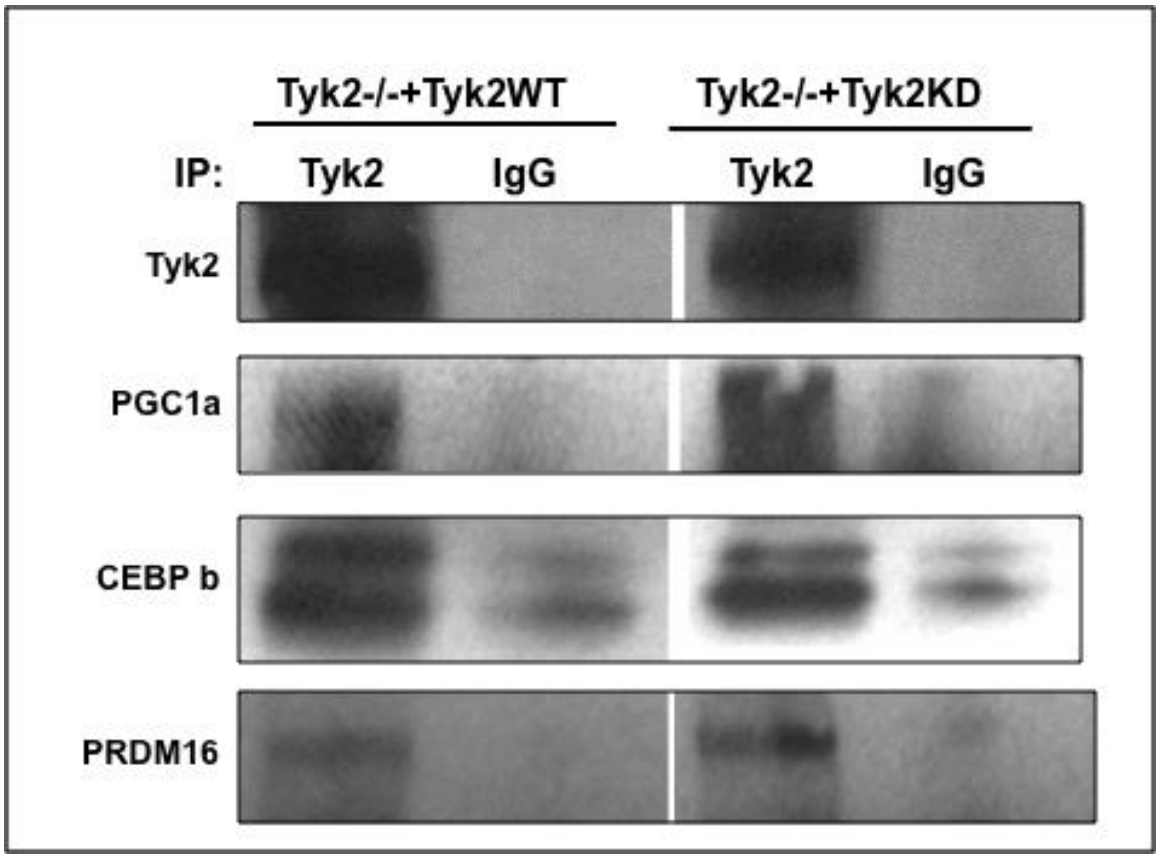
Tyk2-/-+Tyk2WT
Tyk2-/-+Tyk2KD
IP:
Tyk2
IgG
Tyk2
IgG
Tyk2
PGC1a
CEBP b
PRDM16

B

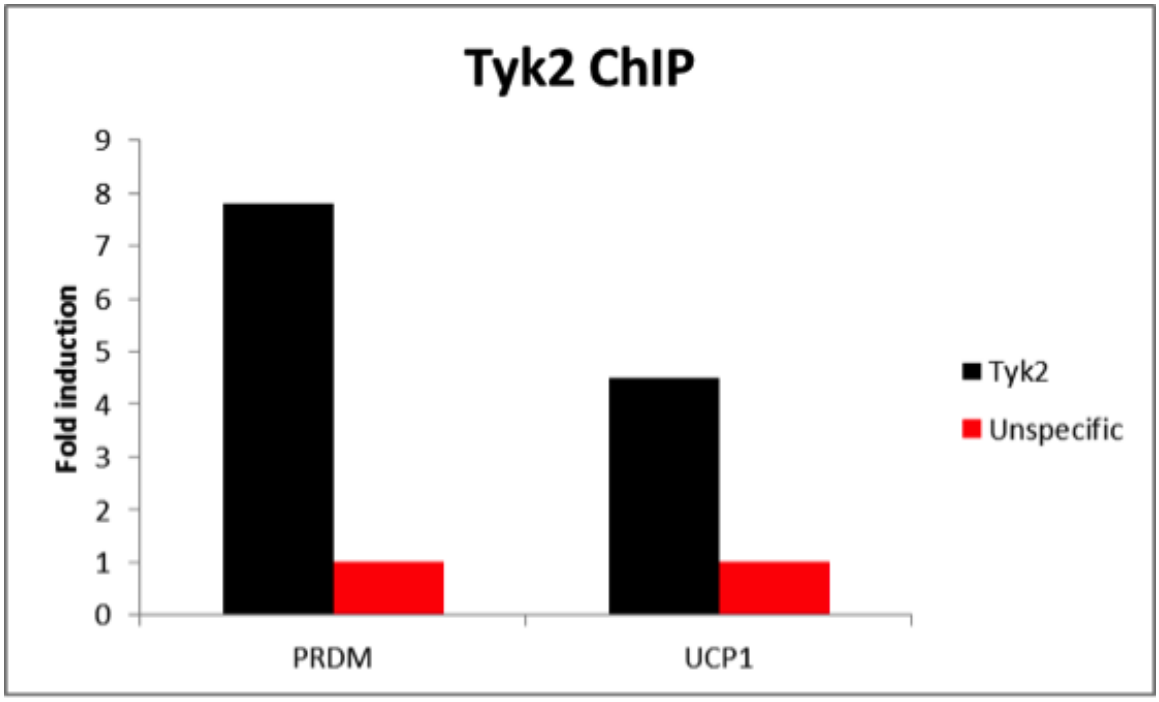
Tyk2 ChIP
Fold induction
9
8
7
6
5
4
3
2
1
0
PRDM
UCP1
Tyk2
Unspecific

C

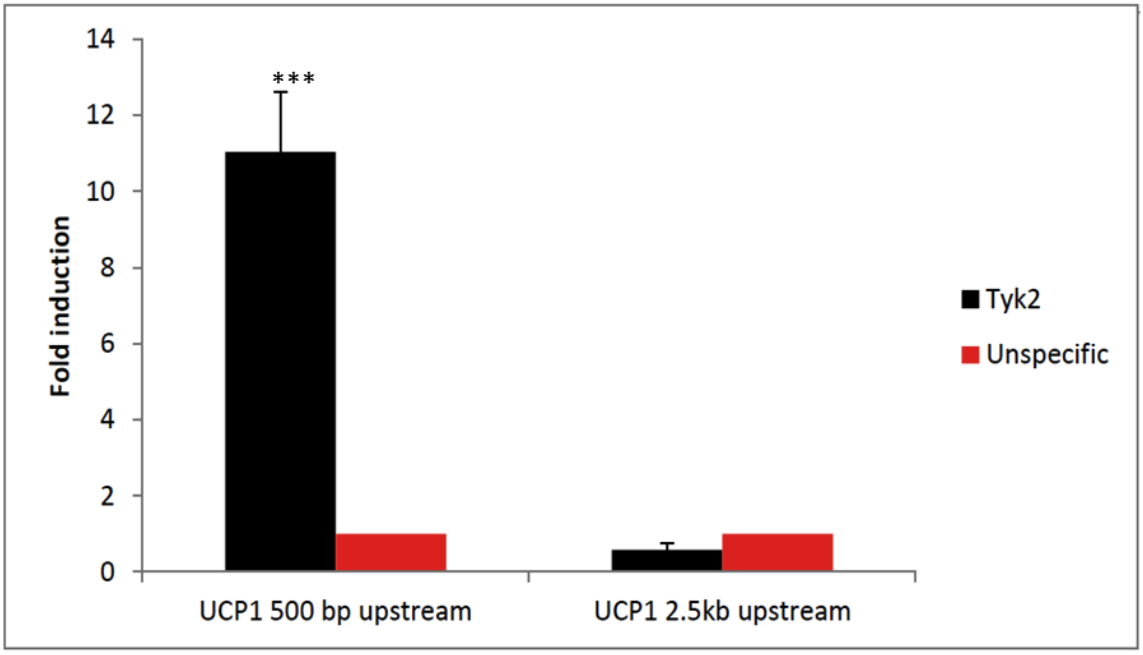

Figure 3.23: Tyk2 interacts with transcription factors involved in BAT differentiation and function: A) Whole cell extracts of BAT from Tyk2WT^{Myf5} and Tyk2KD^{Myf5} mice were immunoprecipitated with antibodies against Tyk2 and western blotted for PGC1α, C/EBPβ and PRDM16. IgG was used as unspecific control. N = 3. ChIP on BAT of 12 week old Tyk2+/+ mice. BAT from age matched Tyk2-/- mice were used as an unspecific control. qPCR was carried out to check for Tyk2 binding at A) UCP1 and PRDM16 promotor regions B) different regions upstream of UCP1 promoter showing the specificity of Tyk2 binding. N = 3, ***p<0.001.

3.24: Interaction of Tyk2 with PGC1α is induced under starvation in SKM

To further investigate whether the involvement of Tyk2 in skeletal muscle function is also beacuse of its nuclear interactions, we immunoprecipitated Tyk2 from SKM of Tyk2+/+ mice and determined its interaction with PGC1α which is important for skeletal muscle function. As seen in Figure 3.24, Tyk2 interacts with PGC1α, under starvation, when PGC1α levels are elevated (82). Interestingly, Tyk2 also interacts with the transcription factor C/EBPβ, which is involved in adult myogenesis. This suggests that Tyk2 may be a part of the transcriptional complex regulating skeletal muscle differentiation and function.

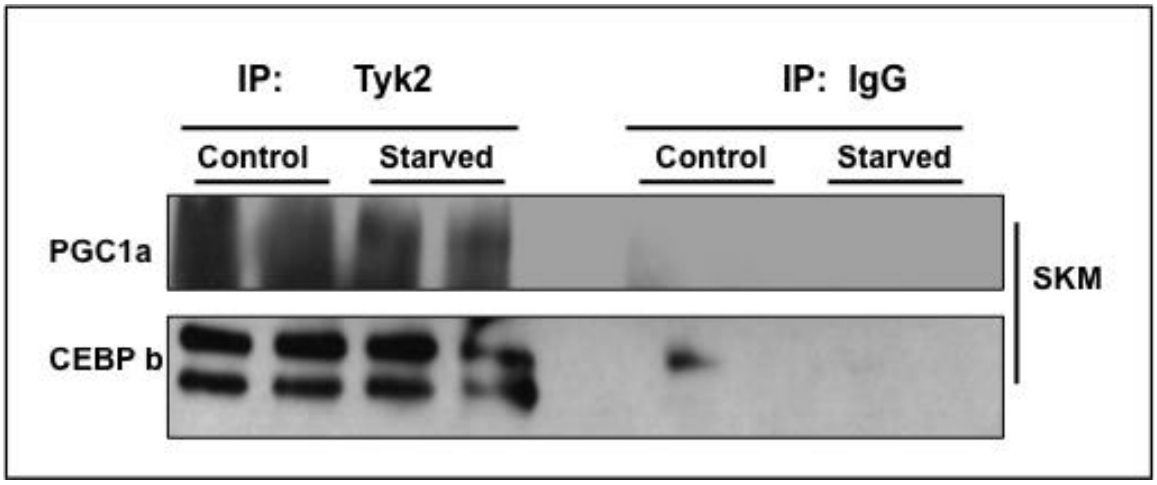

Figure 3.24: Tyk2 intercats with PGC1α in a starvation dependent fashion: Whole cell extracts of SKM Tyk2+/+ mice were immunoprecipitated with antibodies against Tyk2 and western blotted for PGC1α, C/EBPβ. IgG was used as unspecific control. N=3.

Chapter IV: Discussion

The work presented in this thesis highlights the role of Tyk2 in regulating the development and function brown fat and skeletal muscle derived from the Myf5+ progenitors of the mesenchymal lineage. Our previous work characterized the functional defects in brown fat of Tyk2 deficient mice (70).

Since we used a global knockout of Tyk2, the obese phenotype seen in the Tyk2 deficient mice could be a function of not only brown fat, but also other important contributing factors including a defect in the regulation of energy balance mediated by the hypothalamus (83), decreased energy expenditure as a function of skeletal muscle (29, 44) and adipose tissue inflammation leading to insulin resistance (84). Skeletal muscle, like brown fat, is a mitochondria rich tissue, is important in regulating energy expenditure (38) and handles almost 80% of insulin mediated glucose uptake (30). Since both brown fat and skeletal muscle share common embryonic origins, we wanted to investigate the role of Tyk2 in skeletal muscle development and function. Interestingly, Tyk2 along with Jak2 has been observed in regulation of lineage specific determination of mouse embryonic stem cells (85). All JAKs are known to be expressed in mouse embryonic stem cells (mESCs). Tyk2 is phosphorylated along with JAK1 and JAK2 in mESCs following LIF treatment, suggesting their involvement in regulating mESC cell renewal (86).

Body composition of Tyk2 deficient mice by NMR suggested that 3 month old knockout mice have an increased proportion of lean mass as compared to fat mass (A. Gornicka, unpublished data). Interestingly, brown adipose tissue also exhibited an increased

proportion of muscle specific genes (70), suggesting a dysregulation of the Myf5+ descendants. The increased skeletal muscle mass could be a result of hypertrophied muscle. Cross sections of Tyk2 deficient skeletal muscle ruled out muscle hypertrophy, suggesting that there was an increase in overall number of skeletal muscle fibers in the Tyk2 deficient animals. Interestingly, as observed in brown fat, Tyk2 deficient mice did not exhibit an increased expression of skeletal muscle genes in the muscle. On the contrary, levels of muscle creatine kinase, which also regulates the phosphorylation of creatine, was downregulated in these mice. Phospho-creatine is a major source of fuel for the muscles. This suggested an energy imbalance (78) and insufficient supply of fuel to the muscles for contraction.

Tyk2 deficient mice also show decreased expression of troponins, which are involved in regulating skeletal muscle contraction. This defect is observed even in newborn pups suggesting that the defects in muscle contraction are developmental and do not just accumulate with age. Previous studies by our group showed that Tyk2 deficient mice are exercise intolerant (69). This defect could be a function of impaired skeletal muscle contraction and/or dysfunctional mitochondria, which provide the necessary fuel for muscle contraction. Electron micrographs on skeletal muscle show smaller mitochondria with improper cristae formation in Tyk2 deficient mice. Interestingly, the number of mitochondria as observed in the different fiber types (both mitochondria rich type I and mitochondria poor Type II) was not much different between the wild type and Tyk2 deficient mice. These mitochondria are not only structurally defective, but they also exhibit decreased oxygen consumption as a function of decreased activity of complex IV

of the ETC. This suggests a role for Tyk2 in regulating the skeletal muscle contraction and also mitochondria formation and function.

Interestingly, expression of PGC1α, which is an important regulator of mitochondrial biogenesis, is also downregulated in Tyk2 deficient mice. PGC1α regulates the skeletal muscle fiber type determination (22). Tyk2 deficient mice exhibit an increased proportion of Type IIb (glycolytic) fibers, which have relatively low abundance of mitochondria. This could account for the exercise intolerant phenotype observed in Tyk2 deficient mice.

Numerous reports suggest the involvement of JAK-STAT pathway in regulating myogenesis (81, 87). JAK1 is required during initial myoblast proliferation stage whereas JAK2 is activated during the differentiation phage. JAK1 along with STAT1 and STAT3 also functions as a checkpoint to prevent myoblasts from premature differentiation. Knockdown of JAK1 induces increased myogenic differentiation with a concomitant reduction in cell proliferation (88). Interestingly, JAK2 along with STAT2 and STAT3 regulates the myoblast differentiation by activating the transcription factors MyoD and MFE2, which are involved in myogenic differentiation (81). As opposed to JAK1, knockdown of JAK2 inhibited myogenic differentiation, suggesting that JAK2 is required for skeletal muscle differentiation. JAK3, which was known to be restricted to the hematopoetic lineage, was also detected in proliferating myoblasts (89) and shown to play an inhibitory role on proliferating myoblasts. Apart from its involvement in myogenesis, JAK2 was found at the neuro-muscular junction along with ephrin receptor 4A (Epr4A) and shown to regulate the expression of acetylcholine esterase, the critical

enzyme that hydrolyzed the neurotransmitter acetylcholine at the NMJ. This suggests a functional role for JAKs in regulating muscle contraction.

We used an in-vitro system to determine whether Tyk2 plays a role in the development of skeletal muscle. During differentiation of C2C12 myocytes, we observed that Tyk2 protein levels dramatically increase during the initial differentiation phase and stay elevated throughout differentiation. This increase is specific to Tyk2 and not other JAKs. This suggests that although Tyk2 levels are regulated during differentiation of skeletal muscle, it is dispensable for structural development of skeletal muscle. However, is required for the function of skeletal muscle.

The development of obesity in Tyk2 knockout mice was a result of global Tyk2 knockdown. Although expression of constitutively active Stat3 in the brown fat of Tyk2-/- mice, using the fat-specific ap2 cre (expresses in brown fat, white fat or both, after birth) reverted the obese phenotype (70), expression of Tyk2 transgene (Tyk2WT and Tyk2KD) in brown fat alone using the ap2 cre, was not sufficient to revert the obese phenotype (M. Derecka, unpublished data). This suggested that either Tyk2 has to be expressed in tissues other than brown fat and/or the timing of Tyk2 expression is very critical and needs to be expressed early in development. We addressed this issue of temporal and spatial regulation of Tyk2 using two cre systems. Using Myf5 cre, we expressed Tyk2 in both brown fat and skeletal muscle at E8.5 in the mouse embryo. We also used MCK cre, which allowed the expression of Tyk2 in skeletal muscle and heart, but not brown fat. Our earlier studies pointed that expressing a kinase inactive form of Tyk2 in Tyk2-/- brown fat preadipocytes can restore their differentiation in vitro (M.Derecka, unpublished data), suggesting that Tyk2 may not function as a kinase in

brown fat development. To this end, we generated two transgenic mouse lines that carried the wild type and kinase inactive allele of Tyk2. With both transgenes activated under the Myf5 promoter, we observed a complete reversal of the obese phenotype. This effect was observed as early as in 12 week old mice and the lean phenotype was maintained even in 6 month old animals. Cold exposure studies confirmed activation of thermogenesis in the transgenic mice, suggesting the functional rescue of both/either brown fat and skeletal muscle. The in-vitro differentiation of brown fat preadipocytes was also recovered in both the transgenic lines, confirming the novel role of kinase inactive Tyk2 in brown fat differentiation and function.

Using the MCK cre transgenic mice, we wanted to delineate whether expression of Tyk2 in skeletal muscle was sufficient to revert the obese phenotype or it also required the function of brown fat. 12 week old $Tyk2WT^{MCK}$ and $Tyk2KD^{MCK}$ mice are significantly lighter than Tyk2-/- mice, but are still heavy compared to Tyk2+/+ mice. Interestingly, at 24 weeks, the $Tyk2KD^{MCK}$ mice completely revert the obese phenotype, whereas the $Tyk2WT^{MCK}$ mice partially revert the obese phenotype. This suggests that the kinase activity of Tyk2 is not required for its role in skeletal muscle function. Interestingly, these results go along with our in-vitro brown preadipocyte differentiation model where we observe that kinase dead Tyk2 is more effective in rescuing the differentiation in Tyk2-/- preadipocytes. Why the kinase inactive Tyk2 appears to be more effective than the wild-type form of Tyk2 is still not clear. One reason could be that the kinase activity of Tyk2 may have an inhibitory role on its function. Since Tyk2 has been shown to have nuclear actions, it may be possible that Tyk2 could phosphorylate the histones and inhibit transcription of genes that regulate skeletal muscle function. Alternatively, the kinase

inactive Tyk2 is more effective in interacting with proteins regulating muscle function. More studies need to be carried out to address this issue. Unlike the reports suggesting that kinase inactive form of Tyk2 is prone to proteasomal degradation (90), we did not see any differences in the expression of Tyk2 levels in our Tyk2KD^{MCK} and Tyk2KD^{Myf5} transgenic mice. Also, BAT development is not restored in these mice. This suggests that Tyk2 expression is required for proper skeletal muscle function and/or kinase activity of Tyk2 is inhibitory in skeletal muscle function. Co-expression of Tyk2 in brown fat and skeletal muscle may be required for optimal regulation of energy expenditure.

Our results suggest that Tyk2 does not function as a classical JAK-STAT tyrosine kinase, since the kinase dead form of Tyk2 works as effectively as wild type Tyk2 to revert the obese phenotype in Tyk2 deficient mice. Non-classical functions of the JAK kinases are not unheard of. Until recently, involvement of JAKs in gene expression was thought to be restricted to their actions as receptor-associated tyrosine kinases, activating the STAT transcription factors. Recent reports suggest the presence of JAKs in the nucleus and also provide evidence that JAKs also can phosphorylate other target molecules apart from STATs (91). JAK2 in the nucleus was shown to phosphorylate Y41 on histone H3 and regulate genes involved in hematopoiesis and leukemia (52). Reports also suggest a nuclear localization of Tyk2 (54) and its role in gene regulation by binding to their promoters (55). On similar lines, we found an interaction of Tyk2 with PRDM16, PGC1α and C/EBPβ, the transcriptional complex regulating brown fat differentiation and function. In skeletal muscle, we found starvation-induced association of Tyk2 with PGC1α. The FERM domain deletion mutant of Tyk2, which is known to affect its nuclear localization, did not recover the differentiation capacity of Tyk2-/-

brown fat preadipocytes. This suggests that nuclear actions of Tyk2 are required for its role in regulation and differentiation of the thermogenic tissues. We speculate that Tyk2, along with PRDM16, may be a part of the transcriptional machinery regulating the brown fat differentiation.

Our studies suggest that Tyk2 is required at two different stages of development. First, it may be required for the commitment of the Myf5+ progenitors towards developing brown fat and plays an inhibitory role towards commitment of these progenitors towards skeletal muscle (Figure 4.1). Secondly, Tyk2 may also be required for the function of brown fat and skeletal muscle, by regulating the expression of genes involved in brown fat and skeletal muscle differentiation and/or function (Figure 4.2). It is also interesting to note that levels of Tyk2 in the skeletal muscle are much lower compared to other tissues in a mouse (70), suggesting that Tyk2 may play an inhibitory role in maintenance of skeletal muscle progenitors. The role of Tyk2 needs to be further explored with respect to what other genes does it control, how is it activated in response to cold and what other proteins it interacts with.

Therapies for obesity include increasing energy expenditure by exercise and reducing caloric intake. Unfortunately, only a small proportion of obese individuals are able to maintain their reduced body weight on a diet and exercise regime. Bariatric surgery is recommended for extreme obese patients, however it also comes with side effects (5). As of today, FDA has approved three drugs for treatment of obesity which aim at decreasing energy intake. Sibutramine and Phentermine act on the satiety centers in the brain and thus control food intake by obese individuals. Orlistat reduces absorption of fatty acids in the intestine (92). However, apart from the unpleasant side effects that

these drugs possess, clinical studies on patients have shown that once the treatment is stopped, weight gain is accelerated, thus limiting the success of these treatments. Reducing caloric intake also triggers the starvation response in mammals, which may also reduce the efficacy of these drugs.

The other promising treatment for obesity is increasing energy expenditure. Increasing the thermogenic potential of brown fat and skeletal muscle could provide means to increase energy wasting by these tissues, thus potentiating their anti-obesity effects. However, increasing energy expenditure has to be maintained in a controlled manner. If the inherent function of brown fat and skeletal muscle could be modified, which would change the basal metabolic rate (BMR) of an individual, these effects would be beneficial in the long run. In the 1930s, mitochondrial uncoupler 2, 4 dinitrophenol (DNP) gained popularity as an anti-obesity drug. DNP, like UCP1, created a proton leak in the mitochondrial membrane, thus dissipating the potential energy as heat. Although DNP was successful in reducing obesity, continuous use of DNP generated unwanted side effects including hyperthermia, which resulted in death in some cases. Hence, when aiming to develop drugs that increase energy expenditure, careful considerations about not expending excessive energy should be taken into account. If a balance between energy intake and expenditure could be maintained, that will be a better way to combat obesity.

Given the role of Tyk2 in regulating function of brown fat and skeletal muscle, controlled activation of Tyk2 to improve the energy expenditure in these thermogenic tissues could provide an attractive therapy for treatment of obesity.

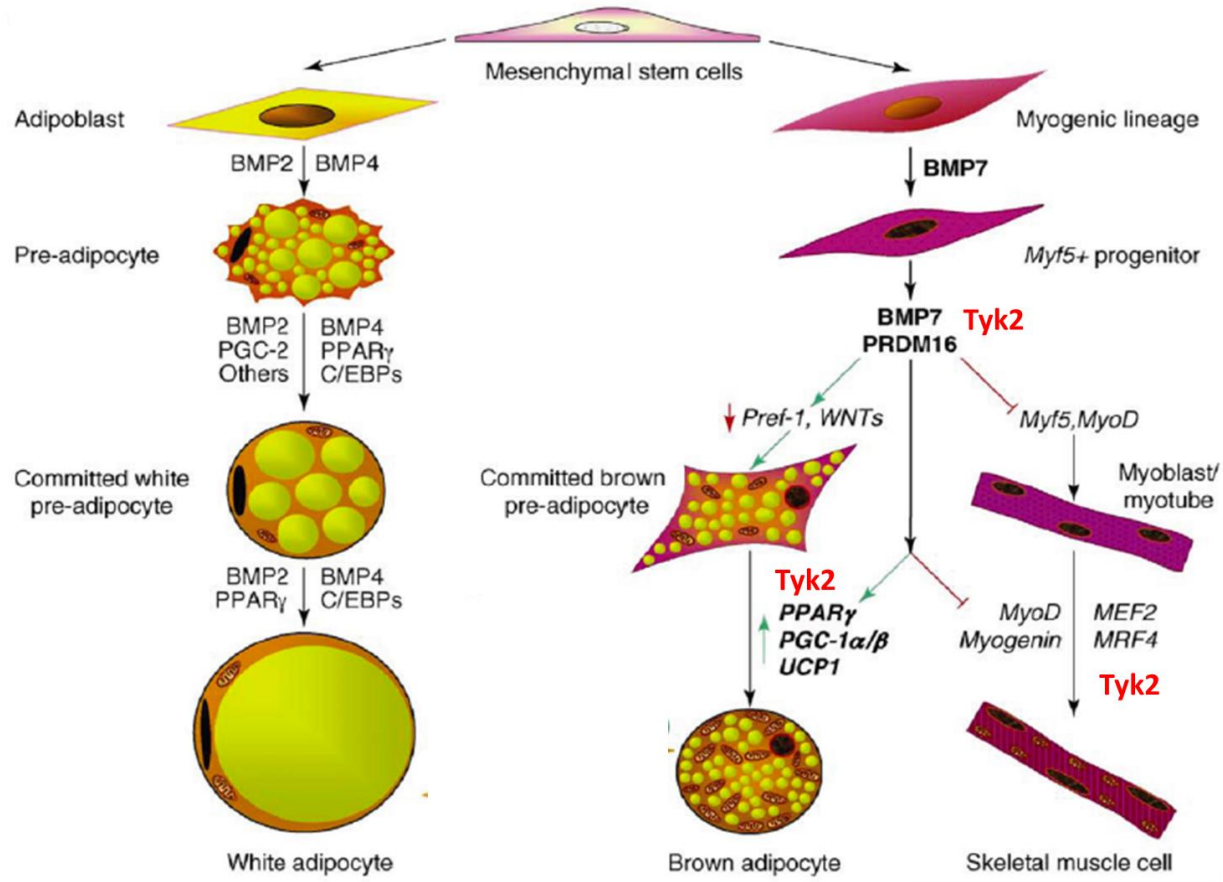

Figure 4.1: Tyk2 may be required for the commitment of Myf5+ progenitors: Tyk2 may be required along with PRDM16 for commitment of Myf5+ mesenchymal stem cells towards brown adipocytes and may also play an inhibitory role in commitment of the Myf5+ cells towards skeletal muscle development.

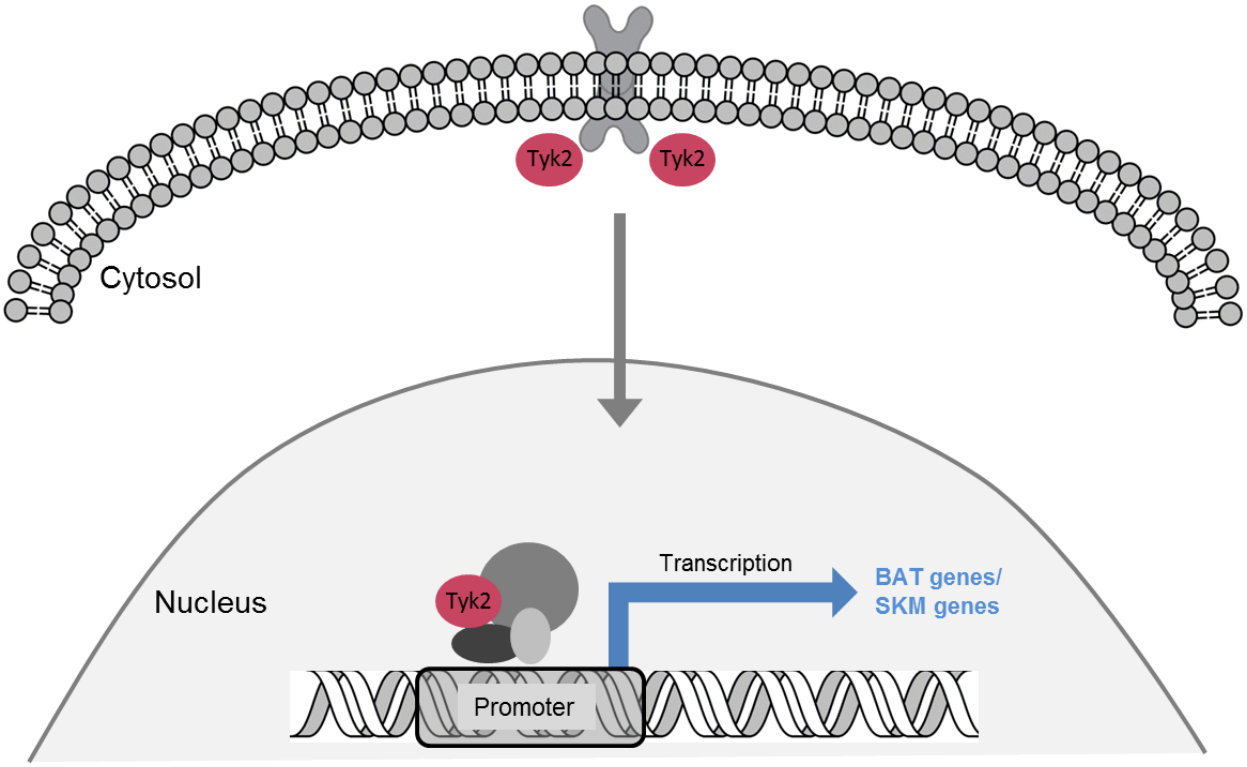

Figure 4.2: Tyk2 regulates genes involved in BAT and SKM differentiation and/or function: Tyk2 may be a part of a multiprotein transcriptional complex regulating genes involved in BAT and SKM differentiation/function.

References

1. Schigt A, Gerdes VE, Cense HA, Berends FJ, van Dielen FM, Janssen I, et al. Bariatric surgery is an effective treatment for morbid obesity. Neth J Med. 2013 Jan;71(1):4-9.

2. Seidell JC. Obesity, insulin resistance and diabetes--a worldwide epidemic. Br J Nutr. 2000 Mar;83 Suppl 1:S5-8.

3. Wu J, Cohen P, Spiegelman BM. Adaptive thermogenesis in adipocytes: Is beige the new brown? Genes Dev. 2013 Feb 1;27(3):234-50.

4. Lopez-Soriano J, Chiellini C, Maffei M, Grimaldi PA, Argiles JM. Roles of skeletal muscle and peroxisome proliferator-activated receptors in the development and treatment of obesity. Endocr Rev. 2006 May;27(3):318-29.

5. Tseng YH, Cypess AM, Kahn CR. Cellular bioenergetics as a target for obesity therapy. Nat Rev Drug Discov. 2010 Jun;9(6):465-82.

6. Cypess AM, Kahn CR. Brown fat as a therapy for obesity and diabetes. Curr Opin Endocrinol Diabetes Obes. 2010 Apr;17(2):143-9.

7. Lowell BB, S-Susulic V, Hamann A, Lawitts JA, Himms-Hagen J, Boyer BB, et al. Development of obesity in transgenic mice after genetic ablation of brown adipose tissue. Nature. 1993 Dec 23-30;366(6457):740-2.

8. Feldmann HM, Golozoubova V, Cannon B, Nedergaard J. UCP1 ablation induces obesity and abolishes diet-induced thermogenesis in mice exempt from thermal stress by living at thermoneutrality. Cell Metab. 2009 Feb;9(2):203-9.

9. Hansen JB, Kristiansen K. Regulatory circuits controlling white versus brown adipocyte differentiation. Biochem J. 2006 Sep 1;398(2):153-68.

10. Nedergaard J, Bengtsson T, Cannon B. Unexpected evidence for active brown adipose tissue in adult humans. Am J Physiol Endocrinol Metab. 2007 Aug;293(2):E444-52.

11. Fruhbeck G, Becerril S, Sainz N, Garrastachu P, Garcia-Velloso MJ. BAT: A new target for human obesity? Trends Pharmacol Sci. 2009 Aug;30(8):387-96.

12. Cannon B, Nedergaard J. Brown adipose tissue: Function and physiological significance. Physiol Rev. 2004 Jan;84(1):277-359.

13. Seale P. Transcriptional control of brown adipocyte development and thermogenesis. Int J Obes (Lond). 2010 Oct;34 Suppl 1:S17-22.

14. Seale P, Kajimura S, Yang W, Chin S, Rohas LM, Uldry M, et al. Transcriptional control of brown fat determination by PRDM16. Cell Metab. 2007 Jul;6(1):38-54.

15. Francetic T, Li Q. Skeletal myogenesis and Myf5 activation. Transcription. 2011 May;2(3):109-14.

16. Cristancho AG, Lazar MA. Forming functional fat: A growing understanding of adipocyte differentiation. Nat Rev Mol Cell Biol. 2011 Sep 28;12(11):722-34.

17. Seale P, Kajimura S, Spiegelman BM. Transcriptional control of brown adipocyte development and physiological function--of mice and men. Genes Dev. 2009 Apr 1;23(7):788-97.

18. Tsukada J, Yoshida Y, Kominato Y, Auron PE. The CCAAT/enhancer (C/EBP) family of basic-leucine zipper (bZIP) transcription factors is a multifaceted highly-regulated system for gene regulation. Cytokine. 2011 Apr;54(1):6-19.

19. Kajimura S, Seale P, Spiegelman BM. Transcriptional control of brown fat development. Cell Metab. 2010 Apr 7;11(4):257-62.

20. Puigserver P, Wu Z, Park CW, Graves R, Wright M, Spiegelman BM. A cold-inducible coactivator of nuclear receptors linked to adaptive thermogenesis. Cell. 1998 Mar 20;92(6):829-39.

21. Lin J, Handschin C, Spiegelman BM. Metabolic control through the PGC-1 family of transcription coactivators. Cell Metab. 2005 Jun;1(6):361-70.

22. Puigserver P. Tissue-specific regulation of metabolic pathways through the transcriptional coactivator PGC1-alpha. Int J Obes (Lond). 2005 Mar;29 Suppl 1:S5-9.

23. Seale P, Kajimura S, Yang W, Chin S, Rohas LM, Uldry M, et al. Transcriptional control of brown fat determination by PRDM16. Cell Metab. 2007 Jul;6(1):38-54.

24. Seale P, Bjork B, Yang W, Kajimura S, Chin S, Kuang S, et al. PRDM16 controls a brown fat/skeletal muscle switch. Nature. 2008 Aug 21;454(7207):961-7.

25. Golozoubova V, Cannon B, Nedergaard J. UCP1 is essential for adaptive adrenergic nonshivering thermogenesis. Am J Physiol Endocrinol Metab. 2006 Aug;291(2):E350-7.

26. Cannon B, Houstek J, Nedergaard J. Brown adipose tissue. more than an effector of thermogenesis? Ann N Y Acad Sci. 1998 Sep 29;856:171-87.

27. Cannon B, Nedergaard J. Brown adipose tissue: Function and physiological significance. Physiol Rev. 2004 Jan;84(1):277-359.

28. Ow YP, Green DR, Hao Z, Mak TW. Cytochrome c: Functions beyond respiration. Nat Rev Mol Cell Biol. 2008 Jul;9(7):532-42.

29. Stump CS, Henriksen EJ, Wei Y, Sowers JR. The metabolic syndrome: Role of skeletal muscle metabolism. Ann Med. 2006;38(6):389-402.

30. Wells GD, Noseworthy MD, Hamilton J, Tarnopolski M, Tein I. Skeletal muscle metabolic dysfunction in obesity and metabolic syndrome. Can J Neurol Sci. 2008 Mar;35(1):31-40.

31. Morimoto S. Sarcomeric proteins and inherited cardiomyopathies. Cardiovasc Res. 2008 Mar 1;77(4):659-66.

32. Gordon AM, Homsher E, Regnier M. Regulation of contraction in striated muscle. Physiol Rev. 2000 Apr;80(2):853-924.

33. Zot AS, Potter JD. Structural aspects of troponin-tropomyosin regulation of skeletal muscle contraction. Annu Rev Biophys Biophys Chem. 1987;16:535-59.

34. Lin J, Wu H, Tarr PT, Zhang CY, Wu Z, Boss O, et al. Transcriptional co-activator PGC-1 alpha drives the formation of slow-twitch muscle fibres. Nature. 2002 Aug 15;418(6899):797-801.

35. Wu Z, Puigserver P, Andersson U, Zhang C, Adelmant G, Mootha V, et al. Mechanisms controlling mitochondrial biogenesis and respiration through the thermogenic coactivator PGC-1. Cell. 1999 Jul 9;98(1):115-24.

36. Wijers SL, Saris WH, van Marken Lichtenbelt WD. Recent advances in adaptive thermogenesis: Potential implications for the treatment of obesity. Obes Rev. 2009 Mar;10(2):218-26.

37. Bal NC, Maurya SK, Sopariwala DH, Sahoo SK, Gupta SC, Shaikh SA, et al. Sarcolipin is a newly identified regulator of muscle-based thermogenesis in mammals. Nat Med. 2012 Oct;18(10):1575-9.

38. van den Berg SA, van Marken Lichtenbelt W, Willems van Dijk K, Schrauwen P. Skeletal muscle mitochondrial uncoupling, adaptive thermogenesis and energy expenditure. Curr Opin Clin Nutr Metab Care. 2011 May;14(3):243-9.

39. Hasty P, Bradley A, Morris JH, Edmondson DG, Venuti JM, Olson EN, et al. Muscle deficiency and neonatal death in mice with a targeted mutation in the myogenin gene. Nature. 1993 Aug 5;364(6437):501-6.

40. Kablar B, Krastel K, Tajbakhsh S, Rudnicki MA. Myf5 and MyoD activation define independent myogenic compartments during embryonic development. Dev Biol. 2003 Jun 15;258(2):307-18.

41. Atit R, Sgaier SK, Mohamed OA, Taketo MM, Dufort D, Joyner AL, et al. Beta-catenin activation is necessary and sufficient to specify the dorsal dermal fate in the mouse. Dev Biol. 2006 Aug 1;296(1):164-76.

42. Timmons JA, Wennmalm K, Larsson O, Walden TB, Lassmann T, Petrovic N, et al. Myogenic gene expression signature establishes that brown and white adipocytes originate from distinct cell lineages. Proc Natl Acad Sci U S A. 2007 Mar 13;104(11):4401-6.

43. Patti ME, Corvera S. The role of mitochondria in the pathogenesis of type 2 diabetes. Endocr Rev. 2010 Jun;31(3):364-95.

44. Kelley DE, He J, Menshikova EV, Ritov VB. Dysfunction of mitochondria in human skeletal muscle in type 2 diabetes. Diabetes. 2002 Oct;51(10):2944-50.

45. Kim JA, Wei Y, Sowers JR. Role of mitochondrial dysfunction in insulin resistance. Circ Res. 2008 Feb 29;102(4):401-14.

46. Cannon B, Nedergaard J. Respiratory and thermogenic capacities of cells and mitochondria from brown and white adipose tissue. Methods Mol Biol. 2001;155:295-303.

47. Harrison DA. The jak/STAT pathway. Cold Spring Harb Perspect Biol. 2012 Mar 1;4(3):10.1101/cshperspect.a011205.

48. Yeh TC, Pellegrini S. The janus kinase family of protein tyrosine kinases and their role in signaling. Cell Mol Life Sci. 1999 Sep;55(12):1523-34.

49. Kisseleva T, Bhattacharya S, Braunstein J, Schindler CW. Signaling through the JAK/STAT pathway, recent advances and future challenges. Gene. 2002 Feb 20;285(1-2):1-24.

50. Yamaoka K, Saharinen P, Pesu M, Holt VE,3rd, Silvennoinen O, O'Shea JJ. The janus kinases (jaks). Genome Biol. 2004;5(12):253.

51. Rawlings JS, Rosler KM, Harrison DA. The JAK/STAT signaling pathway. J Cell Sci. 2004 Mar 15;117(Pt 8):1281-3.

52. Dawson MA, Bannister AJ, Gottgens B, Foster SD, Bartke T, Green AR, et al. JAK2 phosphorylates histone H3Y41 and excludes HP1alpha from chromatin. Nature. 2009 Oct 8;461(7265):819-22.

53. Lobie PE, Ronsin B, Silvennoinen O, Haldosen LA, Norstedt G, Morel G. Constitutive nuclear localization of janus kinases 1 and 2. Endocrinology. 1996 Sep;137(9):4037-45.

54. Ragimbeau J, Dondi E, Vasserot A, Romero P, Uze G, Pellegrini S. The receptor interaction region of Tyk2 contains a motif required for its nuclear localization. J Biol Chem. 2001 Aug 17;276(33):30812-8.

55. Ahmed CM, Noon-Song EN, Kemppainen K, Pascalli MP, Johnson HM. Type I IFN receptor controls activated TYK2 in the nucleus: Implications for EAE therapy. J Neuroimmunol. 2013 Jan 15;254(1-2):101-9.

56. Firmbach-Kraft I, Byers M, Shows T, Dalla-Favera R, Krolewski JJ. Tyk2, prototype of a novel class of non-receptor tyrosine kinase genes. Oncogene. 1990 Sep;5(9):1329-36.

57. Barbieri G, Velazquez L, Scrobogna M, Fellous M, Pellegrini S. Activation of the protein tyrosine kinase tyk2 by interferon alpha/beta. Eur J Biochem. 1994 Jul 15;223(2):427-35.

58. Pellegrini S, Dusanter-Fourt I. The structure, regulation and function of the janus kinases (JAKs) and the signal transducers and activators of transcription (STATs). Eur J Biochem. 1997 Sep 15;248(3):615-33.

59. Velazquez L, Mogensen KE, Barbieri G, Fellous M, Uze G, Pellegrini S. Distinct domains of the protein tyrosine kinase tyk2 required for binding of interferon-alpha/beta and for signal transduction. J Biol Chem. 1995 Feb 17;270(7):3327-34.

60. Yeh TC, Dondi E, Uze G, Pellegrini S. A dual role for the kinase-like domain of the tyrosine kinase Tyk2 in interferon-alpha signaling. Proc Natl Acad Sci U S A. 2000 Aug 1;97(16):8991-6.

61. Gauzzi MC, Velazquez L, McKendry R, Mogensen KE, Fellous M, Pellegrini S. Interferon-alpha-dependent activation of Tyk2 requires phosphorylation of positive regulatory tyrosines by another kinase. J Biol Chem. 1996 Aug 23;271(34):20494-500.

62. Gauzzi MC, Barbieri G, Richter MF, Uze G, Ling L, Fellous M, et al. The amino-terminal region of Tyk2 sustains the level of interferon alpha receptor 1, a component of the interferon alpha/beta receptor. Proc Natl Acad Sci U S A. 1997 Oct 28;94(22):11839-44.

63. Shimoda K, Kato K, Aoki K, Matsuda T, Miyamoto A, Shibamori M, et al. Tyk2 plays a restricted role in IFN alpha signaling, although it is required for IL-12-mediated T cell function. Immunity. 2000 Oct;13(4):561-71.

64. Karaghiosoff M, Neubauer H, Lassnig C, Kovarik P, Schindler H, Pircher H, et al. Partial impairment of cytokine responses in Tyk2-deficient mice. Immunity. 2000 Oct;13(4):549-60.

65. Sheehan KC, Lai KS, Dunn GP, Bruce AT, Diamond MS, Heutel JD, et al. Blocking monoclonal antibodies specific for mouse IFN-alpha/beta receptor subunit 1 (IFNAR-1) from mice immunized by in vivo hydrodynamic transfection. J Interferon Cytokine Res. 2006 Nov;26(11):804-19.

66. Shaw MH, Boyartchuk V, Wong S, Karaghiosoff M, Ragimbeau J, Pellegrini S, et al. A natural mutation in the Tyk2 pseudokinase domain underlies altered susceptibility of B10.Q/J mice to infection and autoimmunity. Proc Natl Acad Sci U S A. 2003 Sep 30;100(20):11594-9.

67. Strobl B, Stoiber D, Sexl V, Mueller M. Tyrosine kinase 2 (TYK2) in cytokine signalling and host immunity. Front Biosci. 2011 Jun 1;16:3214-32.

68. Seto Y, Nakajima H, Suto A, Shimoda K, Saito Y, Nakayama KI, et al. Enhanced Th2 cell-mediated allergic inflammation in Tyk2-deficient mice. J Immunol. 2003 Jan 15;170(2):1077-83.

69. Potla R, Koeck T, Wegrzyn J, Cherukuri S, Shimoda K, Baker DP, et al. Tyk2 tyrosine kinase expression is required for the maintenance of mitochondrial respiration in primary pro-B lymphocytes. Mol Cell Biol. 2006 Nov;26(22):8562-71.

70. Derecka M, Gornicka A, Koralov SB, Szczepanek K, Morgan M, Raje V, et al. Tyk2 and Stat3 regulate brown adipose tissue differentiation and obesity. Cell Metab. 2012 Dec 5;16(6):814-24.

71. Strobl B, Stoiber D, Sexl V, Mueller M. Tyrosine kinase 2 (TYK2) in cytokine signalling and host immunity. Front Biosci. 2011 Jun 1;16:3214-32.

72. Minegishi Y, Saito M, Morio T, Watanabe K, Agematsu K, Tsuchiya S, et al. Human tyrosine kinase 2 deficiency reveals its requisite roles in multiple cytokine signals involved in innate and acquired immunity. Immunity. 2006 Nov;25(5):745-55.

73. Kilic SS, Hacimustafaoglu M, Boisson-Dupuis S, Kreins AY, Grant AV, Abel L, et al. A patient with tyrosine kinase 2 deficiency without hyper-IgE syndrome. J Pediatr. 2012 Jun;160(6):1055-7.

74. Bruning JC, Michael MD, Winnay JN, Hayashi T, Horsch D, Accili D, et al. A muscle-specific insulin receptor knockout exhibits features of the metabolic syndrome of NIDDM without altering glucose tolerance. Mol Cell. 1998 Nov;2(5):559-69.

75. CHANCE B, WILLIAMS GR. A simple and rapid assay of oxidative phosphorylation. Nature. 1955 Jun 25;175(4469):1120-1.

76. Klein J, Fasshauer M, Ito M, Lowell BB, Benito M, Kahn CR. Beta(3)-adrenergic stimulation differentially inhibits insulin signaling and decreases insulin-induced glucose uptake in brown adipocytes. J Biol Chem. 1999 Dec 3;274(49):34795-802.

77. Wende AR, Schaeffer PJ, Parker GJ, Zechner C, Han DH, Chen MM, et al. A role for the transcriptional coactivator PGC-1alpha in muscle refueling. J Biol Chem. 2007 Dec 14;282(50):36642-51.

78. van Deursen J, Ruitenbeek W, Heerschap A, Jap P, ter Laak H, Wieringa B. Creatine kinase (CK) in skeletal muscle energy metabolism: A study of mouse mutants with graded reduction in muscle CK expression. Proc Natl Acad Sci U S A. 1994 Sep 13;91(19):9091-5.

79. Jung C, Higgins CM, Xu Z. Measuring the quantity and activity of mitochondrial electron transport chain complexes in tissues of central nervous system using blue native polyacrylamide gel electrophoresis. Anal Biochem. 2000 Nov 15;286(2):214-23.

80. Trenerry MK, Della Gatta PA, Cameron-Smith D. JAK/STAT signaling and human in vitro myogenesis. BMC Physiol. 2011 Mar 9;11:6,6793-11-6.

81. Wang K, Wang C, Xiao F, Wang H, Wu Z. JAK2/STAT2/STAT3 are required for myogenic differentiation. J Biol Chem. 2008 Dec 5;283(49):34029-36.

82. Potthoff MJ, Inagaki T, Satapati S, Ding X, He T, Goetz R, et al. FGF21 induces PGC-1alpha and regulates carbohydrate and fatty acid metabolism during the adaptive starvation response. Proc Natl Acad Sci U S A. 2009 Jun 30;106(26):10853-8.

83. Williams LM. Hypothalamic dysfunction in obesity. Proc Nutr Soc. 2012 Nov;71(4):521-33.

84. Havel PJ. Role of adipose tissue in body-weight regulation: Mechanisms regulating leptin production and energy balance. Proc Nutr Soc. 2000 Aug;59(3):359-71.

85. Chung BM, Kang HC, Han SY, Heo HS, Lee JJ, Jeon J, et al. Jak2 and Tyk2 are necessary for lineage-specific differentiation, but not for the maintenance of self-renewal of mouse embryonic stem cells. Biochem Biophys Res Commun. 2006 Dec 22;351(3):682-8.

86. Ernst M, Oates A, Dunn AR. Gp130-mediated signal transduction in embryonic stem cells involves activation of jak and ras/mitogen-activated protein kinase pathways. J Biol Chem. 1996 Nov 22;271(47):30136-43.

87. Diao Y, Wang X, Wu Z. SOCS1, SOCS3, and PIAS1 promote myogenic differentiation by inhibiting the leukemia inhibitory factor-induced JAK1/STAT1/STAT3 pathway. Mol Cell Biol. 2009 Sep;29(18):5084-93.

88. Sun L, Ma K, Wang H, Xiao F, Gao Y, Zhang W, et al. JAK1-STAT1-STAT3, a key pathway promoting proliferation and preventing premature differentiation of myoblasts. J Cell Biol. 2007 Oct 8;179(1):129-38.

89. Jang YN, Lee IJ, Park MC, Baik EJ. Role of JAK3 in myogenic differentiation. Cell Signal. 2012 Mar;24(3):742-9.

90. Prchal-Murphy M, Semper C, Lassnig C, Wallner B, Gausterer C, Teppner-Klymiuk I, et al. TYK2 kinase activity is required for functional type I interferon responses in vivo. PLoS One. 2012;7(6):e39141.

91. Zouein FA, Duhe RJ, Booz GW. JAKs go nuclear: Emerging role of nuclear JAK1 and JAK2 in gene expression and cell growth. Growth Factors. 2011 Dec;29(6):245-52.

92. Padwal RS, Majumdar SR. Drug treatments for obesity: Orlistat, sibutramine, and rimonabant. Lancet. 2007 Jan 6;369(9555):71-7.